Journal of Chemical&Engineering Data

pubs.acs.org/jced Review

Comprehensive Review of the Impact of Thermodynamic Inhibitors and the Predictive Power of Machine Learning Models on Hydrate Formation Pressure and Temperature

Mohammad Amin Behnam Motlagh, Rohallah Hashemi,* Zahra Taheri Rizi, Mohsen Mohammadi, Mahbobeh Mohammadtaheri, and Behnam Zarei Eslam

Cite This: https://doi.org/10.1021/acs.jced.5c00025 Read Online

ACCESS | Metrics & More | Article Recommendations

ABSTRACT: Gas hydrate formation presents challenges in the petroleum and gas industry, such as pipeline blockages. This study evaluates thermodynamic inhibitors, including amino acids, ionic liquids, salts, and commercial inhibitors, using 213 data entries covering a range of gases and inhibitors over pressures from 0.13 to 200 MPa and temperatures from 238.15 to 333.15 K. Glycine is identified as the most effective amino acid inhibitor, especially when combined with methanol. The inhibition efficiency of ionic liquids depends on functional groups (e.g., OH, NH_2) and side chain lengths, while salts like $MgCl_2$ perform well due to high ionic charge densities. Methanol and monoethylene glycol remain effective in high-flow systems. Machine learning models, including random forest (RF), support vector machines (SVM), deep neural networks (DNN), and convolutional neural networks (CNN), were applied to predict hydrate formation conditions. The RF model showed the best accuracy with an R^2 of 0.96 and a root-mean-square error (RMSE) of 1.51 MPa for pressure, and an R^2 of 0.92 and an RMSE of 2.66 K for temperature. Compared to physically based models, these machine learning methods demonstrated better generalization across varied compositions and inhibitor types, particularly in cases involving complex nonlinear interactions, offering a powerful approach to optimize hydrate control strategies in operations.

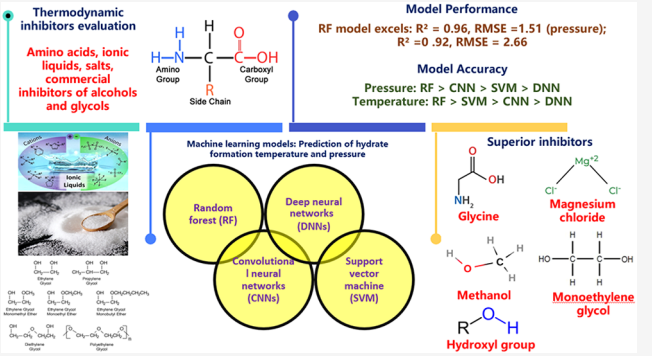

1. INTRODUCTION

Gas clathrates are a member of a particular group of substances known as clathrate that generate crystalline forms similar to ice by combining water molecules (hosts) and gas particles (guests) such as methane, ethane, propane, carbon dioxide, and hydrogen sulfide. These guests are confined within enclosures established by the hydrogen tie between water particles. Despite the absence of covalent bonding between the guests and hosts, the former molecules are free to rotate within the cells created by the latter molecules.[1] Different crystallographic structures were formed in accordance with the dimensions of the guest molecules, among which the most frequently occurring ones are designated as structure I, structure II (sII), and structure H. In 1965, McMullan and Jeffrey made the initial observation of the hydrate I structure during the process of hydrate creation, wherein ethylene oxide was employed as a guest molecule.[2] The structure I is a cubic lattice structure about 12 Å in size. This structure has two small cavities (5^{12}), each composed of 12 pentagonal faces and containing 20 water molecules, and six large cavities ($5^{12}6^2$), each composed of 12 pentagonal and 2 hexagonal faces and containing 26 water molecules. By way of illustration, the creation of structure I is expedited through the utilization of light gases and small molecules such as CH_4, C_2H_6, and CO_2.[1,3] Mak and McMullan's studies in 1965 on the phenomenon of X-ray diffraction caused by the creation of hydrogen sulfide hydrate led to the discovery of the structure of type II or sII hydrates.[4]

It should be noted that structure II (sII) contains two different types of cavities, including 12 pentagonal plates (5^{12}) and 8 large cavities, including 12 pentagonal plates and 4 hexagonal plates ($5^{12}6^4$) with 136 water molecules.[1,5] The third crystallographic hydrate structure (sH structure) was found by Ripmeester and co-worker in 1987,[6] which is a hexagonal structure that, unlike the previous two structures, requires large and small molecules for stability. Structure H is composed of

Received: January 15, 2025
Revised: August 14, 2025
Accepted: August 28, 2025

three distinct categories of cavities (3 small cavities, 2 medium cavities, and 1 large cavity) with 34 water molecules. It is noteworthy to specify that structure H gas hydrate is generated with larger molecules such as cyclohexane in the presence of smaller molecules such as nitrogen and methane.[5,7]

In underground reservoirs, natural gas and crude oil are generally in contact with water. During oil and gas production, gas hydrate formation may occur under favorable conditions such as low temperature and high pressure. While gas hydrates have been investigated for potential applications such as energy storage, transportation, and gas separation, their primary commercial significance currently lies in two areas: preventing hydrate formation in oil and gas production systems, and dissociating naturally occurring hydrates as a source of methane. These broader applications remain largely at the research stage and require further technological development.[1,8−12] It should be noted that the existence of water molecules, light hydrocarbons, and favorable thermodynamic circumstances improve the development of gas hydrate.[13−15]

In this review, all critical published data on the subject were comprehensively summarized, providing clear insights into thermodynamic inhibitors and their application in gas hydrate prevention. The review incorporates over 200 equilibrium measurements, which were gathered from multiple sources and span a wide range of gases and inhibitor types. This compilation of data serves as a comprehensive database for understanding hydrate behavior under different conditions. For comparison, the work presented here is aligned with recent databases, such as the one constructed by Zhu, which provides a similarly extensive set of equilibrium data for industrially relevant systems.[16] The findings of this research assist in selecting the most efficient inhibitors based on operational parameters and offer a foundation for further innovation in the field. The first part of the review discusses various methods to prevent gas hydrate formation, while the second part categorizes and describes different types of thermodynamic inhibitors, including amino acids, salts, ionic liquids (ILs), and commercial inhibitors. The third part highlights critical research on thermodynamic inhibitors, focusing on key parameters such as inhibitor type, concentration, and environmental conditions. Additionally, this study introduces advanced machine learning models (MLM) used to predict hydrate formation temperature (HFT) and pressure with high accuracy. These models complement experimental findings by enabling precise and efficient inhibitor selection based on specific operational needs. The integration of experimental and predictive modeling insights paves the way for researchers to develop new thermodynamic inhibitors with enhanced performance while also optimizing their application in industrial scenarios. This combined approach provides a robust framework for advancing hydrate management strategies in oil and gas operations.

In this study, several novel contributions to the field of gas hydrate inhibition are introduced. The research explores the integration of new inhibitors, including amino acids, ionic liquids, salts, and commercial inhibitors, showing how their combinations enhance inhibition effectiveness, improving safety and efficiency in natural gas transport. One of the innovative aspects of this research is the investigation of the synergistic effect observed between commercial inhibitors and salts, which, through the analysis of a wide range of experimental data, introduces an optimal combination of these materials that could serve as a solution for the industry. Additionally, the use of machine learning models allows for more accurate prediction of hydrate formation conditions, optimizing inhibitor selection. The study also presents new insights into the mechanisms of inhibition, particularly the effectiveness of hydroxyl-functionalized ionic liquids with shorter alkyl chains. Furthermore, unlike previous studies, this research comprehensively examines all categories of thermodynamic inhibitors, offering a complete approach that could open new doors for researchers and industry professionals in the future. Finally, the research offers environmentally friendly and cost-effective alternatives to traditional inhibitors, contributing to more sustainable solutions for hydrate prevention in industrial applications.

2. METHODS OF PREVENTING GAS HYDRATE FORMATION

Gas hydrate formation can be prevented using various methods, including pressure control, temperature regulation, water removal, mechanical cleaning, and chemical inhibitors. Pressure control involves maintaining the pressure below hydrate formation levels, though this is often impractical due to operational requirements.[7,17] Temperature control employs pipeline insulation and heating systems to keep fluids above hydrate formation temperatures but is costly in cold environments and risks pipeline damage from hydrate decomposition.[15,18,19] Removing water from fluids effectively hinders hydrate formation, though it fails if water is dissolved in oil or gas.[19] Mechanical cleaning, or pigging, uses scrapers to clear hydrates and debris from pipelines, maintaining production efficiency but increasing labor and equipment maintenance costs.[15,20] Lastly, chemical inhibitors are widely used to alter hydrate formation kinetics or phase equilibria, making them an effective and commonly preferred method.

3. TYPES OF INHIBITORS

Chemical inhibitors are essential for preventing or delaying hydrate formation in gas transmission lines and are categorized into low-dosage hydrate inhibitors (LDHIs) and thermodynamic hydrate inhibitors (THIs). LDHIs are effective at low concentrations and include antiagglomerates (AAs) and kinetic hydrate inhibitors (KHIs). AAs, as surfactants, prevent hydrate crystals from merging by dispersing hydrate particles into the liquid phase, forming a transportable slurry that helps avoid pipeline blockages. KHIs, on the other hand, are water-soluble polymers that delay hydrate nucleation and/or growth by extending the induction time. Despite their efficiency, LDHIs face limitations in high-pressure or low-temperature conditions and depend on factors like wellhead temperature, water salinity, and the availability of condensates.[15,18,21,22] THIs, such as methanol and monoethylene glycol (MEG), are widely used to suppress hydrate formation by shifting the hydrate phase boundary to higher pressures and lower temperatures. This shift occurs because these inhibitors interact with the hydrogen bonding network of water molecules. By disrupting the ability of water molecules to form strong hydrogen bonds, THIs effectively compress the hydrate stability zone. This compression prevents hydrate formation under typical conditions and facilitates the removal of existing blockages. As a result, hydrate formation is delayed, and the risk of blockage in pipelines is reduced, allowing for safer and more efficient operations in the oil and gas industry. While alcohols and glycols like methanol and MEG are highly effective

https://doi.org/10.1021/acs.jced.5c00025
J. Chem. Eng. Data XXXX, XXX, XXX−XXX

inhibitors, with methanol typically ranking as the most effective in most applications, other inhibitors, such as diethylene glycol (DEG) and triethylene glycol (TEG), are less efficient and are primarily used for dehydration purposes.[15,18,21,23,24] Within their respective categories, alcohols and glycols tend to be the most effective, followed by ionic liquids and salts, which show moderate efficacy in shifting the equilibrium curve. The least effective inhibitors include certain amines and heavier glycols. Figure 1 illustrates the equilibrium diagram for hydrate

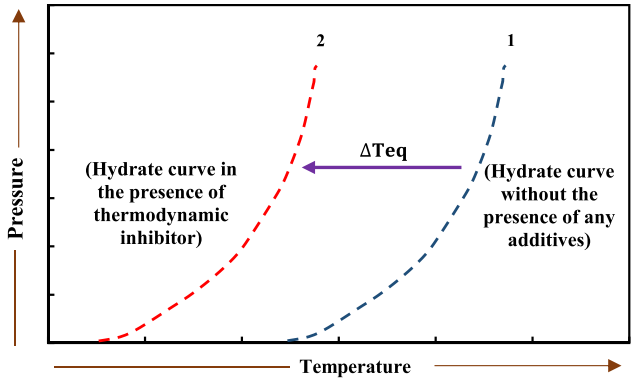

Figure 1. Schematic of the thermodynamic behavior of hydrate in the existence and absence of inhibitor.

formation with and without thermodynamic inhibitors. The addition of thermodynamic inhibitors shifts the equilibrium curve to lower temperatures, expanding the safe zone for nonhydrate formation and effectively preventing hydrates. This suppression, represented by ΔT_{eq}, depends on factors such as gas composition, the type and amount of inhibitor used. Different thermodynamic inhibitors have unique effects on hydrate formation, requiring careful selection based on specific conditions. The choice of inhibitor also depends on the intended use of the production fluid. For example, methanol may not be ideal for liquefied natural gas (LNG) feed due to its potential effects on cryogenic processes, whereas it is commonly used in gas pipeline networks to prevent hydrate formation. The impact of the selected inhibitor varies depending on the specific type employed and the application.[25] This suggests that each inhibitor type should be carefully considered for its unique effects. The following sections present the results of studies on various kinds of hydrates and the impact of inhibitors on their hydrate formation conditions.

In this review, we explore novel research findings that significantly advance our understanding of gas hydrate inhibition. A key contribution of this study is the combination of various inhibitors, including amino acids, ionic liquids, salts, and commercial inhibitors such as alcohols and glycols, as well as their synergistic effects when used together. This novel approach, which integrates traditional and newer types of inhibitors, has shown that the synergy between amino acids and ionic liquids offers a more efficient and environmentally friendly method to inhibit hydrate formation under extreme temperature and pressure conditions. Furthermore, this study highlights the use of machine learning models to predict hydrate formation conditions with significantly greater accuracy compared to traditional experimental methods. These models not only enhance the prediction of hydrate formation pressure (HFP) and temperature but also optimize the selection of inhibitors, making them a valuable tool in the field of hydrate management. Figure 2 provides a schematic overview of the research methodology, including the classification of thermodynamic inhibitors (such as amino acids, ionic liquids, salts, and commercial inhibitors) and the machine learning models employed. The flowchart highlights the data gathering process for hydrate formation conditions (temperature and pressure), followed by performance evaluation of inhibitors and prediction of hydrate formation using various machine learning models.

4. RESEARCH FINDINGS

The inhibitors that operate based on thermodynamics can be classified into five distinct categories of inhibitors, which encompass amino acids, ionic liquids, salts, commercial inhibitors (such as alcohols and glycols), and a blend of commercial inhibitors and salts. The present study highlights the inhibitory effect of salts as an inhibitor separately, given

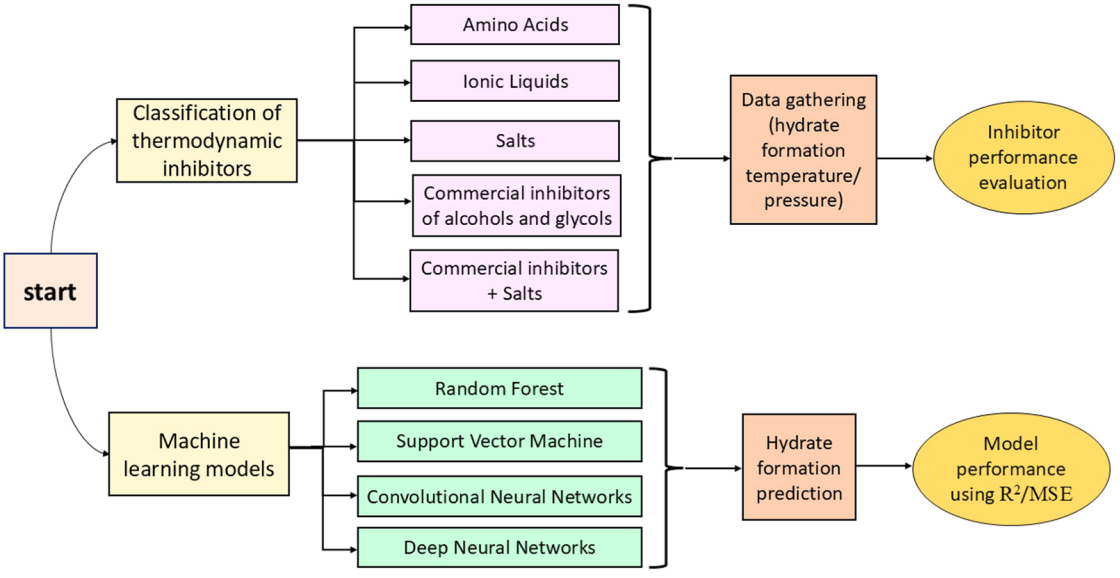

Figure 2. Schematic of the workflow for thermodynamic inhibitor classification and machine learning-based hydrate formation prediction.

https://doi.org/10.1021/acs.jced.5c00025
J. Chem. Eng. Data XXXX, XXX, XXX−XXX

that salts typically exist in the brine of pipelines. Subsequently, we assessed the impact of the presence of salts in combination with commercial inhibitors such as ethanol and glycols on the inhibition conditions of gas hydrates.

4.1. Amino Acids. It has been proposed that naturally occurring amino acids possess the ability to act as potential agents for suppressing the formation of gas hydrates.[26] This is owing to their capacity to elicit potent electrical charges and electrostatic interactions with water in the form of zwitterions, as well as their capability to intermingle strongly with water particles through robust hydrogen bonds by virtue of their hydrophilic nature. Consequently, they demonstrate excellent inhibitory properties. The interaction of amino acids and water molecules through electrostatic forces serves to diminish the crystalline formation akin to ice in water particles that are bound through hydrogen bond, which results in a negative cohesion between them.[27−29]

Sa et al. investigated the use of hydrophobic amino acids, including glycine ($C_2H_5NO_2$), alanine ($C_3H_7NO_2$), and valine ($C_5H_{11}NO_2$), as thermodynamic at concentrations of 0.42−16.74 wt % to prevent CO_2 hydrate formation in the temperature range of 273.05−281.45 K and pressures from 14.1 to 35.2 bar.[30] The study found that factors such as water history, additive quantity, and amino acid side chain properties influenced the inhibition efficiency, with valine, alanine, and glycine showing the most effective inhibition in that order.

Sa et al. studied the impact of amino acids, including proline ($C_5H_9NO_2$), serine ($C_3H_7NO_3$), alanine, and glycine, on CH_4 and natural gas hydrate formation.[31] The results showed that amino acids acted as thermodynamic inhibitors, enabling hydrate formation under high pressure and low temperature. The inhibition effect was directly related to the inhibitor concentration, with proline, serine, alanine, and glycine showing varying degrees of temperature reduction at 7.77 wt %. The influence of amino acid injection on hydrate creation condition in the H_2O-CO_2 system was investigated by Roosta et al.[32] The amino acid studied were histidine ($C_6H_9N_3O_2$), proline, serine, threonine ($C_4H_9NO_3$), and glutamine ($C_5H_{10}N_2O_3$), with concentrations ranging from 0.5 to 2 wt %.[32] The findings of the study discovered that the reduction in the growth rate of hydrates followed a decreasing trend in the sequence of $C_6H_9N_3O_2 > C_5H_9NO_2 \sim C_3H_7NO_3 \sim C_4H_9NO_3 > C_5H_{10}N_2O_3$. Furthermore, there was a noticeable increase in the extent of inhibition observed at higher concentrations.

Bavoh et al. undertook a study on the impact of amino acid injection, encompassing glycine, alanine, proline, serine, and arginine ($C_6H_{14}N_4O_2$) with concentrations ranging from 5 to 20 wt %, on CO_2 hydrate.[33] Their investigation demonstrated that the inhibition influence of amino acids followed the order of $C_2H_5NO_2 > C_3H_7NO_2 > C_5H_9NO_2 > C_3H_7NO_3 > C_6H_{14}N_4O_2$, respectively. Furthermore, the most significant decrease in temperature was observed for glycine with a concentration of 10 wt %, wherein the temperature drop was 1.83 K. It has been ascertained that an escalation in glycine concentration results in a corresponding elevation in its inhibitory impact. Bavoh et al. executed a study to examine the thermodynamic impact of five different amino acids, present in concentrations of 5−20 wt %, on the phase equilibrium state of CH_4 hydrate, using pressure and temperature scope of 3.86−9.98 MPa and 276.5−286 K, respectively.[34] The results of this study suggest that glycine exhibits optimal inhibitory performance, as evidenced by its ability to lower the equilibrium temperature by 1.78 K at a concentration of 10 wt %. The experimental results demonstrate a particular order in which amino acids inhibit CH_4 hydrate at a concentration of 10 wt %. Specifically, the inhibition influence follows the sequence: $C_2H_5NO_2 > C_3H_7NO_2 > C_5H_9NO_2 > C_3H_7NO_3 > C_6H_{14}N_4O_2$. Mannar et al. studied the thermodynamic inhibitory effects of lysine ($C_6H_{14}N_2O_2$) on CH_4 and CO_2 hydrates at concentrations of 5 and 10 wt % under pressures of 1.87−10.45 MPa and temperatures of 276.45−285.15 K.[35] The results showed that lysine effectively shifted the equilibrium to lower temperatures and higher pressures, with a greater inhibitory effect on CO_2 hydrate formation, enhancing the equilibrium temperature by 1.44 K for CH_4 and 1.49 K for CO_2 at 10 wt %.

Bavoh et al. surveyed the thermodynamic effect of four amino acids, including L-valine, L-threonine, L-asparagine ($C_4H_8N_2O_3$), and L-phenylalanine ($C_9H_{11}NO_2$) at concentrations of 1 and 5 wt % on CH_4 hydrate, in the 3.52−10.25 MPa pressure range and 275.71−286.10 K temperature range.[36] Their research has shown that the presence of L-valine amino acid at a concentration of 5 wt % is capable of acting as the most influential inhibitor by reducing the equilibrium temperature to 0.529 K. Furthermore, it has been noted that the inhibitory influence of amino acids in decreasing the equilibria temperature of CH_4 hydrate creation at a concentration of 5 wt % follows the order of $C_9H_{11}NO_2 < C_4H_8N_2O_3 < C_4H_9NO_3 < C_5H_{11}NO_2$, respectively. Long et al. studied CH_4 hydrate equilibrium using the pressure-search method with isochoric step-heating at pressures of 4.78−12.20 MPa and temperatures of 273.3−287.8 K.[37] They examined the synergistic effect of ethylene glycol and glycine inhibitors at concentrations of 1−30 wt %. The results showed that the combination of glycine and ethylene glycol reduced the temperature of CH_4 hydrate formation, with the most effective inhibitors being ethylene glycol, followed by ethylene glycol−glycine mixtures and glycine alone. These findings suggest that glycine, as a synergist, has significant potential for industrial applications, particularly in oil/gas transfer and flow safety.

Lee et al. evaluated the thermodynamic inhibition of CH_4 hydrate by glycine, alanine, and methanol at concentrations of approximately 11.41, 13.26, and 5.21 wt %, respectively.[38] The study showed that these inhibitors shifted the equilibrium toward lower temperatures or higher pressures, with inhibition potency following the order: alanine < glycine < methanol.

Qureshi et al. studied the thermodynamic inhibition of CH_4 hydrate by glycine, L-alanine, histidine, and conventional inhibitors like methanol, ethylene glycol, and sodium chloride at 1−2 wt % concentrations and 4−12 MPa pressures.[39] The results showed that amino acids enhanced the inhibition potency of commercial inhibitors, with glycine demonstrating the best performance when combined with classical inhibitors.

Qureshi et al. investigated the impact of water fractions and L-proline on methane hydrate equilibrium under pressures of 4−12 MPa.[40] Their results showed that water fraction had minimal effect on equilibrium, but L-proline (5 wt %) shifted the equilibrium by 0.9−1.3 °C at 4 MPa and 0.4−0.8 °C at 6 MPa, with higher water fractions enhancing inhibition slightly. Moreover, the inhibition potency of L-proline was greater than alanine and glycine, following the order: glycine > alanine > proline.

Bharathi et al. studied the synergistic effect of glycine and monoethylene glycol (MEG) on CO_2 hydrate inhibition using the T-cycle method at pressures of 2−4 MPa and temperatures of 274.70−282.55 K.[41] The results showed that all systems

https://doi.org/10.1021/acs.jced.5c00025
J. Chem. Eng. Data XXXX, XXX, XXX−XXX

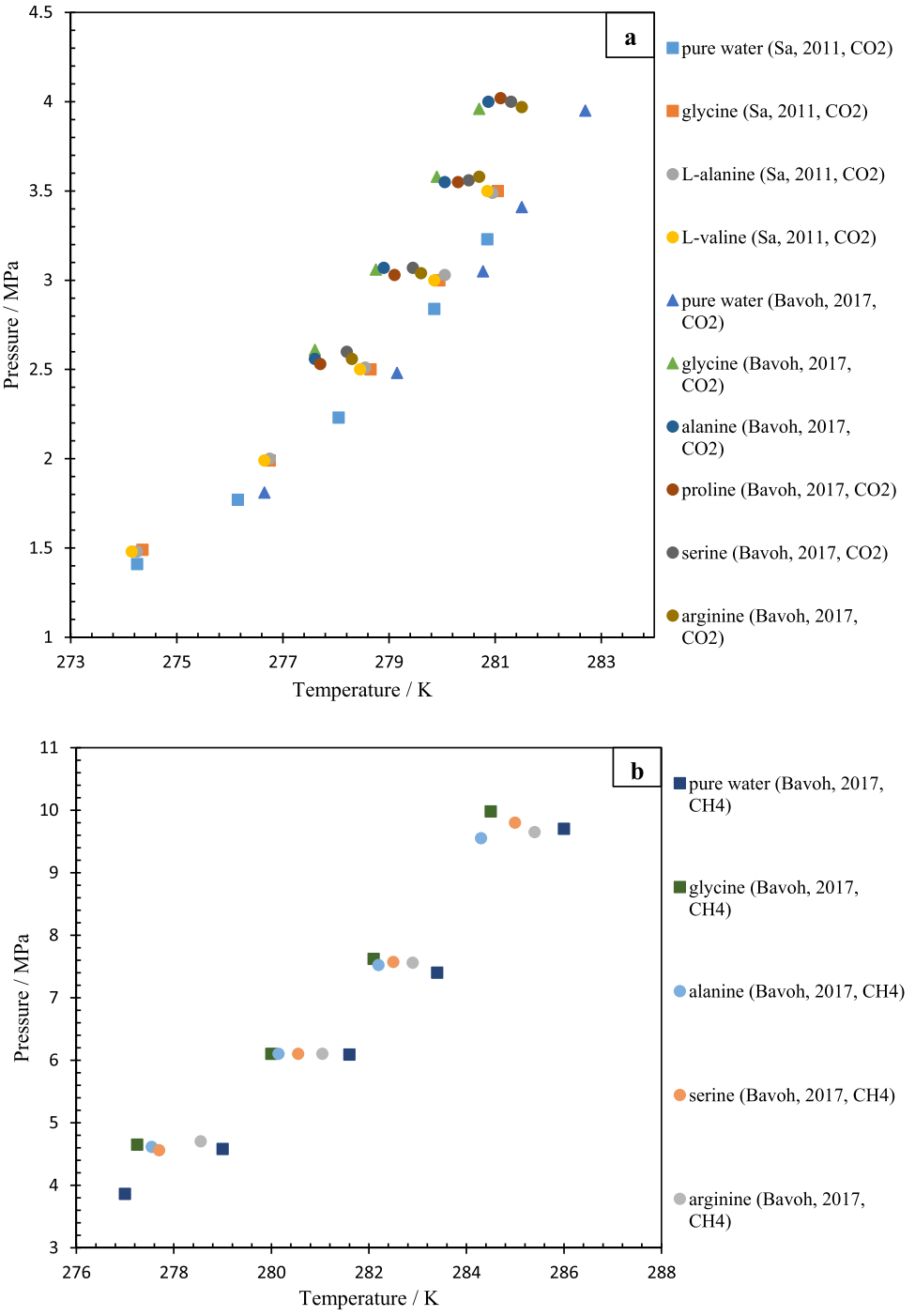

Figure 3. Comparison between the equilibrium diagram of various gas hydrates in the presence of various inhibitors. (a) CO_2 gas with glycine, alanine, and valine additives,[30] and CO_2 gas with glycine, alanine, proline, serine, and arginine additives;[33] (b): CH_4 gas and glycine, alanine, proline, serine, and arginine additives.[34]

shifted the CO_2 hydrate equilibrium to lower temperatures, with the inhibition potency following the order: 15 wt % MEG + 15 wt % glycine > 10 wt % MEG + 10 wt % glycine > 5 wt % MEG + 5 wt % glycine. The combination of MEG and glycine exhibited superior inhibition, making glycine a suitable synergist for industrial use.

Figure 3a,b exhibits the diagram of equilibrium for CH_4 and CO_2 hydrate in the existence of various amino acids. The laboratory data of Sa et al. research is employed to depict the CO_2 hydrate equilibria diagram in the existence of 0.5 mol % amino acids glycine, alanine, and valine.[30] Similarly, the equilibrium diagram of CH_4 hydrate and CO_2 is drawn for the research of Bavoh et al. with the existence of glycine, alanine, proline, serine, and arginine inhibitors having a concentration of 10 wt %.[33,34] It is noteworthy to mention that glycine is the weakest inhibitor when the concentration of inhibitors is based on molar percentage, as demonstrated in Figure 3. However, a change in the concentration unit to weight percentage highlights that glycine manifests better performance than other amino acids in hydrate inhibition.

It can be inferred from the outcomes of the conducted research that multiple factors, inclusive of the concentration of

https://doi.org/10.1021/acs.jced.5c00025
J. Chem. Eng. Data XXXX, XXX, XXX−XXX

Table 1. Research Studies on the Subject of Gas Hydrate Formation in the Presence of Amino Acids

author (publication date)	gas	type of thermodynamic inhibitor	concentration of inhibitors (wt %)	T/K	P/MPa	result	ref
Sa et al. (2011)	CO_2	$C_2H_5NO_2$	0.415, 2.051, 5.202, 8.568, 11.414	273.05−281.45	1.41−3.52	$C_5H_{11}NO_2 > C_3H_7NO_2 > C_2H_5NO_2$	30
		$C_3H_7NO_2$	0.492, 2.424, 6.114, 10.008, 13.263				
		$C_5H_{11}NO_2$	0.647, 3.164, 7.887, 12.758, 16.741				
Sa et al. (2016)	CH_4	$C_2H_5NO_2$	2.051, 5.202, 8.568, 11.414	274.65−285.15	3−9	$C_5H_9NO_2 > C_3H_7NO_3 > C_3H_7NO_2 > C_2H_5NO_2$	31
		$C_3H_7NO_2$,	2.424, 6.114, 10.008, 13.263				
	NG	$C_5H_9NO_2$	3.111, 7.762, 12.566, 16.5	276.15−287.95	1−4		
		$C_3H_7NO_3$	2.847, 7.133, 11.597, 15.281				
Roosta et al. (2016)	CO_2	$C_6H_9N_3O_2$, $C_5H_9NO_2$, $C_3H_7NO_3$, $C_4H_9NO_3$, $C_5H_{10}N_2O_3$	0.5, 1, 1.5, 2	275.15−285.15	1.58−3	$C_6H_9N_3O_2 > C_5H_9NO_2 \sim C_3H_7NO_3 \sim C_4H_9NO_3 > C_5H_{10}N_2O_3$	32
Bavoh et al. (2017)	CO_2	$C_2H_5NO_2$, $C_5H_9NO_2$, $C_3H_7NO_3$, $C_3H_7NO_2$, $C_6H_{14}N_4O_2$	5, 10, 15, 20	279.15−282.70	2.53−4	$C_2H_5NO_2 > C_3H_7NO_2 > C_5H_9NO_2 > C_3H_7NO_3 > C_6H_{14}N_4O_2$	33
Bavoh et al. (2017)	CH_4	$C_2H_5NO_2$, $C_5H_9NO_2$, $C_3H_7NO_3$, $C_3H_7NO_2$, $C_6H_{14}N_4O_2$	5, 10, 15, 20	279.15−282.70	2.53−4	$C_2H_5NO_2 > C_3H_7NO_2 > C_5H_9NO_2 > C_3H_7NO_3 > C_6H_{14}N_4O_2$	34
Mannar et al. (2017)	CH_4	$C_6H_{14}N_2O_2$	5, 10	279−286	4.58−9.70	the inhibitory impact of lysine on CO_2 hydrate is greater than that on CH_4 hydrate	35
	CO_2			276.65−282.70	1.87−3.78		
Bavoh et al. (2018)	CH_4	$C_5H_{11}NO_2$, $C_4H_9NO_3$, $C_4H_8N_2O_3$, $C_9H_{11}NO_2$	1, 5	275.71−286.10	3.52−10.25	$C_5H_{11}NO_2 > C_4H_9NO_3 > C_4H_8N_2O_3 > C_9H_{11}NO_2$	36
Long et al. (2018)	CH_4	$C_2H_6O_2$, $C_2H_5NO_2$	0.5 MEG + 0.5 glycine, 2.5 MEG + 2.5 glycine, 5 MEG + 5 glycine, 10 MEG + 10 glycine, 15 MEG + 15 glycine	273.3−287.8	4.78−12.20	glycine could act as a suitable inhibitor synergist	37
Lee et al. (2019)	CH_4	$C_2H_5NO_2$	11.41	273.4−283.3	3.22−9.35	$CH_3OH > C_2H_5NO_2 > C_3H_7NO_2$	38
		$C_3H_7NO_2$	13.26				
		CH_3OH	5.21				
Qureshi et al. (2020)	CH_4	$C_2H_5NO_2$, $C_3H_7NO_2$, $C_6H_9N_3O_2$, CH_3OH, $C_2H_6O_2$, NaCl	1, 2	277.15−287.15	4−12	glycine presented the best inhibition performance along with classical inhibitors	39
Qureshi et al. (2021)	CH_4	$C_2H_5NO_2$, $C_2H_5NO_2$, $C_5H_9NO_2$	5	276.53−287.12	4−12	$C_2H_5NO_2 > C_2H_5NO_2 > C_5H_9NO_2$	40
Bharathi et al. (2021)	CO_2	$C_2H_6O_2$, $C_2H_5NO_2$	5 glycine + 5 MEG, 10 glycine + 10 MEG, 15 glycine + 15 MEG	274.70−282.55	2−2	as the inhibitor concentration increases, the inhibitory power increases; glycine could act as a suitable inhibitor synergist	41

https://doi.org/10.1021/acs.jced.5c00025
J. Chem. Eng. Data XXXX, XXX, XXX−XXX

additives, concentration unit of inhibitors, length, and the nature of the side chains of amino acids, have a substantial impact on the inhibitory properties. It is possible to make the claim that an elevation in the level of amino acids results in a significant enhancement of their inhibitory impacts. Additionally, the equilibrium diagram of gas hydrates has undergone a change in the direction of areas featuring lower temperatures and greater pressures. Furthermore, in the scenario of the unit of amino acid concentration, wherein the molar percentage serves as the unit of inhibitors, the amino acids having a higher molecular weight (i.e., longer side chain length) exhibit a greater inhibitory potential, whereas the employment of the inhibitor concentration unit as a weight percentage indicates that amino acids with a lower molecular weight (i.e., shorter side chain lengths) exhibit more pronounced inhibition effects. Nevertheless, weight percentage is a more prevalent approach in centralized industrial research owing to its proximity to practical applications. Consequently, glycine can be identified as the most effective thermodynamic inhibitor among amino acids based on weight percentage. It is also remarkable that glycine can serve as a fitting synergist in augmenting the thermodynamic inhibitory potential of commercial inhibitors, such as methanol. Regarding the molecular stability of amino acids, they generally exhibit good chemical stability under a wide range of pressures and temperatures typically encountered in oil and gas production. In terms of regenerability, amino acids like glycine and alanine may retain their inhibitory properties even after repeated exposure to hydrate formation conditions, though the extent of regeneration can vary depending on the concentration and specific environmental factors. This makes amino acids a potentially more sustainable option compared to single-use commercial inhibitors.[42] A comprehensive summary of the studies conducted in the domain of gas hydrates in the existence of amino acids is shown in Table 1. To summarize, the key findings in the field of amino acids are as follows:

- Amino acids possess strong potential as inhibitors of gas hydrate formation due to their ability to interact with water molecules through electrostatic forces and hydrogen bonding.
- Studies show that amino acids such as glycine, alanine, and valine demonstrate varying levels of inhibition, with glycine showing the most effective inhibition in the context of CO_2 hydrate formation.
- The concentration of amino acids directly influences their effectiveness, with higher concentrations leading to greater inhibitory effects.
- Inhibitory potency follows a specific sequence, with glycine being the most effective, followed by alanine and valine.
- Amino acids such as glycine and alanine have demonstrated superior performance when compared to other inhibitors, particularly in terms of shifting the equilibrium temperature and pressure.
- The change in concentration units from molar to weight percentage alters the performance ranking, with glycine exhibiting superior performance when expressed in weight percentage.
- The molecular weight and the length of the amino acid side chains have a significant impact on their inhibitory effects, with shorter chain amino acids showing better inhibition when the concentration is given in weight percentage.
- Amino acids such as glycine can enhance the thermodynamic inhibition effects of commercial inhibitors like methanol, highlighting their synergistic potential.
- Amino acids generally exhibit good molecular stability under typical oil and gas production conditions, making them potentially more sustainable options compared to single-use inhibitors.

4.2. Ionic Liquids (ILs). Ionic liquids (ILs), which are compounds consisting of cations and anions, bear similarities to salts and are characterized by their liquid state at room temperature. These distinctive materials have garnered much attention due to their exceptional properties, including zero volatility, thermal stability, low vapor pressure, electric conductivity, and dual functionality in gas hydrate inhibition. Owing to these unique properties, ILs have become prevalent in a myriad of applications, particularly in preventing the creation of gas hydrates. While ILs are effective for hydrate inhibition, it is important to note that their separation and recovery can be achieved in certain cases, depending on the specific type of IL and the operational conditions. For example, some ILs are recoverable and reusable, though the process may require additional steps to purify and regenerate them. Regarding solubility, while some ionic liquids are water-soluble, others may have limited solubility depending on their chemical structure, specifically the cation and anion components.[43] It is noteworthy that the ability of ILs to impede thermodynamic activity can be attributed to their competence in generating hydrogen bonds with unbound water molecules.[26,44] The impact of ILs on thermodynamic inhibition depends on their cations, anions, and concentration. Similar to other thermodynamic inhibitors, increasing the concentration of ILs shifts the hydrate equilibrium curve to lower temperatures, enhancing their inhibitory effect. Furthermore, the efficacy of ILs tends to decrease with the elongation of their alkyl chains.[14]

Li et al. executed an inquiry pertaining to the compulsory circumstances for the creation of equilibria hydrates of CH_4 in the existence of dialkyl imidazolium-based ionic liquids and tetraalkylammonium-based ionic liquids.[45] The dialkyl imidazolium-based ionic liquids which were utilized in the study comprised 1,3-dimethyl-imidazolium iodide ([MMIM]-I), 1-ethyl-3-methyl-imidazolium iodide ([EMIM]-I), and 1-hydroxyethyl-3-methyl-imidazolium chloride ([OH-C_2MIM]-Cl). The tetraalkylammonium-based ionic liquids examined were tetramethylammonium chloride ([$N_{1,1,1,1}$]-Cl) and hydroxyethyl-trimethylammonium chloride ([$N_{1,1,1,eOH}$]-Cl). The isochoric approach was applied to determine the data in the pressure scope of 3−17 MPa and the temperature scope of 276.15−289.15 K. Based on the experimental results, it was detected that the incorporation of ionic liquids induces a modification in the equilibria phase frontier of CH_4 hydrate, leading to conditions of temperature and pressure that are unsuitable for hydrate creation. Furthermore, it can be posited that the hydroxyl-functionalization of the cation in dialkyl imidazolium-based ionic liquids improves their inhibition effectiveness. Specifically, it has been observed that ionic liquids containing shorter alkyl groups are more operative in inhibiting the formation of hydrates than those with longer alkyl groups. When considering tetraalkylammonium-based

https://doi.org/10.1021/acs.jced.5c00025
J. Chem. Eng. Data XXXX, XXX, XXX−XXX

ionic liquids, it has been noted that those with shorter alkyl groups exhibit superior thermodynamic inhibition effects when compared to those containing hydroxylated longer alkyl groups of the cations. Ultimately, it has been determined that $[N_{1,1,1,1}]$-Cl is the most efficacious thermodynamic inhibitor among all of the studied ionic liquids. In the scientific study conducted by Tumba and colleagues, the impact of an aqueous solution comprising an ionic liquid called tributyl-methyl phosphonium methylsulfate ($[3C_4C_1P][MeSO_4]$) on the equilibrium state of CO_2 and CH_4 clathrate hydrates was investigated.[46] The dissociation conditions of hydrates were determined through the utilization of the isochoric pressure-search method for two distinct systems, namely, carbon dioxide + tributyl-methyl phosphonium methylsulfate + water and methane + tributyl-methyl phosphonium methylsulfate + water. The temperature ranges considered in this study were 273.5−282.2 K, while the pressures differed between 4.35 and 14.77 MPa. Additionally, the mass fractions of tributyl-methyl phosphonium methylsulfate utilized in the system were 0, 0.2611, and 0.5007. The study's outcomes imply that the existence of tributyl-methyl phosphonium methylsulfate retards the development of clathrate hydrates of CO_2 and CH_4, unlike their formation in its nonexistence.

Keshavarz et al. performed an experiment to determine the conditions at which CH_4 hydrate dissociates.[47] They tested this in the presence of pure water and different aqueous solutions. These solutions included 1-butyl-3-methylimidazolium tetrafluoroborate (BMIM-BF_4) at 10, 15, and 20 wt %, 1-butyl-3-methylimidazolium dicyanamide (BMIM-$N(CN)_2$) at 10 wt %, and tetraethylammonium chloride ($N_{2,2,2,2}$-Cl) at 10 wt %. Experimental measurements were conducted over a range of pressures spanning from 2.48 to 6.58 MPa and temperatures ranging from 272.1 to 282.0 K. The experimental procedure involved the use of a high-pressure balance enclosure and the application of the isochoric pressure examination technique. The researchers noted that when using BMIM-BF_4 with a concentration of 10 wt %, the dissociation circumstances of CH_4 hydrate at pressures between 2.5 and 7.0 MPa occurred at a slightly lower temperature of around 1 K. On the other hand, the temperature was found to be around 1.5 K for the same aqueous solution with a concentration of 0.2 mass fraction. Hence, it can be deduced that an escalation in the concentration of BMIM-BF_4 in aqueous medium results in a corresponding increase in the inhibitory impacts of this ionic liquid for methane hydrate. Furthermore, the findings suggest that the inhibitory effect of tetraalkylammonium-based ionic liquid on the formation of CH_4 hydrate typically diminishes as the length of the alkyl chain rises. Zare et al. conducted a comprehensive study to investigate the conditions under which CH_4 hydrate dissociates in the existence of different imidazolium-based aqueous ionic liquid solutions.[48] These solutions included 1-butyl-3-methylimidazolium methylsulfate ($[BMIM][MeSO_4]$), 1-ethyl-3-methylimidazolium hydrogen sulfate ($[EMIM][HSO_4]$), 1-ethyl-3-methylimidazolium ethyl sulfate ($[EMIM][EtSO_4]$), ($[BMIM][BF_4]$), and 1-(2-hydroxyethyl)-3-methylimidazolium tetrafluoroborate ([OH-EMIM]-$[BF_4]$). Concentrations of 1-ethyl-3-methylimidazolium ethyl sulfate ($[EMIM][EtSO_4]$) in the aqueous phase are 8 and 10 wt %. Also, the thermodynamic inhibition influences of the other mentioned ionic liquids with 10 wt % concentration are studied. The isochoric methodology was employed to obtain experimental data at a temperature and pressure scope of 281.9−287.4 K and 7.08−12.16 MPa, respectively. The ionic liquids under investigation displayed a thermodynamic inhibition behavior on CH_4 hydrate, thereby leading to a displacement of the hydrate balance separation circumstances to greater pressures and lesser temperatures. Notably, [OH-EMIM][BF_4] possess the highest level of efficiency as a thermodynamic inhibitor. The thermodynamic inhibitory properties of $[EMIM][HSO_4]$ and $[BMIM][MeSO_4]$ were found to be more practical compared with $[EMIM][EtSO_4]$ among the ionic liquids containing alkyl sulfate. Richard et al. investigated the effectiveness of 1-ethyl-3-methylimidazolium chloride (EMIM-Cl) in preventing the creation of CH_4 hydrate at both low and high concentrations of ionic liquid. They carried out their experiments under pressure conditions ranging from 10 to 20 MPa.[49] Experiments were conducted to examine the potential synergetic effects of assorted ionic liquid and orthodox inhibitors, including NaCl and MEG, and a combination of two ionic liquids, EMIM-Cl and 1-ethyl-3-methylimidazolium bromide (EMIM-Br), on CH_4 hydrate dissociation conditions. The separation circumstances of CH_4 hydrate in the existence of EMIM-Cl at concentrations of 5, 20, 30, and 40 wt % were measured at pressures of roughly 10, 15, and 20 MPa. The detachment circumstances of CH_4 hydrate were systematically measured in the presence of mixed solution containing EMIM-Cl and MEG using a 1:1 mixture at concentrations of 10 wt % (5 wt % EMIM-Cl + 5 wt % MEG), 20 wt % (10 wt % EMIM-Cl + 10 wt % MEG), and 30 wt % (15 wt % EMIM-Cl + 15 wt % MEG). Measurements are also accomplished on a mixture of 5 wt % EMIM-Cl + 5 wt % NaCl and a mixture of two ILs, i.e., 10 wt % EMIM-Cl + 10 wt % EMIM-Br. It has been observed that solutions composed of solely the EMIM-Cl component display a gradual escalation in their inhibitory effect as their concentration increases. This effect has the potential to exceed the efficiency of MEG at high levels of concentration. While combinations of EMIM-Cl and MEG do not exhibit any synergetic properties at low pressures as far as thermodynamic inhibition performance is concerned, higher pressures do elicit such effects. Moreover, there is a synergistic effect observed when EMIM-Cl and EMIM-Br are mixed together at higher pressures. Inhibitors that contain EMIM-Cl or EMIM-Br, as opposed to MEG or NaCl, exhibit a growth in their inhibition efficacy as pressure rises.

Sabil et al. studied an inquiry on the decomposition temperature of CH_4 hydrate in the existence of nine aqueous solutions of ionic liquid under different pressure conditions, spanning from 3.6 to 11.2 MPa.[50] The aqueous ionic liquid solutions were thoroughly analyzed while maintaining a mass fraction of 0.10. The ILs used were 1-butyl-3-methylimidazolium methylsulfate $[BMIM][CH_3SO_4]$, 1-butyl-3-methylimidazolium hydrogen sulfate $[BMIM][HSO_4]$, 1-butyl-3-methylimidazolium trifluoromethanesulfonate $[BMIM][CF_3SO_3]$, 1-butyl-3-methylimidazolium dicyanamide $[BMIM][N(CN)_2]$, 1-butyl-3-methylimidazolium chloride [BMIM][Cl], 1-butyl-3-methylimidazolium bromide [BMIM][Br], 1-butyl-3-methylimidazolium perchlorate $[BMIM][ClO_4]$, 1-(2-hydroxyethyl) 3-methylimidazolium chloride [OH-EMIM][Cl], and 1-(2-hydroxyethyl) 3-methylimidazolium bromide [OH-EMIM]-[Br]. The discovery was made that the ILs have the ability to transfer the equilibria diagram of methane hydrate (liquid + vapor) toward a reduced temperature and increased pressure. The effectiveness of the ILs as THI was decreasing in the order of [OH-EMIM][Cl] > $[BMIM][HSO_4]$ > [OH-EMIM][Br] > [BMIM][Cl] > [BMIM][Br] > $[BMIM][N(CN)_2]$ >

https://doi.org/10.1021/acs.jced.5c00025
J. Chem. Eng. Data XXXX, XXX, XXX−XXX

[BMIM][CF_3SO_3] > [BMIM][CH_3SO_4] > [BMIM][ClO_4]. By comparing the performance of [OH-EMIM][Cl], [OH-EMIM][Br], [BMIM][Cl], and [BMIM][Br], it was shown that the performance of ILs with $[OH\text{-}EMIM]^+$ is better than that of $[BMIM]^+$. This might be because $[OH\text{-}EMIM]^+$ has a shorter alkyl substituent, which decreases its hydrophobicity. Furthermore, the existence of hydroxyl cluster in $[OH\text{-}EMIM]^+$, which could create hydrogen bonds to the water molecules, increases its strength as a gas hydrate inhibitor. For the ILs with $[BMIM]^+$, the strong electrostatic charges of halides (Cl^- and Br^-) in the solutions result in their performance to be made them more effective than $[ClO_4]^-$, $[CH_3SO_4]^-$, $[CF_3SO_3]^-$, and $[N(CN)_2]^-$ as hydrate inhibitor. The stronger inhibition of Cl^- compared to Br^- was due to the higher electronegativity of the anion. It should be noted that [BMIM][HSO_4] also shows a strong tendency toward hydrate inhibition. This may be attributed to the ionization of $[HSO_4]^-$ into H^+ and SO_4^{2-}, thereby facilitating the creation of additional hydrogen bonds between H^+ and the oxygen atoms present in water.

Su et al. observed the influence of alkyl group size in natural salts on the constancy of methane hydrate. The study involved the measurement of hydrate phase equilibrium for tetramethylammonium bromide (TMAB), tetraethylammonium bromide (TEAB), tetrapropylammonium bromide (TPrAB), tetrabutylammonium bromide (TBAB), and tetrapentylammonium bromide (TPeAB).[51] The procedure of ascertaining the equilibrium measurements for the hydrate phase was executed by employing the pressure examination procedure with step-by-step heating. This was carried out within a particular temperature range spanning from 278.94 to 291.85 K and pressure fluctuating from 4.79 to 14.32 MPa. The findings of the study demonstrated that the introduction of TBAB or TPeAB had a substantial influence on the phase equilibria of CH_4 semiclathrate hydrates, leading to a reduction in pressure and an increase in temperature. Upon analysis, it was observed that TBAB exhibited superior thermodynamic properties compared to TPeAB in terms of stimulating methane hydrate formation, consistently producing more favorable outcomes at equivalent doses. Conversely, the use of TMAB, TEAB, or TPrAB resulted in a slight shift in phase equilibrium circumstances toward a greater pressure and lesser temperature range, thus indicating a thermodynamic inhibitory effect. Khan et al. directed an experimental assessment of thermodynamic performance related to tetramethylammonium hydroxide (TMAOH) for CH_4 and CO_2 gas hydrates.[52] The study involved the implementation of a conventional T-cycle practice coupled with an isochoric step heating technique to distinguish the thermodynamic impediments. The findings showed that TMAOH successfully shifts the hydrate equilibria figure to greater pressure and lower temperature zones for both the methane + TMAOH + water system and the carbon dioxide + TMAOH + water system. The methane + TMAOH + water system exhibited a mean reduction in temperature of virtually 1.06 °C, while the prevention impact for carbon dioxide + TMAOH + water system was practically 2.09 °C.

Khan et al. measured the inhibition impact of three aqueous ammoniums of tetraethylammonium hydroxide (TEAOH), tetramethylammonium chloride (TMACl), and tetrapropylammonium hydroxide (TPrAOH) based on ionic liquids (ILs) in concentrations of 1, 5, and 10 wt % on CO_2 hydrate.[53] The frequent method called T-cycle was employed to determine the hydrate equilibrium circumstances of ammonium-based ionic liquids (AILs) + CO_2 + H_2O in the temperature scope of 274−283 K and pressure scope of 1.80−4.20 MPa. It was observed that all AILs studied exhibited inhibition of CO_2 hydrate, with the degree of inhibition growing with the concentration of AILs. Among the various AILs that were examined, the one containing 10 wt % of TEAOH showed the most pronounced inhibitory influence, as evidenced by its average suppression temperature ($\Delta\overline{T}$) of 1.7 K. This was tracked by TMACl ($\Delta\overline{T}$ = 1.6 K) and TPrAOH ($\Delta\overline{T}$ = 1.2 K), which also demonstrated some degree of impediments. The greater inhibition efficiency of TEAOH as compared with TMACl and TPrAOH can be linked to the existence of the hydroxyl OH^- group, which is known to be the most suitable anion for H-bonding. The presence of OH^- in TEAOH enhances its H-bonding affinity, leading to greater disturbance in the water activity during hydrate formation and further contributing to effective hydrate inhibition. Long et al.[54] conducted an investigation to study the circumstances of phase equilibria for CH_4 hydrate in solitary ionic fluid aqueous systems. The solutions were composed of low levels of 1-ethyl-3-methylimidazolium nitrate ([Emim][NO_3]) at dosages of 1, 2.5, and 5 wt %. The researchers employed an isochoric step-by-step heating pressure examination technique to calculate the phase equilibrium circumstances over a pressure range of 3.50−15.0 MPa.[54] The investigation of the thermodynamic impediment influence of mixed ionic liquids including [Emim][NO_3] coupled with 1-ethyl-3-methylimidazolium chloride ([Emim][Cl]) in the presence of 1:1 mixture at mass fractions of 0.01 (0.005 [Emim][NO_3] + 0.005 [Emim][Cl]), 0.05 (0.025 [Emim][NO_3] + 0.025 [Emim][Cl]), 0.1 (0.05 [Emim][NO_3] + 0.05 [Emim][Cl]), and 0.2 (0.1 [Emim][NO_3] + 0.1 [Emim][Cl]) on the formation of CH_4 hydrate was also explored to ascertain the feasible existence of synergistic impacts. It was witnessed that for all the inhibitor systems that incorporate [Emim][NO_3] or [Emim][Cl], the impact of inhibition is seen to gradually augment with the rise in concentration and pressure. Among all the investigated mass fractions, the incorporation of the ionic liquid [Emim][NO_3] into water resulted in a shift of the phase equilibria curve toward a lower temperature and greater pressure zone, which is indicative of the expected behavior of thermodynamic inhibitors. The inhibition efficacy showed an incremental improvement with an augmentation in [Emim][NO_3] concentration. Importantly, it was observed that the inhibitory influence of [Emim][NO_3] at 0.01 mass fraction was so feeble that the decomposition figure practically coincided with that of pure water. Conversely, at the same pressure of 6.40 MPa, the anticipated temperature modification was nearly 0.3 K from 0.01 to 0.025 mass fraction, 0.4 K from 0.025 to 0.05 mass fraction, 0.6 K from 0.05 to 0.1 mass fraction, and 1.2 K from 0.1 to 0.2 mass fraction. Moreover, the inhibitory influence became more pronounced as the pressure increased. Importantly, the phase equilibria figures obtained with the mixed [Emim][NO_3] and [Emim][Cl] at each mass fraction, except 0.01, exhibited a significant reduction in the decomposition temperature at a given pressure compared with that of methane hydrate in unadulterated water. At higher concentrations, there were optimiztic contacts between [Emim][NO_3] and [Emim][Cl], which could potentially occur at higher pressures.

Khan et al. conducted an exploration on the effects of four ammonium-based ionic liquids (AILs) on a gas hydrate system containing a mixture of 70 mol % carbon dioxide and 30 mol %

https://doi.org/10.1021/acs.jced.5c00025
J. Chem. Eng. Data XXXX, XXX, XXX−XXX

methane from a thermodynamic inhibition perspective.[55] The alkylated ionic liquids (AILs) that were examined in this study were tetramethylammonium hydroxide, tetraethylammonium hydroxide, tetrapropylammonium hydroxide, and tetrabutylammonium hydroxide (TBAOH). The results obtained clearly indicate that the inhibitory effect of AILs is highly dependent on the alkyl chain length of the cation. Therefore, shorter alkyl chains provide improved thermodynamic inhibition. The findings revealed that when the gas mixture is enriched with CO_2, the existence of 10 wt % shorter alkyl chain AILs (TMAOH, TEAOH, and TPrAOH) triggers a change in the boundary of the hydrate phase toward lower temperature and greater pressure regions. However, 10 wt % TBAOH does not function as a thermodynamic inhibitor. Instead, it modifies the hydrate liquid vapor equilibrium curve toward greater temperature regions and ultimately acts as a gas hydrate promoter. The thermodynamic hydrate inhibitors influence AILs found in a descending order of significance, with TMAOH being the most influential, followed by TEAOH, TPrAOH, and TBAOH. The TMAOH is able to provide supreme inhibition ($\Delta\overline{T}$ = 1.56 K) among the studied AILs linked to the shortest alkyl chain, while TBAOH ($\Delta\overline{T}$ = −1.04 K) exhibits a promotional effect attributable to its relatively longer alkyl chain together with conceivable semiclathrate behavior. Nashed et al.[56] undertaken an assessment on the influence of ionic liquids with a concentration of 10 wt % on the phase border of CH_4 hydrate. Their method involved calculating the detachment temperature of CH_4 hydrate within the confines of the pressure spectrum that ranges from 5.1 to 11.1 MPa, utilizing a high-pressure differential scanning calorimeter (DSC).[56] The ionic liquids that were scrutinized are as follows: 1-methyl-3-octylimidazolium chloride [MOIM-Cl], 1-methylimidazolium hydrogen sulfate [H-MIM-HSO_4], tetraethylammonium iodide [TEA-I], and 1-hexyl-3-methyl-imidazolium iodide [HMIM-I]. The findings demonstrated that the inhibitory effect on CH_4 hydrate was more potent in the following order: [H-MIM-HSO_4] > [MOIM-Cl] > [TEA-I] > [HMIM-I]. The process of deterrence was initiated by virtue of the significant influence exerted by anions and alkyl chain length with respect to the inhibition of hydrate, as observed in the case of ionic liquids. Thus, the exemplary performance of [HMIM-HSO_4] in hydrate inhibition can be attributed to the influence of both its anionic and cationic components. The $[H\text{-}MIM]^+$ cation, with its abbreviated alkyl chain, evinces greater hydrophilicity compared to its lengthier counterpart, thereby manifesting a more pronounced inhibitory effect. Conversely, the sulfate anion $[HSO_4]^-$ undergoes ionization in an aqueous medium, generating H_3O^+ and SO_4^{2-} species, which foster greater hydrogen bonding interactions between H_3O^+ and the oxygen atoms of water.

Gupta et al. investigated a study in which they examined the impact of eight ionic liquids (ILs) from two categories of ILs, specifically, aromatic and aliphatic ILs, on the phase performance of CH_4 hydrate.[57] The authors utilized five aromatic-based ILs with various cations such as 1-butyl-3-methyl imidazolium, 1-hexyl-3-methyl imidazolium $[HMIM]^+$, 1-octyl-3-methyl imidazolium $[OMIM]^+$, and numerous anions such as $[HSO_4]^-$, $[Cl]^-$, $[Br]^-$, and also three aliphatic-based ILs with several cations such as diethylammonium $[Et_2NH_2]^+$, tripropyl-ammonium $[Pr_3NH]^+$, tributyl-ammonium $[Bu_3NH]^+$, and $[HSO_4]^-$ anion. The experiments were conducted within the parameters of hydrate equilibria pressure and temperature, ranging from 3.86 to 7.66 MPa and 276.68 to 283.18 K, respectively. It has been detected that all of the surveyed ionic liquids demonstrate an inhibitory impact on the CH_4 hydrate system. Aromatic ionic liquids are more prevalent in CH_4 hydrate inhibition than aliphatic ionic liquids. Ionic liquids with similar cation classes but differing carbon chain lengths do not notably enhance hydrate inhibition. However, replacing anion with $[HSO_4]^-$ in imidazolium-based ILs ameliorates CH_4 hydrate prevention. 1-Butyl-3-methyl imidazolium sulfate ($[BMIM]^+[HSO_4]^-$) was detected to be the most effective CH_4 hydrate inhibitor among all considered ILs. Gupta and colleagues conducted an assessment on the impact of quaternary ammonium salts (QAS) belonging to the bromide group, specifically tetramethyl, tetraethyl, and tetrabutyl ammonium bromide (TMAB, TEAB, and TBAB), which were used in aqueous solutions at two varying concentrations (5, 10 wt %), on the hydrate−liquid−vapor (H−L−V) phase equilibria of the circumstances of CH_4 hydrate development.[58] Through the utilization of the isochoric pressure examination methodology, numerous experimental procedures were conducted to acquire phase equilibrium information within the confines of an equilibrium pressure scope of 4.2−7.6 MPa and a temperature span of 276.8−282.4 K. The results indicated that the introduction of TMAB and TEAB led to a change in the phase equilibria figure of CH_4 hydrate toward greater pressure and lower temperature circumstances. It was found that TMAB and TEAB exhibited thermodynamic prevention, whereas TBAB demonstrated a promotion effect. The level of inhibition found in the aqueous solution of TMAB is slightly greater than that of TEAB at both 5 and 1 wt %. The mean degree of temperature depression, also known as ΔT_{eq} for hydrate inhibition, was measured for both TMAB and TEAB at 5 wt %, yielding 1.20 and 1.01 K, respectively, and at 10 wt %, resulting in 1.55 and 1.08 K, respectively. These outcomes successfully demonstrate the influence of alkyl chain length on ionic liquids in relation to the phase equilibria of the CH_4 hydrate system. It has been determined that ionic liquids possessing shorter alkyl chains exhibit a more pronounced ability to inhibit hydrate development as opposed to those with longer chains. It is worth noting that particular QASs, namely, TMAB and TEAB, have displayed thermodynamic prevention of hydrate development, which stands in contrast to the observed promotion of hydrate creation by TBAB.

Khan et al. directed an experimental survey on the thermodynamic impediments comprising a binary combination of 70 mol % CH_4 + 30 mol % CO_2.[59] The inhibitory influences of four different ionic liquids based on ammonium (AILs)—tetramethylammonium hydroxide, tetraethylammonium hydroxide, tetrapropylammonium hydroxide, and tetrabutylammonium hydroxide—were analyzed using the T-cycle procedure. The equilibrium between liquid and vapor states of hydrate was examined in the studied systems using aqueous AILs solutions with a concentration of 10 wt %. The assessment was steered at pressures extending from 3.0 to 7.50 MPa and temperatures spanning from 275.0 to 286.0 K. The outcomes revealed that the AILs altogether, other than TBAOH, exhibited the thermodynamic influence by altering the HLwVE of CH_4-enriched mixed gas hydrates. In addition, the mean temperature of hydrate decomposition ($\Delta\overline{T}$) decreased as the alkyl chain length of AILs augmented. The impact of various amines on the prevention of gas hydrate creation was evaluated. Among the amines studied, TMAOH exhibited the highest level of prevention at a mass fraction of

https://doi.org/10.1021/acs.jced.5c00025
J. Chem. Eng. Data XXXX, XXX, XXX−XXX

0.01, with a $\Delta\overline{T}$ value of 1.28 K. The other amines, namely, TEAOH, TPrAOH, and TBAOH, displayed lower levels of prevention with $\Delta\overline{T}$ values of 0.8, 0.7, and −0.84 K, respectively. Interestingly, TBAOH acted as a gas hydrate promoter due to its relatively higher alkyl chain cation (butyl) content, leading to its semiclathrate hydrate behavior. The THI efficiency of AILs was found to rise in the order of TBAOH < TPrAOH < TEAOH < TMAOH. Due to its shorter alkyl chain, TMAOH was found to be the most influential inhibitor with a $\Delta\overline{T}$ value of 1.28 K among all the assessed AILs.

Khan et al. evaluated the dual functional (thermodynamic and kinetic) comportment of quaternary ammonium salt, specifically TMACl, for both CH_4 and CO_2 hydrates.[60] The equilibrium between hydrate liquid and vapor, also known as HLwVE, pertaining to CH_4 and CO_2, has been assessed in the existence and nonexistence of aqueous TMACl solutions (1, 5, and 10 wt %) through the T-cycle procedure with the isochoric step-heating methodology under diverse temperature and pressure situations. The thermodynamic and kinetic outcomes procured have demonstrated that TMACl has acted as a double-functional hydrate inhibitor for CH_4 and CO_2 gases. Obtained outcomes imitated that the thermodynamic prevention efficiency of TMACl + H_2O + CH_4 for every system is composition-dependent; higher concentration, i.e., 10 wt % TMACl, supplies more inhibition than lower concentrations (1 or 5 wt %). In addition, the phase behavior of diverse aqueous TMACl solutions, i.e., 1, 5, and 10 wt % on CO_2 hydrates, showed that the TMACl was able to display thermodynamic stimulus by altering the HLwVE toward lower temperatures and greater pressures. Like the CH_4 hydrates, the THI influence of TMACl is also contingent on the composition, perhaps owing to the augmented action of TMACl in the aqueous phase resulting in superior prevention for the concentration of 10 wt %. The THI evaluation divulged that 10 wt % TMACl substantially diminished the hydrate phase frontier of CH_4 and CO_2 hydrates up to 1.42 and 1.60 K, respectively. Kazemi et al. executed a survey on the impact of BMIM-BF_4 and tetraethylammonium chloride (TEACl) on the thermodynamic constant of CH_4 clathrate hydrate.[61] BMIM-BF_4 and TEACl diverse aqueous solutions (4.77 wt % (0.57 mol %) TEACl + 4.85 wt % (0.43 mol %) BMIM-BF_4, 9.15 wt % (0.20 mol %) TEACl + 9.38 wt % (0.90 mol %) BMIM-BF_4, and 11.82 wt % (1.63 mol %) TEACl + 11.82 wt % of BMIM-BF_4 (1.20 mol %) in aqueous solution) were used as thermodynamic inhibitors. The experiments were conducted at constant volume from the temperature and pressure ranges of 274.6−283.2 K and 3.18−7.93 MPa, utilizing an isochoric pressure examination procedure. The trialed findings indicate that mixtures of ionic liquids (ILs) demonstrate a higher degree of efficacy in comparison to individual ILs at equivalent concentrations. Furthermore, it is observed that an augmentation in ILs concentration within the aqueous solution serves to enhance the inhibitory effect of the ILs. Consequently, the combination of 11.82 wt % (1.63 mol %) of TEACl + 11.82 wt % of BMIM-BF_4 (1.20 mol %) mixture can reduce methane hydrate equilibrium temperature to a greater extent than two other IL mixtures examined. Ultimately, the results evince an increase in the inhibitory effect of the studied ILs as a function of system pressure augmentation.

de Menezes et al. evaluated the function of 1-butyl-3-methylimidazolium chloride and 1-butyl-3-methylimidazolium bromide as CH_4 hydrate inhibitors.[62] New data on the dissociation of hydrates were acquired via high-pressure calorimetry for aqueous solutions containing these inhibitors at concentrations ranging approximately from 3.6 to 63.107 wt % for [BMIM][Cl] and 4.5 to 68.21 wt % for [BMIM][Br], under pressures ranging from 9.6 to 100 MPa using microcalorimetric measurements. The findings indicate that [BMIM][Cl] exhibits superior inhibitory effects, as evidenced by the onset and peak temperatures. When chloride-based IL is present, hydrates form at lower dissociation temperatures. Moreover, it is noteworthy that the suppressive impact of [BMIM][Cl] is more conspicuous than that of [BMIM][Br] when the IL fractions are elevated. The electrical conductivity of [BMIM][Cl] in aqueous solutions surpasses that of [BMIM][Br], which is conjectured to be linked to the thermodynamic efficacy of the IL as a gas hydrate inhibitor. The infrared spectra manifest that chloride ionic liquids establish more robust hydrogen bonds with water molecules, which potentially explains the superior functionality of [BMIM][Cl] as a gas hydrate inhibitor. Even though these supplements encourage hydrate growth at low levels, they all act as thermodynamic inhibitors for methane hydrates, prompting the phase equilibria figures to alter in the way to lesser temperatures. The thermodynamic inhibition effect is greatly enhanced by increasing the content of these ILs, mainly for [BMIM][Cl]. Qasim et al.[63] inspected the equilibrium states of CH_4 hydrate under varying pressures of 3.45−8.3 MPa and temperatures of 274−284.6 K. To accomplish this, they employed the isochoric thermodynamic cycle (T-cycle) practice and incorporated three distinct quaternary ammonium salts, specifically tetraethylammonium iodide (TEAI), TMAB, and TEAB, as well as monoethylene glycol at 0.01, 0.05, and 0.1 mass fraction.[63] The analyses indicated an augmentation in the inhibition effect with a rise in the quantity of chemicals. Furthermore, the results revealed that TMAB exhibited a superior effect on hydrate suppression in comparison with TEAB and TEAI, both in unadulterated form and when mixed with MEG.

Soromenho et al. considered the influence of two thiouronium-based ionic liquids, called 2-ethylthiouronium bromide [C_2th][Br] and 2-(hydroxyethyl)thiouronium bromide [C_2OHth][Br], at a 10 wt % concentration on the inhibition of carbon dioxide hydrate in the pressure scope of 1.70−3.50 MPa and temperature of 275.40−282.02 K, employing the isochoric pressure examination procedure.[64] The findings of their scrutiny evinced that both ionic liquids evinced an inhibitory effect by inducing a shift in the equilibria figure of CO_2 hydrate to regions with lower temperatures and higher pressure. Nevertheless, the inhibitory effect of both ionic liquids was not particularly robust, and the equilibrium diagram of CO_2 hydrate underwent an alteration of only 1.2 K.

Wang et al. examined the inhibition impact of five types of ionic liquids, namely, ethyltributylphosphonium hexafluorophosphate ($[P_{2\,4\,4\,4}][PF_6]$), tributylhexylphosphonium hexafluorophosphate ($[P_{6\,4\,4\,4}][PF_6]$), tetraethylammonium bromide ($[N_{2\,2\,2\,2}]Br$), tetraethylammonium bistrifluoromethanesulfonimide ($[N_{2\,2\ \ 2\,2}][NTf_2]$), and tetraethylammonium hexafluorophosphate ($[N_{2\,2\,2\,2}][PF_6]$) (at concentrations of 0.25, 0.63, 0.95, 1.25, 3.75, 6.25, and 10 wt %) on the inhibition of carbon dioxide hydrate in the temperature span of 277.65−277.15 K and pressures less than 2 MPa.[65] The results of their experiments showed that $[P_{2\,4\ \ 4\,4}][PF_6]$ and $[P_{6\,4\,4\,4}][PF_6]$ are not able to impede the creation of CO_2 hydrate and the phase equilibria diagram of CO_2 hydrate

https://doi.org/10.1021/acs.jced.5c00025
J. Chem. Eng. Data XXXX, XXX, XXX−XXX

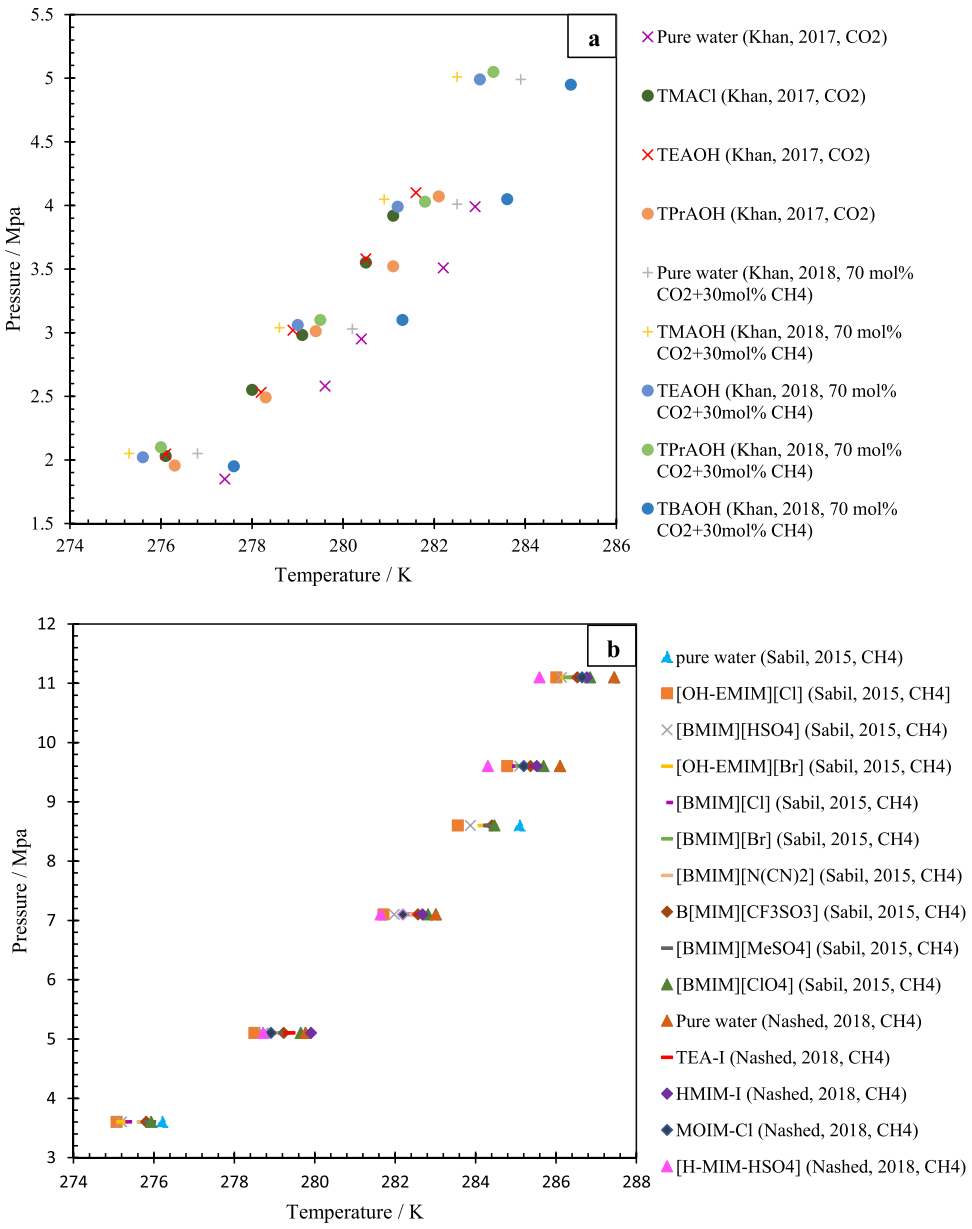

Figure 4. Comparison between the equilibrium diagrams of different gas hydrates in the presence of various inhibitors. (a) CO_2 gas and TEAOH, TMACl, TPrAOH additives,[53] mixture of 70 mol % CO_2 + 30 mol % CH_4 gas and TMAOH, TEAOH, TPrAOH, TBAOH additives,[55] and CH_4 gas and [MOIM-Cl], [H-MIM-HSO_4], [TEA-I], [HMIM-I] additives;[56] (b) CH_4 gas and [BMIM][CH_3SO_4], [BMIM][HSO_4], [BMIM][CF_3SO_3], [BMIM][$N(CN)_2$], [BMIM][Cl], [BMIM][Br], [BMIM][ClO_4], [OH-EMIM][Cl], [OH-EMIM][Br] additives.[50]

shifted slightly to higher temperatures. On the other hand, [$N_{2\,2\,\,2\,2}$]Br, [$N_{2\,2\,\,2\,2}$][NTf_2], and [$N_{2\,2\,\,2\,2}$][PF_6] showed inhibition properties by altering the phase equilibria temperature figure of CO_2 hydrate toward lesser temperatures. Also, at the concentration of 10 wt %, these three types of ionic liquids [$N_{2\,2\,\,2\,2}$]Br, [$N_{2\,2\,\,2\,2}$][NTf_2], and [$N_{2\,2\,\,2\,2}$][PF_6] showed more inhibition power by reducing the equilibrium temperature of CO_2 hydrate with values of 5.60, 3.20, and 1.40 K, respectively. This indicates that the inhibition impact augmented as the size of anion lessened or the charge density of anion raised.

Figure 4a,b provides an illustrative diagram depicting the equilibrium of diverse gas hydrates, such as CH_4, CO_2, and a hybrid comprising 70 mol % CO_2 + 30 mol % CH_4 under varying ionic liquids. The CH_4 hydrate equilibrium diagram has been derived from the laboratory experimentation of Sabil et al. and is presented in the existence of 10 wt % ionic liquids, which include [BMIM][CH_3SO_4], [BMIM][HSO_4], [BMIM][CF_3SO_3], [BMIM][$N(CN)_2$], [BMIM][Cl], [BMIM][Br], [BMIM][ClO_4], [OH-EMIM][Cl], [OH-EMIM][Br].[50] Similarly, the equilibrium diagram of CO_2 gas hydrate has been included, based on the research steered by Khan et al. in the presence of inhibitors like TEAOH, TMACl, TPrAOH, in a concentration of 10 wt %.[53] Furthermore, the equilibrium graph for the hybrid of 70 mol % CO_2 + 30 mol % CH_4, as reported by Khan et al., has been presented, where the inhibitors used were TMAOH, TEAOH, TPrAOH, TBAOH, in a concentration of 10 wt %.[55] The circumstances of the creation of CH_4 hydrate have also been shown in the existence of 10 wt % of [MOIM-Cl], [H-MIM-HSO_4], [TEA-I], [HMIM-I], as stipulated in the research by Nashed et al.[56] As evident from Figure 4, the ionic liquid [OH-EMIM][Cl]

https://doi.org/10.1021/acs.jced.5c00025
J. Chem. Eng. Data XXXX, XXX, XXX−XXX

exhibits superior inhibitory properties compared with other ionic liquids in Sabil et al.'s[50] research due to the existence of $[OH\text{-}EMIM]^+$, a shorter alkyl substituent, which subsequently decreases its hydrophobicity, the hydroxyl group in $[OH\text{-}EMIM]^+$, creating hydrogen ties with water molecules, and the higher electronegativity of the anion Cl^- in comparison to Br^-. Additionally, in the study by Khan et al.,[53] TEAOH shows better inhibition compared to other inhibitors, owing to the existence of hydroxyl OH^-, which causes more disturbance in the activity of water during hydrate creation, and the cation TEA^+, which has a shorter alkyl chain and is less hydrophobic. Furthermore, TMAOH exhibited superior inhibitory effects compared to other ionic liquids that were considered by Khan et al.,[55,59] owing to its possession of the shortest alkyl chain. Additionally, Nashed et al.[56] discovered that $[H\text{-}MIM\text{-}HSO_4]$ demonstrated greater inhibition efficacy than other ionic liquids, as a consequence of its shorter alkyl chain $[H\text{-}MIM]^+$, which in turn resulted in heightened hydrophilicity. Overall, the nature of the cation and anion, as well as the type and length of the side chain, are significant factors that contribute to the manifestation of a more potent inhibitory property within ionic liquids.

Studies conducted in the field of ionic liquid inhibitors have indicated a wide-reaching scope of research within this category. It is noteworthy that no superior inhibitor has been introduced in this group. However, it can be inferred that the addition of ionic liquids to the system in greater concentration is directly proportional to the displacement of the equilibrium curve toward lower temperatures, thereby resulting in highly effective thermodynamic inhibition. Additionally, it is evident that the inhibition potential of the cation's shorter side chain in ionic liquids is superior to that of the longer side chain. For example, in a study by Li et al. on the inhibition influence of ionic liquids, including [MMIM]-I, [EMIM]-I, $[OH\text{-}C_2MIM]$-Cl, $[N_{1,1,1,1}]$-Cl, and $[N_{1,1,1,eOH}]$-Cl on CH_4 hydrate, it was established that $[N_{1,1,1,1}]$-Cl is the most efficacious thermodynamic inhibitor among all ionic liquids, owing to the shorter length of its alkyl cation chain.[45] Furthermore, it is important to emphasize that ionic liquids with suitable hydrogen bonding functional groups, such as OH, NH_2, and NHCO, have greater potential as gas hydrate inhibitors compared with unsubstituted ionic liquids.

Moreover, it is notable that the hydroxyl OH^- group can be classified as the most appropriate anion for hydrogen bonding. This particular group has been observed to cause a greater degree of disturbance in the water activity during the formation of hydrates, which in turn leads to the effective inhibition of hydrates. To illustrate this point, it is worth mentioning the investigation carried out by Khan et al.[53] on the phase equilibria circumstances of CO_2 hydrates in the existence of ionic liquids such as TEAOH, TMACl, and TPrAOH. The findings of this study indicated that TEAOH demonstrated a superior inhibition effect compared to other ionic liquids owing to the existence of a hydroxyl OH^- group and a TEA^+ cation with a shorter alkyl chain.[53] Table 2 presents a compendium of investigations conducted on gas hydrates when exposed to ionic liquids. To summarize, the key findings in the field of ionic liquids are as follows:

- ILs, composed of cations and anions, show potential as effective thermodynamic inhibitors due to their unique properties, including zero volatility, thermal stability, and low vapor pressure.
- ILs inhibit gas hydrate formation by forming hydrogen bonds with unbound water molecules, contributing to the displacement of the equilibrium curve to lower temperatures and higher pressures.
- The inhibitory impact of ILs depends on their cations, anions, and concentration. Shorter alkyl chains in ILs result in superior inhibition effects compared to longer alkyl chains.
- Some ILs can be recovered and reused, though their regeneration may require additional steps, depending on their chemical structure and operational conditions.
- ILs with hydroxyl-functionalized cations, such as $[OH\text{-}EMIM][Cl]$, show stronger inhibitory effects due to enhanced hydrogen bonding capabilities.
- Ionic liquids with shorter alkyl chains tend to be more effective in inhibiting hydrate formation compared to those with longer chains.
- Combinations of ionic liquids, such as $[EMIM][NO_3]$ and [EMIM][Cl], show synergistic effects at higher concentrations and pressures, resulting in more effective inhibition.
- Ionic liquids, especially those with shorter alkyl chains and appropriate functional groups (e.g., OH, NH_2), offer a promising alternative to traditional hydrate inhibitors, providing environmentally friendly and cost-effective solutions for industrial applications.

4.3. Salts. Electrolytes are a highly efficacious category of thermodynamic inhibitors. By undergoing conversion to cation and anion ions within a solution, salts serve to diminish the water activity. Subsequently, these electrolytes interact vigorously with water dipoles via a robust electrostatic force, leading to the transference of hydrate phase equilibria lines to lower temperatures and higher pressures. It has been duly noted that the creation of hydrate networks necessitates a lower temperature at a given pressure. Notably, sodium chloride is among the most extensively researched electrolytes and is utilized on an industrial level as a gas hydrate inhibitor in drilling operations.[23]

Lu et al. conducted an investigation that delved into the multifarious functions of cations and anions in the hindrance of hydrate creation and its stability conditions in various electrolyte solutions.[66] Their experimental findings revealed that changes in the concentration of Cl^- and SO_4^{2-} anions have a greater impact on CH_4 hydrate stability than Na^+ and Mg^{2+} cations. This is primarily due to changes in the equilibria temperature of hydrate creation occurring significantly more by changing the concentration of anions than cations. Furthermore, the regression line slope for different electrolyte solutions is similar for C_3H_8 hydrate when coexisting with salts such as sodium chloride, potassium chloride, and calcium chloride, indicating little variation in the inhibition of these salts for C_3H_8 hydrate. However, irrespective of the electrolyte solution cation, modifications in the equilibrium state of propane hydrate demonstrated a strong correlation with the concentration of chlorine. Consequently, it is reasonable to assert that the stability of C_3H_8 hydrate in the electrolyte solution is predominantly influenced by the Cl^- anion, with the cation having a relatively minor effect. As such, the anion's impact on influencing gas hydrate constancy in an electrolyte solution is more significant than that of the cation. This phenomenon can be linked to the various hydration properties of cations and anions in an electrolyte solution, as hydrated

https://doi.org/10.1021/acs.jced.5c00025
J. Chem. Eng. Data XXXX, XXX, XXX−XXX

Table 2. Studies Pertaining to the Creation of Gas Hydrates in the Presence of Ionic Liquids

author (publication date)	gas	type of thermodynamic inhibitor	concentration of inhibitors (wt %)	T/K	P/MPa	result	ref
Li et al. (2011)	CH_4	[MMIM]-I, [EMIM]-I, [OH-C_2MIM]-Cl, [$N_{1,1,1,1}$]-Cl, [$N_{1,1,1,eOH}$]-Cl	10	276.15−289.15	3−17	the cations that possess shorter alkyl substituents exhibit superior performance in the prevention of hydrate formation in comparison to those that have longer alkyl substituents	45
Tumba et al. (2011)	CO_2	[3C_4C_1P][$MeSO_4$]	26.11, 50.07	273.5−282.2	4.35−14.77	tributylmethylphosphonium methylsulfate has an inhibition influence on the creation of CO_2 and CH_4 hydrate	46
	CH_4			273.3−288.5			
Keshavarz et al. (2013)	CH_4	BMIM-BF_4, BMIM-N(CN)$_2$, $N_{2,2,2,2}$-Cl	10 μ_BIM-N(CN)$_2$, $N_{2,2,2,2}$-Cl, 10, 15, 20 μ_BIM-BF_4	272.1−282.0	2.48−6.58	increasing the concentration of BMIM-BF_4 results in an increase in inhibition effects	47
Zare et al. (2013)	CH_4	[BMIM][$MeSO_4$], [EMIM][HSO_4], [EMIM][$EtSO_4$], [BMIM][BF_4], [OH-EMIM][BF_4], [EMIM][$EtSO_4$]	8, 10	281.9−287.4	7.08−12.16	the most influential thermodynamic inhibitor was [OH-EMIM][BF_4]	48
Richard et al. (2013)	CH_4	EMIM-Cl, EMIM-Br, NaCl, MEG	5, 20, 30, 40 EMIM-Cl, 5, 10, 15 EMIM-Cl + 5, 10, 15 MEG, 5 EMIM-Cl + 5 NaCl, 10 EMIM-Cl + 10 EMIM-Br	273.6−292	10−20	improvement of the thermodynamic inhibition effect of single-component solutions of EMIM-Cl was observed by increasing its concentration; in contrast to MEG or NaCl, inhibitors that comprise EMIM-Cl or EMIM-Br have exhibited a rise in their inhibition potency with an escalation in pressure	49
Sabil et al. (2015)	CH_4	[BMIM][CH_3SO_4], [BMIM][HSO_4], [BMIM] [CF_3SO_3], [BMIM] [N(CN)$_2$], [BMIM][Cl], [BMIM][Br], [BMIM][ClO_4], [OH-EMIM][Cl], [OH-EMIM][Br]	10	275.07−287.45	3.6−11.2	[OH-EMIM][Cl] > [BMIM][HSO_4] > [OH-EMIM][Br] > [BMIM][Cl] > [BMIM][Br] > [BMIM][N(CN)$_2$] > [BMIM][CF_3SO_3] > [BMIM][CH_3SO_4] > [BMIM][ClO_4]	50
Su et al. (2016)	CH_4	TMAB	2.177, 4.497	278.94−291.85	4.79−14.32	TBAB and TPeAB showed hydrate promotion properties, while TMAB, TEAB, and TPrAB exhibited hydrate inhibition effects by shifting phase equilibrium circumstances to areas with higher pressures and lesser temperatures	51
		TEAB	3.078, 6.296				
		TPrAB	3.963, 8.029				
		TBAB	4.832, 9.70				
		TPeAB	5.685, 11.31				
Khan et al. (2016)	CO_2	TMAOH	10	276.55−282.7	2−4	the utilization of TMAOH results in a notable upward alteration of the hydrate equilibrium curve toward zones of higher pressure and lower temperature	52
	CH_4			276.25−282.45	3.5−8		
Khan et al. (2017)	CO_2	TEAOH, TMACl, TPrAOH	1, 5, 10	274−283	1.80−4.20	TEAOH showed the highest inhibition effect due to the hydroxyl OH^- group	53
Long et al. (2017)	CH_4	[Emim][NO_3], [Emim][Cl]	1, 2.5, 5 [Emim][NO_3], 0.5, 2.5, 10 [Emim][NO_3] + 0.5, 2.5, 10 [Emim][Cl]	272.6−289	3.40−14.91	the extent of inhibition rises in a gradual manner as the concentration and pressure levels are heightened across all inhibitor systems; in addition, the inhibition effect became stronger at higher pressures	54
Khan et al. (2018)	CO_2 + CH_4	TMAOH, TEAOH, TPrAOH, TBAOH	1, 5, 10	275.0−286.0	3.0−7.50	TMAOH > TEAOH > TPrAOH > TBAOH	55
Nashed et al. (2018)	CH_4	[MOIM-Cl], [H-MIM-HSO_4], [TEA-I], [HMIM-I]	10	278.8−286.8	5.1−11.1	[H-MIM-HSO_4] > [MOIM-Cl] > [TEA-I] > [HMIM-I]	56
Gupta et al. (2018)	CH_4	[BMIM][Cl], [BMIM][Br], [HMIM][Br], [OMIM][Cl], [BMIM][HSO_4], [Et_2NH_2][HSO_4], [Pr_3NH][HSO_4], [Bu_3NH][HSO_4]	10	276.68−283.18	3.86−7.66	the compound $[BMIM]^+[HSO_4]^-$ has been determined to be the optimal inhibitor of CH_4 hydrate in comparison to all other studied ILs	57
Gupta et al. (2018)	CH_4	TMAB, TEAB, TBAB	5, 10	276.8−282.4	4.20−7.60	the hydrate prevention is observed to be more pronounced for the lengthier alkyl chain length (TBAB) of ionic liquids, while the shorter alkyl chain length (TMAB and TEAB) appears to have a lesser effect	58
Khan et al. (2018)	CH_4 + CO_2	TMAOH, TEAOH, TPrAOH, TBAOH	10	275.0−286.0	3.0 − 7.50	TBAOH < TPrAOH < TEAOH < TMAOH	59
Khan et al. (2019)	CH_4	TMACl	1, 5, 10	275.9−284.8	3.52−8.05	the THI evaluation showed that 10 wt % TMACl significantly diminished the hydrate phase boundary of CH_4 and CO_2 hydrates up to 1.42 and 1.60 K, respectively	60
	CO_2			276.1−282.9	1.85−4		
Kazemi et al. (2019)	CH_4	BMIM-BF_4, TEACl	4.77 TEACl + 4.85 μ_BIMBF_4, 9.15 TEACl + 9.38 μ_BIM-BF_4, 11.82 TEACl + 11.82 μ_BIM-BF_4	274.6−283.2	3.18−7.93	ILs mixtures are more effective than each single IL at equal concentration	61

https://doi.org/10.1021/acs.jced.5c00025
J. Chem. Eng. Data XXXX, XXX, XXX−XXX

Table 2. continued

author (publication date)	gas	type of thermodynamic inhibitor	concentration of inhibitors (wt %)	T/K	P/MPa	result	ref
de Menezes et al. (2020)	CH_4	[BMIM][Cl]	3.6, 17.27, 30.66, 41.43, 63.107	271.92−305.08	9.6−100	the suppressive impact of [BMIM][Cl] is more pronounced than [BMIM][Br] under heightened IL fractions	62
		[BMIM][Br]	4.5, 21.3, 39.022, 57.464, 68.21				
Qasim et al. (2020)	CH_4	TEAI, TMAB, TEAB	1, 5, 10	274−284.6	3.45−8.30	TMAB demonstrated a superior ability to suppress hydrate formation when compared to TEAB and TEAI	63
Soromenho et al. (2022)	CO_2	[C_2th][Br], [C_2OHth][Br]	10	275.40−282.02	1.70−3.50	both ionic liquids serve as thermodynamic inhibitors when present at a concentration of 10 wt % and effectively suppress the equilibrium of CO_2 hydrate by approximately 1.2 K	64
Wang et al. (2022)	CO_2	[P_{2444}][PF_6] [P_{6444}][PF_6], [N_{2222}]Br, [N_{2222}][NTf_2], [N_{2222}][PF_6]	0.25, 0.63, 0.95, 1.25, 3.75, 6.25, 10	270.65−277.15	under 2	[P_{2444}][PF_6] and [P_{6444}][PF_6] act as promoters; [N_{2222}]Br, [N_{2222}][NTf_2], and [N_{2222}][PF_6] act as inhibitors	65

anions have a considerably more potent ability than cations to disrupt the water network by fading the H-bond of water particles. Jager and Sloan measured the circumstances of equilibrium for the creation of CH_4 hydrate in the existence of 6.208, 10.83, 17.15, and 21.997 wt % of sodium chloride salt by experimental Raman spectroscopy technique up to pressures of 70 MPa.[67] In the experimental approach employed by the researchers, the temperature and pressure conditions were adjusted to a degree where the final hydrate crystal vanished, and this was considered the point of equilibrium for hydrate formation. This methodology has the added benefit of not only facilitating the identification of hydrate structures but also the determination of the equilibrium point. Through their experimentation, the researchers discovered that methane hydrate is inhibited by sodium chloride salt, and as the concentration of salt rises, the equilibria zone alters toward regions with higher pressure and lower temperature. Furthermore, it was noted that the configuration of the hydrate structure generated in every solution was of type I. Atik et al. scrutinized the circumstances of methane hydrate creation utilizing the isochoric method in the existence of magnesium chloride salt in concentrations of 1, 5, 10, and 15 wt %, calcium chloride salt in the mass fraction of 0.1705 wt %, and also the mixture of sodium chloride (5 wt %) and magnesium chloride salts (6.09 wt %), in the temperature span of 237−229 K and at pressures up to 23 MPa.[68] The results derived from their study have exposed that magnesium chloride salt displays exceptional inhibitory characteristics in contrast to other forms of salts. As a result, the inhibitory effect of the amalgamation of salts including magnesium chloride and sodium chloride exceeds that of the mixture of calcium chloride and sodium chloride salts.

Mohammadi et al. investigated hydrate decomposition circumstances of CH_4, C_2H_6, C_3H_8, and CO_2 gases separately and in the presence of sodium chloride, potassium chloride, and calcium chloride salts, in concentrations of 5 wt %, 5 and 10 wt %, and 5 and 15 wt %, respectively, using the isochoric method.[69] The conducted experiments have indicated that the augmentation of potassium chloride and calcium chloride salts' concentration resulted in an escalation of their inhibition attribute in the formation of hydrates for sundry gases. Calcium chloride, of all the salts, demonstrated the most substantial effect of inhibition.

Mohammadi et al. checked CH_4 hydrate decomposition circumstances in the presence of aqueous solutions containing 5 and 10 wt % sodium bromide, potassium bromide, magnesium chloride, and potassium carbonate salts and also in the presence of 5 and 15 wt % of calcium bromide salt using isochoric pressure search.[70] The research conducted by the aforementioned individuals has substantiated that a rise in the concentration of salts has a direct correlation with the augmentation of the inhibition property of CH_4 hydrate formation. Furthermore, it was observed that magnesium chloride exhibited the most pronounced inhibitory effect among the various salts analyzed. Haghighi et al. inspected the decomposition circumstances of methane hydrate in the presence of aqueous solutions, including sodium chloride at concentrations of 15 and 20 wt %, potassium chloride at a concentration of 15 wt %, and magnesium chloride at a concentration of 10 wt %, using the isochoric step-heating method.[71] The findings of their study have demonstrated that the current salts have exerted a substantial influence on the equilibria hydrate formation conditions, whereby the con-

https://doi.org/10.1021/acs.jced.5c00025
J. Chem. Eng. Data XXXX, XXX, XXX−XXX

ditions have shifted toward lower temperatures and higher pressures. Furthermore, it has been detected that among the three salts tested, namely, sodium chloride, magnesium chloride, and potassium chloride, the latter exhibited the least inhibitory influence in impeding the creation of CH_4 hydrate.

Sabil et al.[72] conducted a relative study on the impact of seven distinct electrolytes, specifically metal halides, comprising sodium chloride, calcium chloride, magnesium chloride, potassium bromide, sodium fluoride, potassium chloride, and sodium bromide. The study aimed to investigate their effect on the decomposition circumstances of CO_2−THF at a temperature spectrum of 275−305 K and a pressure range of 0.9−7.10 MPa.[72] The results of their experimental investigations indicate a significant impact of the existence of salts on the equilibrium diagram of hydrate creation, leading to a shift toward the right of the equilibrium region. Moreover, it has been observed that the suppressive capacity of salts in the formation of hydrates was diminished by tetrahydrofuran owing to its capability to dissolve in water. Additionally, the inhibitory impact of diverse metal halides on the balance circumstances of CH_4 hydrate was in the following order: NaF < KBr < NaCl < NaBr < $CaCl_2$ < $MgCl_2$. Concerning cations and anions, the potency of inhibition on hydrates was found to be Mg^{2+} > Ca^{2+} > Na^+ > K+ and Br^- > Cl^- > F^-, respectively.

Ngema et al. guided an inquiry into the circumstances of gas hydrate decomposition for R134a refrigerant, in the existence of different concentrations of sodium chloride salt (5, 10, and 15 wt %), in the temperature range of 268.1−280.6 K and pressure of 0.086−0.383 MPa and also for R410a or R507 refrigerants, in the existence of different quantity of sodium chloride salt (5 and 10 wt %), in the temperature span of 273.9−290.9 K and a pressure ranging from 0.226 to 1.345 MPa, using isochoric pressure examination procedure.[73] The empirical findings indicated by the researchers demonstrate that the existence of sodium chloride in an aqueous solution exerts a considerable thermodynamic influence on refrigerants, leading to the alteration of the phase equilibria boundaries of the hydrate diagram toward lower dissociation temperatures. Additionally, the inhibitory potency of sodium chloride on the equilibrium conditions of distinct refrigerants was observed to vary in the order of R410a < R507 < R143a, respectively. Windmeier and Oellrich measured the dissociation pressure for CH_4 gas hydrate under the influence of aqueous solutions containing lithium bromide (with 5, 10, 15, and 20 wt %) and lithium chloride (with 5, 10, 15, and 26.55 wt %) in the temperature scope of 260−290 K and for pressures up to 22.5 MPa using isochoric method.[74] The findings from their experimental investigations illustrated that the equilibrium diagram's inclination toward regions characterized by lesser temperatures and further pressures heightened as the quantity of salts amplified. Additionally, the inhibitory potency followed the order of LiCl > LiBr, attributed to the discrepant degrees of hydration arising from the varying anion sizes. Unsurprisingly, lithium chloride salt evinced a more substantial inhibition effect than lithium bromide.

Ngema et al. considered the decomposition circumstances of gas hydrate for R134a refrigerant, in the existence of different concentrations of magnesium chloride salt (2.407, 4.942, and 7.633 wt %), in the temperature scope of 277.1−283 K and pressure span of 0.114−0.428 MPa and also for R410a or R507 refrigerants, in the existence of various concentrations of magnesium chloride salt (2.407 and 4.942 wt %), within the temperature and pressure scope of 274.3−293 and 0.154−1.421 MPa, respectively, utilizing isochoric pressure examination method.[75] The findings of their investigation demonstrate that magnesium chloride salt can facilitate the transfer of the equilibrium diagram of refrigerants to zones with higher pressures and lower temperatures via the thermodynamic inhibition effect. Furthermore, the inhibitory capacity of salts on various refrigerants was observed to follow the sequence R410a < R134a < R507. Sylva et al. examined equilibria conditions of CH_4 hydrate in the existence of intermediate salts, including sodium chloride, calcium chloride, silver nitrate, copper sulfate, iron chloride, iron sulfate, and magnesium sulfate, at concentrations ranging approximately from 1.60 to 11.74 wt % for NaCl, 3.00 to 20.59 wt % for $CaCl_2$, 4.55 to 27.50 wt % for $AgNO_3$, 4.32 to 26.19 wt % for $CuSO_4$, 3.48 to 23.40 wt % for $FeCl_2$, 4.15 to 25.86 wt % for $FeSO_4$, and 3.33 to 22.07 wt % for $MgSO_4$, using the differential scanning calorimeter (DSC) method.[76] The findings have demonstrated that the suppression of CH_4 hydrate formation by various salts occurred in the following order: $FeCl_3$ > NaCl > $CaCl_2$ > ≈ $AgNO_3$ ≈ $MnSO_4$ > $CuSO_4$ ≈ $FeSO_4$. Additionally, it was observed that salts comprising larger sulfate anions exhibited a lesser reduction in dissociation temperature as opposed to salts incorporating smaller chloride anions. Conversely, a lesser reduction in dissociation temperature was noted for salts containing smaller Fe^{2+} cations when compared to those containing larger cations such as Ag^+ and Mn^{2+}. Cai et al. explored the decomposition circumstances of cyclopentane (CP)−methane binary sII-type hydrate in the existence of sodium chloride salt in concentrations of 3.5 and 7 wt % within the pressure scope of 1.09−3.26 MPa, by means of the isochoric method.[77] The research conducted by the aforementioned individuals has demonstrated that the utilization of inhibitors with elevated concentrations evokes a shift in the locus of the hydrate equilibria diagram toward regions of lesser temperatures and higher pressures. Additionally, it has been observed that at a concentration of 3.5 wt % of sodium chloride, the dissociation temperature was reduced to approximately 1 K. Furthermore, at a concentration of 7 wt % of sodium chloride, the dissociation temperature experienced a reduction of approximately 3 K. Holzammer et al. considered the efficiency of sodium chloride injection on the creation of CO_2 hydrate.[78] Their research has demonstrated that the inclusion of sodium chloride salt in solution leads to the encirclement of Na^+ and Cl^- ions by hydrate shells that contain water molecules. The disruption of water molecule interactions has resulted in the creation of weakened hydrogen bonds. Conversely, salt, comparable to water, displays polar properties, whereas most gases, including CO_2, exhibit nonpolar properties. The polar nature of water molecules makes them more susceptible to adsorption onto the polar ions of salt as opposed to the nonpolar molecules of CO_2. As a result, a smaller amount of water molecules was available to construct hydrate shelves around carbon dioxide, resulting in a reduction in CO_2 solubility. The outcomes of their findings indicate that an augmentation in salinity has led to a diminution in the temperature of CO_2 hydrate creation. At the maximum injection salt concentration of 20 wt %, the hydrate formation temperature was observed to have diminished by 12 K.

Hu et al. evaluated the equilibrium circumstances of CH_4 hydrate formation in the existence of a mixture of brine solution containing sodium chloride, potassium chloride,

https://doi.org/10.1021/acs.jced.5c00025
J. Chem. Eng. Data XXXX, XXX, XXX−XXX

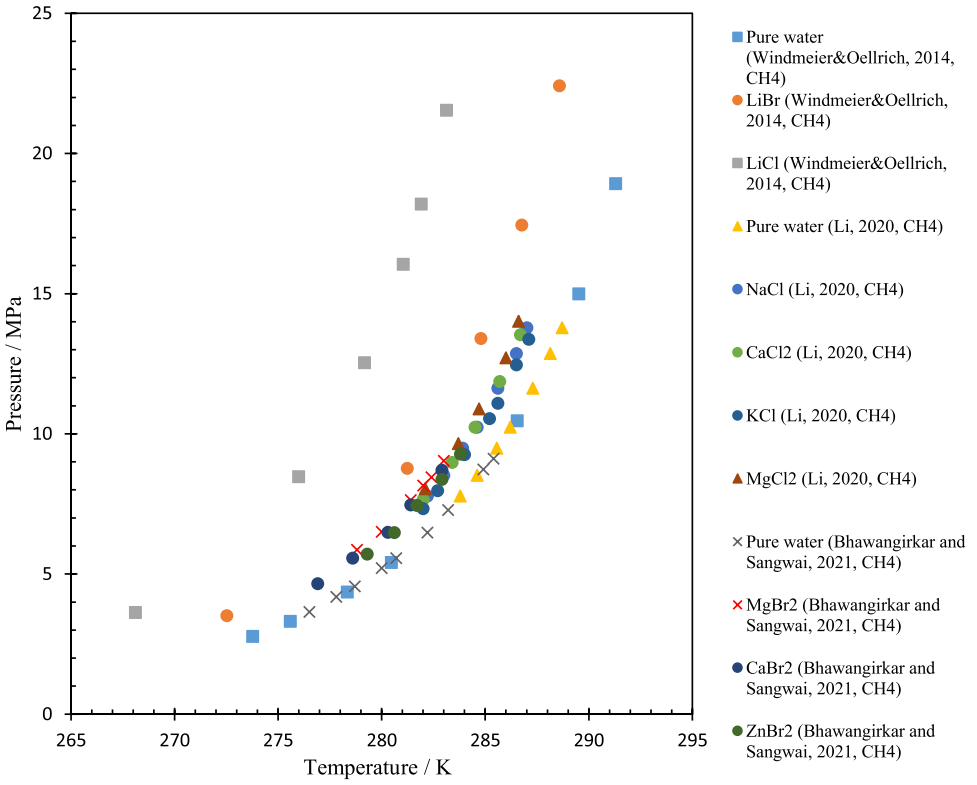

Figure 5. Comparison between the equilibria diagram of distinct gas hydrates in the company of diverse salts, including CH_4 gas and LiCl and LiBr salts,[74] CH_4 gas and NaCl, KCl, $CaCl_2$, and $MgCl_2$ salts,[83] and CH_4 gas and $MgBr_2$, $CaBr_2$, and $ZnBr_2$ salts.[85]

calcium chloride, and magnesium chloride with a maximum concentration of 29.2 wt % in the pressure span of 20−200 MPa utilizing isochoric method.[79] The research conducted by the scholars has demonstrated that the Ca^{2+} ion holds a greater potential for inhibition in comparison to K^+ ion, owing to its greater flux density. As a consequence, the inhibitory power of the salts in isolation and the combination of salts can be expressed as KCl < $CaCl_2$ and NaCl + KCl < NaCl + $CaCl_2$, respectively. Furthermore, the calcium chloride salt has exhibited a more significant inhibitory effect than the sodium chloride salt, due to the lower inhibitory potential of the Na^+ cation in opposition to Ca^{2+}.

Ho-Van et al. inspected the equilibria circumstances of cyclopentane hydrate in the existence of sodium chloride, potassium chloride, calcium chloride, and a mixture of sodium chloride and potassium chloride salts in 0−23 wt % and concentrations of 0−20 wt % of potassium chloride and calcium chloride using isochoric method.[80] The experiments conducted by the researchers demonstrated that a rise in the concentration of salts triggers a significant reduction in the equilibrium temperature. Furthermore, it was detected that calcium chloride and sodium chloride salts, in amounts above and below 16% by weight, respectively, exhibited the most pronounced inhibitory impact on cyclopentane hydrate. Additionally, the inhibitory potential of various salts in concentrations below 16 wt % was observed to be in the order of KCl < NaCl-KCl < $CaCl_2$ < NaCl, whereas in concentrations above 16 wt %, the order was KCl < NaCl-KCl < NaCl < $CaCl_2$. Lv et al. considered the equilibrium circumstances of the CH_4−C_5H_{10} hydrate system containing different ions (K^+, Na^+, Mg^{2+}, Ca^{2+}, Cl^-, and SO_4^{2-}).[81] The findings of their experiments have manifested that the suppression effect of ions can be enhanced through the increase of charge and decrease of radius. The role of ion radius outweighs that of ion charge in altering the equilibrium conditions of hydrates. Additionally, the temperature required for hydrate formation exhibits a decrease as ion concentration increases. Furthermore, the inhibition influences of cations and anions were observed to follow the order of Mg^{2+} > Ca^{2+} > Na^+ > K^+ and Cl^- > SO_4^{2-}, respectively.

Choi et al. inspected the equilibria situations of Pentafluoroethane hydrate in the existence of sodium chloride salt in mass fractions of 0.035 and 0.08, in the temperature span of 276.6−283.8 K and the pressure of 0.16−0.89 MPa, applying isochoric method.[82] The outcomes of the investigation demonstrate that sodium chloride displays thermodynamic inhibitory attributes through modification of the equilibrium diagram of pentafluoroethane hydrate, resulting in areas with reduced temperatures and elevated pressures. Additionally, the inhibitory characteristics of sodium chloride have been observed to increase in tandem with concentration escalation. Conversely, the potential of NaCl to generate inhibitory traits can be linked to the interference of sodium chloride ions with the hydrogen ties of guest water particles.

Li et al. utilized isochoric step-heating to evaluate the phase equilibria circumstances of CH_4 hydrate at temperatures and pressures ranging from 281.9 to 287.1 K and 7.14−33.02 MPa, respectively, in the existence of 3.5 wt % salts of $CaCl_2$, KCl, NaCl, and $MgCl_2$ individually.[83] Their research showed $MgCl_2$ salt had the best performance among all salts in inhibiting methane hydrate creation. Pourranjbar et al. scrutinized the impact of tetra-*n*-butyl ammonium chloride (TBAC) additive at mass fractions of 0.05 and 0.20, and sodium chloride and magnesium chloride at a mass fraction of 0.05 on methane hydrate formation.[84] The present study employed the isochoric pressure examination technique with the step-by-step heating

https://doi.org/10.1021/acs.jced.5c00025
J. Chem. Eng. Data XXXX, XXX, XXX−XXX

Table 3. Studies Pertaining to the Formation of Gas Hydrates in the Existence of Ionic Salts

author (publication date)	gas	type of thermodynamic inhibitor	concentration of inhibitor (wt %)	T/K	P/MPa	result	ref
Lu et al. (2001)	CH_4, C_3H_8	NaCl, $CaCl_2$, KCl, $MgCl_2$, $MgSO_4$	0−17.725 Cl^-, 9.606 SO_4^{2-}, 4.598 Na^+, 2.43 Mg^{2+}	274−283	3−8.2	the influence of gas hydrate constancy in an electrolyte solution is more significantly affected by anions compared to cations	66
Jager and Sloan (2001)	CH_4	NaCl	6.208, 10.83, 17.15, 21.997	270.66−303.48	6.60−72.26	sodium chloride salt possesses an inhibition impact on methane hydrate	67
Atik et al. (2006)	CH_4	NaCl, $CaCl_2$, $MgCl_2$	1, 5, 10, 15 $MgCl_2$, 17.05 $CaCl_2$, 5 NaCl + 6.09 $MgCl_2$	237−229	11.11−22.93	magnesium chloride salt acted as the best inhibitor among all salts	68
Mohammadi et al. (2008)	CH_4,	NaCl, $CaCl_2$, KCl	5 NaCl, 5, 10 KCl, 5, 15 $CaCl_2$	268−283.6	3.39−9.01	calcium chloride had the highest inhibition effect	69
	C_2H_6,			270−284.7	0.44−2.90		
	C_3H_8,			272−276.2	0.18−0.46		
	CO_2			270.2−280.2	1.37−3.73		
Mohammadi et al. (2009)	CH_4	NaBr, KBr, $MgCl_2$, K_2CO_3, $CaBr_2$	5, 10 NaBr, KBr, $MgCl_2$, K_2CO_3, 5, 15 $CaBr_2$	272.5−285.5	2.85−11.90	magnesium chloride showed the most significant inhibitory effect	70
Haghighi et al. (2009)	CH_4	NaCl, KCl, $MgCl_2$	15, 20 NaCl, 15 KCl, 10 $MgCl_2$	268.55−287.38	3.93−26.50	potassium chloride salt showed the most negligible inhibition effect	71
Sabil et al. (2010)	CO_2-THF	NaCl	3.172, 9.116, 14.58	275−305	0.9−7.10	NaF < KBr < NaCl < NaBr < $CaCl_2$ < $MgCl_2$	72
		KCl	2.04				
		$CaCl_2$	3.002, 5.857				
		$MgCl_2$	2.586, 5.067				
		KBr	3.212, 6.253				
		NaF	1.157, 2.30				
		NaBr	2.789, 5.453				
Ngema et al. (2014)	R134a	NaCl	5, 10, 15	268.1−280.6	0.086−0.383	the inhibition efficiency of sodium chloride on the equilibrium conditions of different refrigerants was R410a < R507 < R143a	73
	R410a, R507		5, 10	273.9−290.9	0.226−1.345		
Windmeier and Oellrich (2014)	CH_4	LiBr	5, 10, 15, 20	260−290	2.7−22.5	LiCl < LiBr	74
		LiCl	5, 10, 15, 26.55				
Ngema et al. (2016)	R134a,	$MgCl_2$	2.407, 4.947, 7.633	277.1−283	0.114−0.428	the inhibitory power of salts on different refrigerants was R410a < R134a < R507, respectively	75
	R410a, R507		2.407, 4.947	274.3−293	0.154−1.421		
Sylva et al. (2016)	CH_4	NaCl	1.604, 3.172, 6.208, 11.74	273.1−286	5.51−9.65	$FeCl_3$ > NaCl > $CaCl_2$ > ≈ $AgNO_3$ ≈ $MnSO_4$ > $CuSO_4$ ≈ $FeSO_4$	76
		$CaCl_2$	3.002, 5.857, 11.165, 20.166				
		$AgNO_3$	4.523, 8.694, 16.134, 27.884				
		$CuSO_4$	4.261, 8.212, 15.309, 26.648				
		$FeCl_2$	3.414, 6.634, 12.553, 22.39				
		$FeSO_4$	4.064, 7.847, 14.679, 25.693				
		$MgSO_4$	3.248, 6.321, 11.997, 21.506				
Cai et al. (2016)	CH_4−C_5H_{10}	NaCl	3.5, 7	288.5−296.9	1.09−3.26	using an amount of 3.5 wt % of sodium chloride, the dissociation temperature was reduced by about 1 K; at a concentration of 7 wt % of sodium chloride, the dissociation temperature was decreased by about 3 K	77
Holzammer et al. (2016)	CO_2	NaCl	2.8, 5.5, 10.7, 15.5, 20	268−283	5−15	increasing the salinity has led to a diminution in the temperature of CO_2 hydrate creation	78
Hu et al. (2017)	CH_4	NaCl, $CaCl_2$, KCl, $MgCl_2$	5.2 NaCl + 6.6 KCl, 5 NaCl + 9.5 $CaCl_2$, 6.9 NaCl + 9.3 $CaCl_2$, 9.5 NaCl + $CaCl_2$, 8.9 NaCl + 14.6 $MgCl_2$, 15.7 $CaCl_2$ + 13.5 $MgCl_2$, 10.4 NaCl + 8.2 $CaCl_2$ + 7.1 $MgCl_2$, 2.1 NaCl + 2.6 KCl + 3.9 $CaCl_2$ + 3.4 $MgCl_2$, 6.7 NaCl + 8.6 KCl + 4.3 $CaCl_2$ + 3.7 $MgCl_2$	238.15−333.15	20−200	KCl < $CaCl_2$, NaCl + KCl < NaCl + $CaCl_2$	79

https://doi.org/10.1021/acs.jced.5c00025
J. Chem. Eng. Data XXXX, XXX, XXX−XXX

Table 3. continued

author (publication date)	gas	type of thermodynamic inhibitor	concentration of inhibitor (wt %)	T/K	P/MPa	result	ref
Ho-Van et al. (2018)	C_5H_{10}	NaCl, KCl, $CaCl_2$	0−23 NaCl, 0−20 KCl, 0−22 NaCl + KCl, 0−25 NaCl + $CaCl_2$	253.55−280.85		the inhibitory power of different salts in concentrations below 16 wt % was KCl < NaCl−KCl < $CaCl_2$ < NaCl and in concentrations above 16 wt % as KCl < NaCl−KCl < NaCl < $CaCl_2$	80
Lv et al. (2018)	CH_4−C_5H_{10}	NaCl, $CaCl_2$, KCl, Na_2SO_4, $MgCl_2$	0.23, 0.46, 0.69 Na^+, 0.391, 0.782, 1.173 K^+, 0.355, 0.709, 1.064 Cl^-, 0.122, 0.243, 0.365 Mg^{2+}, 0.48, 0.961, 1.441 SO_4^{2-}	287−300	0.7−5.5	the inhibition effect of cations and anions was Mg^{2+} > Ca^{2+} > Na^+ > K^+ and Cl^- > SO_4^{2-}	81
Choi et al. (2019)	C_2HF_5	NaCl	3.5, 8	276.6−283.8	0.16−0.89	sodium chloride can show thermodynamic inhibition properties	82
Li et al. (2020)	CH_4	NaCl, $CaCl_2$, KCl, $MgCl_2$	3.5	281.9−287.1	7.14−33.02	magnesium chloride salt had the best performance among all salts	83
Pourranjbar et al. (2020)	CH_4	NaCl, $MgCl_2$, $C_{16}H_{36}ClN$	5, 20 $C_{16}H_{36}ClN$, 5 NaCl, $MgCl_2$	282.2−291.8	1.27−5.46	increasing the concentration of $C_{16}H_{36}ClN$ to 20 wt %, along with the concentration of 5 wt % of salts, the equilibrium diagram of CH_4 hydrate formation is transferred to areas with lower temperatures, so in this case, thermodynamic inhibition property was observed	84
Bhawangirkar and Sangwai (2021)	CH_4	$MgBr_2$, $CaBr_2$, $ZnBr_2$	0.1, 0.25, 0.5, 0.75, 1, 3, 5, 10, 15	276.5−285.4	3.65−9.56	$MgBr_2$ > $CaBr_2$ > $ZnBr_2$	85
Porgar and Rahmanian (2022)	CH_4 + C_2H_6			274.8−304.1	1.28−6.08	CH_3OH > NaCl > KCl	86
	C_2H_6	CH_3OH, NaCl, KCl	5	277.8−287.2	0.99−9.99		

https://doi.org/10.1021/acs.jced.5c00025
J. Chem. Eng. Data XXXX, XXX, XXX−XXX

procedure to investigate the effects of various concentrations of TBAC additive, as well as NaCl and $MgCl_2$ salts, on the equilibrium temperature of CH_4 hydrate formation. The temperature and pressure scope of the study were 282.2−291.8 K and 1.27−5.46 MPa, respectively. The outcomes of the examination discovered that the TBAC additive, at both 5 and 20 wt % concentrations, acted as a promoter of CH_4 hydrate stability conditions by increasing the equilibrium temperature of CH_4 hydrate formation by 8 and 12 K, respectively. Additionally, when used in conjunction with 5 wt % concentrations of sodium chloride and magnesium chloride salts, the TBAC additive, at a mass fraction of 0.05, exhibited inhibition influences on CH_4 hydrate creation by increasing the equilibrium temperature of CH_4 hydrate creation by 11 and 14 K, respectively. Furthermore, when the concentration of TBAC was increased to 20 wt %, along with the concentration of 5 wt % of salts, the equilibria diagram of CH_4 hydrate formation was altered to areas with lower temperatures, thus exhibiting thermodynamic inhibition property.

Bhawangirkar and Sangwai investigated the effect of various concentrations of salts (0.1, 0.25, 0.5, 0.75, 1, 3, 5, 10, 15 wt %) including $MgBr_2$, $CaBr_2$, and $ZnBr_2$ on the formation conditions of CH_4 in the temperature scope of 276.5−285.4 K and pressure scope of 3.65−9.56 MPa, utilizing the isochoric pressure examination method.[85] The research findings indicate that the utilization of salts at low concentrations ranging from 0.1 to 0.75 wt % does not substantially inhibit CH_4 hydrate. Nonetheless, the inhibition influence is observed to rise considerably beyond 1 wt % and is markedly high at 3 wt % salt concentration. Furthermore, it is evident that the potency of salts inhibition augments with their increasing concentrations. Finally, based on the hydrated radii, which are $Mg^{2+} > Ca^{2+} > Zn^{2+}$, it can be deduced that the inhibitory potential of various salts diminishes in the descending order of $MgBr_2 > CaBr_2 > ZnBr_2$.

Porgar and Rahmanian considered the formation conditions of the dual mixture of CH_4 and C_2H_6 with a different CH_4 content in the temperature scope of 274.8−304.1 K and pressure span of 1.28−6.08 MPa and also the equilibrium circumstances of pure C_2H_6 in the existence of different inhibitors including methanol, potassium chloride, and sodium chloride in a mass fraction of 0.05 and the temperature and pressure scope of 277.8−287.2 K and 0.99−9.99 MPa, respectively.[86] The outcomes showed that the higher the CH_4 content in the mixture of CH_4 and C_2H_6, the higher the pressure of hydrate formation would be. Moreover, in the case of pure C_2H_6 without and with additives, the outcomes showed that the effectiveness of diverse inhibitors in 5 wt % was decreased in the form of $CH_3OH > NaCl > KCl$.

The equilibria diagram of CH_4 hydrate in the presence of different salts including lithium bromide and lithium chloride at the concentration of 10 wt % is shown in Figure 5, which has been taken from the research of Windmeier and Oellrich.[74] In addition, the equilibrium circumstances of CH_4 hydrate from the research of Li et al. are depicted in the concentration of 3.5 wt % of sodium chloride, calcium chloride, potassium chloride, and magnesium chloride,[83] and by considering the research of Bhawangirkar and Sangwai, the equilibrium diagram of CH_4 hydrate is drawn in the existence of 20 wt % of magnesium bromide, calcium bromide, and zinc bromide.[85] As is demonstrated in Figure 5, it is quite apparent that the various additives, including LiCl, $MgCl_2$, and $MgBr_2$, display vastly superior inhibitory effects when compared to other salts within each respective system. This notable phenomenon can be primarily attributed to the ionic radius and ion charge values, wherein salts exhibiting higher charge densities (i.e., greater ionic charge) possess relatively smaller ionic radii. Consequently, there is an increase in the strength of the electrostatic interaction between the ions and water molecules, which leads to a considerable disturbance in the interaction between water molecules. The aforementioned perturbation consequently results in a decline in water activity, ultimately culminating in a substantial inhibition of hydrate creation in comparison to the other salts present.

According to the findings of research on gas hydrate inhibition in the presence of diverse salts, it can be posited that these materials impede hydrate creation via transformation into cationic and anionic ions within a solution. Subsequently, they engage with the dipoles present in water via a potent electrostatic force, leading to a lessening in water activity and a shift in hydrate phase equilibria lines toward regions of lesser temperatures and greater pressures. The inhibition capacity of salts is primarily recognized by their ion charge density. Higher charge densities, arising from large ion charges or small ionic radii, result in more significant inhibition effects, disrupting hydrogen bonds more effectively and impeding the creation of the hydrate structure of water. Additionally, it is worth noting that anions hold a more prominent position in determining the constancy of gas hydrates in an electrolytic solution, in comparison to cations. This occurrence can be linked to the distinct hydration properties of cations and anions in an electrolyte solution, as hydrated anions possess a much stronger ability to disrupt the water network by weakening H-bonds of water molecules. Overall, for different hydrate systems in the presence of various salts and ions, $MgCl_2$ salt and Mg^{2+} ions are recognized as superior inhibitors compared to other salts, respectively. A summary of studies of different gas hydrates in the presence of different types of salt inhibitors is given in Table 3. To summarize, the key findings in the field of salts are as follows:

- Salts are effective thermodynamic inhibitors due to their ability to dissociate into cations and anions in a solution, decreasing water activity and shifting the hydrate equilibrium to lower temperatures and higher pressures.
- Sodium chloride is one of the most extensively studied salts and widely used as a gas hydrate inhibitor in industrial applications like drilling operations. Its inhibitory effect increases with concentration.
- The anion component of salts plays a more significant role in inhibiting gas hydrate formation than the cation. Chlorine anions (Cl^-) have a stronger impact on hydrate stability than the cations.
- Magnesium chloride exhibits superior inhibitory properties compared to other salts such as sodium chloride and potassium chloride, especially at higher concentrations.
- The charge density of the cations and the ionic radius of the anions are critical in determining the inhibitory capacity of salts. Salts with higher charge densities (smaller ionic radii and higher ionic charge) are more effective at disrupting water molecules and preventing hydrate formation.
- Hydrated anions are more effective than cations in disturbing the water network, weakening hydrogen

https://doi.org/10.1021/acs.jced.5c00025
J. Chem. Eng. Data XXXX, XXX, XXX−XXX

bonds, and shifting the hydrate equilibrium, thus enhancing inhibition.

- The combination of salts like magnesium chloride and sodium chloride shows enhanced inhibition compared to individual salts.
- Calcium chloride also demonstrates strong inhibitory effects, particularly at higher concentrations, and is more effective than sodium chloride due to its greater ion charge density.
- Salts, especially those with higher charge densities, offer a promising, cost-effective solution for industrial applications where gas hydrate inhibition is critical, such as in oil and gas transportation.

4.4. Commercial Inhibitors of Alcohols and Glycols. Commercial inhibitors, including alcohols and glycols, are extensively utilized as thermodynamic inhibitors for impeding the formation of hydrate masses. This procedure of prevention involves the creation of hydrogen bonds with water particles through the hydroxyl group, thus hindering the process of hydrate creation. In the field of chemical engineering, this is a widely accepted practice.[18] Methanol and monoethylene glycol, for example, are often utilized in concentrations of up to around 60% to inhibit hydrate formation in pipelines. It should be stated that alcohols are more volatile than glycols, resulting in their rapid evaporation at upstream points and subsequent transport to cold points of the pipeline through the gas stream. Furthermore, methanol has a lower viscosity compared to monoethylene glycol, and its high vapor pressure leads to methanol loss in the gas phase. The amount of inhibitor used varies depending on operational conditions, although their high consumption often necessitates the use of a recovery unit.[15,21,24] Methanol recycling is a complex and costly process; hence, these materials are typically consumed without recycling. However, it is worth noting that methanol regeneration is more commonly employed in Russia and CSTO states. As a result, if the aim is to inhibit hydrate formation at high flow rates, monoethylene glycol is often the preferred thermodynamic inhibitor. The usage of diethylene glycol and triethylene glycol as thermodynamic inhibitors in industry is limited due to their low inhibitory efficacy, although they are broadly employed in gas dehydration processes.[87]

Wu et al. investigated the creation circumstances of natural gas hydrates (including 85 mol % CH_4, 2.5 mol % CO_2, 11 mol % C_2H_6, 1 mol % C_3H_8, and 0.5 mol % H_2O) in the existence of methanol and monoethylene glycol inhibitors utilizing the method of lowering of the freezing point.[88] The investigation conducted by the authors exhibited that adding inhibitors to the reactor, while maintaining the same pressure, led to a reduction in the temperature of hydrates creation. Additionally, the pressure of hydrate formation was observed to have increased under the same temperature conditions. Furthermore, it was noted that the application of greater inhibition values resulted in a substantial decrease in temperature. Additionally, subsequent to the inclusion of the inhibitor, the unloaded masses disrupted the network of liquid water molecules, which arise from hydrogen bonding, through the creation of several interaction forces with water molecules. Based on the findings of the experiments, it was concluded that the addition of 10 wt % of methanol and glycol can effectively impede the creation of hydrates within the reactor. Afzal et al. measured the equilibria circumstances of CH_4 and CO_2 hydrates in the existence of a thermodynamic inhibitor of triethylene glycol in the temperature range of 264.8−275.8 K for CH_4 hydrate and 264.7−282.6 K for CO_2 hydrate by using the isochoric experimental method.[89] The concentration of triethylene glycol inhibitor used in the experiment was 5, 10, 15, and 20 wt % for CO_2 hydrate and 24.5, 40, and 50 wt % for CH_4 hydrate. The findings have established that the existence of triethylene glycol has impeded the development of both CH_4 and CO_2 hydrates. As the inhibitor concentration increased, the hydrate equilibrium diagram has shifted toward regions characterized by lower temperatures, thus suggesting a more pronounced inhibitory effect.

Afzal et al. evaluated the equilibrium circumstances of CH_4, C_2H_6, C_3H_8, and CO_2 hydrates in the presence of diethylene glycol inhibitor, in the temperature span of 274.3−282.5 K for CH_4 hydrate, 275.7−285.7 K for C_2H_6 hydrate, 272.2−277 K for C_3H_8 hydrate, and 272.1−281.4 K for CO_2 hydrate using isochoric method.[90] The thermodynamic inhibitor concentrations used in their experiments for CH_4, C_2H_6, C_3H_8, and CO_2 hydrates were 6.6 and 16.8, 7.1 and 16.3, 7.3 and 16.4, and 7.4 and 16.3 wt %, respectively. The findings have demonstrated that the formation of hydrates for the gases in the experiments experienced inhibition as a result of the presence of diethylene glycol. Furthermore, an escalation in the amount of the inhibitor led to an alteration of the hydrate equilibrium diagram toward regions with lower temperatures. This shift is indicative of an enhancement in the effectiveness of diethylene glycol as an inhibitor. Mohammadi et al. examined hydrate equilibrium conditions of C_2H_6 and C_3H_8 gases in the presence of methanol, monoethylene glycol, and triethylene glycol inhibitors with mass fractions of 0.05 and 0.15, in the temperature span of 268.2−281.5 and 266.3−276.8 K for C_2H_6 and C_3H_8 hydrate, respectively, by using isochoric experimental method.[91] The findings indicate that the presence of methanol, ethylene glycol, and triethylene glycol unveiled a hindrance effect on the hydrate creation circumstances of C_2H_6 and C_3H_8 gases. Furthermore, it was detected that the hydrate equilibrium figure moved to regions with lesser temperatures upon the augmentation of inhibitor concentration, signifying the inhibition effect of inhibitors. Conversely, the inhibitory potency of distinct inhibitors increased in the subsequent order: triethylene glycol < monoethylene glycol < methanol.

Mohammadi et al. considered the phase equilibria circumstances of CH_4 hydrate in the existence of poly(ethylene glycol) inhibitor with a mole fraction of approximately 400 g/mol (PEG-400) by the isochoric pressure examination method.[92] The temperature scope of the experiment in the presence of inhibitor with concentrations of 10 and 40 wt % was 276.8−287.3 and 276.1−285.6 K, respectively. The study executed by the investigators has illustrated that the aqueous resolution comprising a minimal level of inhibitor PEG-400 (10 wt %) does not have a substantial impact on the disintegration state of CH_4 hydrate. Conversely, at high concentrations, this effect is non-negligible. The existence of a mass fraction of 0.4 of poly(ethylene glycol) has resulted in the thermodynamic hindrance efficiency, which has decreased the decomposition temperature of CH_4 hydrate by about 4 K. Additionally, it should be asserted that the introduction of inhibitors, specifically ethylene glycol, diethylene glycol, and triethylene glycol at a mass fraction of 0.4 has significantly decreased the dissociation temperature by about 16, 10.5, and 8.5 K, respectively. Therefore, the inhibitory power of poly(ethylene glycol) on CH_4 hydrate is much lower than

https://doi.org/10.1021/acs.jced.5c00025
J. Chem. Eng. Data XXXX, XXX, XXX−XXX

that of ethylene glycol, diethylene glycol, and triethylene glycol inhibitors.

Mohammadi and Richon scrutinized an analysis of the circumstances of equilibrium for hydrates of C_2H_6, CO_2, and H_2S in the existence of ethylene glycol inhibitors with varying mass fractions of 0.1, 0.2, 0.35, and 0.5 and CH_4 hydrate equilibrium condition in the existence of methanol with mass fractions of 0.55 and 0.65, utilizing the isochoric pressure examination method.[93] The inquiry carried out by the scholars has evinced that the relocation of the hydrate creation zone to regions of lesser temperatures occurs with an augmentation in the concentration of inhibitors. Furthermore, the methanol inhibitor exhibited superior inhibitory performance when compared to ethylene glycol and methanol. In addition, studies have indicated that with regard to the inhibitory potency of ethylene glycol concerning various hydrates of gases, the mean equilibria temperature of CO_2 hydrate has experienced a greater decline than C_2H_6 and H_2S gases. Moreover, the mean equilibria temperature of H_2S hydrate has undergone a lesser decrease compared to C_2H_6 hydrate in the existence of the ethylene glycol substance. Maekawa measured the equilibrium circumstances of CO_2 hydrate in the existence of aqueous solutions of methanol, ethanol, ethylene glycol, diethylene glycol, triethylene glycol, and glycerol inhibitors at the temperature range of 264.1−283.1 K and pressure up to a maximum of 4.54 MPa, utilizing the isochoric step-heating method.[94] The inquiry conducted by the researchers has yielded substantiation that the presence of diverse chemical compounds has led to a reduction in the equilibria temperature associated with the decomposition of CO_2 hydrate. Additionally, the equilibrium diagram has been found to shift toward the left of the region associated with hydrate decomposition. Also, the inhibition impact of diverse inhibitors based on mass fraction was in the form of triethylene glycol < diethylene glycol < glycerol < monoethylene glycol < ethanol < methanol, respectively.

Mohammadi and Richon presented a comprehensive exposition on the equilibria circumstances of CH_4 hydrate in the existence of thermodynamic inhibitors comprising ethylene glycol (at a weight percentage of 65%), diethylene glycol (at weight percentages of 20, 35, and 50%), and triethylene glycol (at weight percentages of 20, 35, and 50%), over a temperature range of 247.4−250.7, 265.0−283.2, and 266.3−284.6 K, respectively, utilizing the isochoric pressure examination method.[95] The findings of their research have revealed that the inhibitory ability of inhibitors on the formation conditions of CH_4 hydrate follows the order of triethylene glycol < diethylene glycol < monoethylene glycol. The aforementioned statement suggests that the existence of a monoethylene glycol inhibitor prompts a significant displacement of the CH_4 hydrate equilibrium figure to the left of the hydrate equilibrium diagram when in the existence of unadulterated water.

Maekawa conducted a study to evaluate the state of equilibria of C_2H_6 hydrate under the influence of aqueous solutions containing methanol, ethanol, ethylene glycol, diethylene glycol, triethylene glycol, and glycerol.[96] The study was carried out utilizing the isochoric method and involved subjecting the hydrate to a range of temperatures between 261.6 and 285.9 K, as well as pressures of up to 3.12 MPa. Concentrations of glycerol, diethylene glycol, and triethylene glycol inhibitors used in the experiments were 10, 20, 30, 40, and 50 wt %, concentrations of ethylene glycol were 10, 20, 30, and 40 wt %, and the concentrations of ethanol and methanol were 10, 20, and 30 wt %. The findings of their investigation have revealed that the existence of certain chemicals impedes the circumstances required for the creation of C_2H_6 hydrate. The degree of inhibition based on mass fraction manifested itself in the following hierarchy: methanol > ethanol > ethylene glycol > diethylene glycol ≈ glycerol > triethylene glycol.

Cha et al. surveyed the equilibria circumstances of artificial natural gas hydrate, containing CH_4 (0.90 mole fraction), C_2H_6 (0.06 mole fraction), C_3H_8 (0.03 mole fraction), and *n*-C_4H_{10} (0.01 mole fraction) in the temperature scope of 269.7−294.7 K and the existence of ethylene glycol inhibitor at 0.10, 0.30, and 0.50 mass fractions.[97] The findings indicate that synthetic gas hydrate can be formed under specific conditions at a pressure of 10 MPa without the existence of monoethylene glycol inhibitor, given a temperature of 293.9 K. With the inclusion of monoethylene glycol inhibitor at concentrations of 10, 30, and 50 wt %, at the same pressures, the equilibria temperature of natural gas hydrate formation was detected to be 291.6, 284.5, and 270.9 K, respectively. This indicates a depression in equilibrium temperature (ΔT_{eq}) of 2.3, 9.4, and 23 K in the presence of inhibitor, relative to the unadulterated water.

Mech et al. directed an inquiry into the equilibria circumstances of CH_4 hydrate when exposed to an aqueous solution of poly(ethylene glycol) with varying molecular weights—200 (PEG-200), 400 (PEG-400), and 600 (PEG-600) kg/kmol—at mass fractions ranging from 0.077 to 0.46.[98] This study was carried out within the temperature scope of 270.75−281.45 K and pressure range of 4.60−7.05 MPa, utilizing the isochoric pressure examination procedure. The outcomes divulged those inhibitors possessing a smaller molecular weight, particularly PEG-200, manifested a more substantial inhibitory impact in dropping the temperature of CH_4 hydrate creation than those possessing greater molecular mass, despite having comparable mass fractions. Conversely, when comparing similar mole fractions at 0.022, the prevention influence was more significant for PEG-600 than PEG-200, with an augmentation in concentration. Interestingly, at lesser concentrations of the same mole fraction (0.007), the poly(ethylene glycol) inhibitor with a molecular weight of 200 kg/kmol had a more profound impact on dropping the temperature of CH_4 hydrate creation than the 600 kg/kmol counterpart. Additionally, when considering the identical mass proportion (e.g., 0.2) of ethylene glycol and poly(ethylene glycol), it was detected that ethylene glycol illustrated a higher capability of prevention for the CH_4 hydrate system compared to poly(ethylene glycol). However, it has been noticed that when the mass fraction of PEG-200 reaches 0.4, the inhibition effect is significantly greater than that of ethylene glycol at a mass fraction of 0.2 and 0.1. In comparison, the prevention impact of a mass fraction of 0.2 of PEG-200 is similar to that of a mass fraction of 0.2 of ethylene glycol. Furthermore, the stage equilibria figures of PEG-400 and PEG-600 suppressors at 0.4 mass fraction virtually coincide with the figure at 0.2 mass fraction of ethylene glycol.

Maekawa conducted an in-depth investigation into the equilibrium conditions of xenon gas hydrate, with a focus on its interaction with aqueous solutions of alcoholic, glycolic, and glycerol.[99] The study was carried out over the temperature scope of 263.6−289.6 K and the pressure with the maximum range up to 1 MPa, utilizing the isochoric approach. The amounts of methanol, ethanol, and ethylene glycol inhibitors

https://doi.org/10.1021/acs.jced.5c00025
J. Chem. Eng. Data XXXX, XXX, XXX−XXX

used in the experiment were 10, 20, and 30 wt %, and the amounts of glycerol, diethylene glycol, and triethylene glycol were 20 and 40 wt %. Their research has substantiated that the adding of chemicals to water has brought about a diminution in the equilibrium temperature of xenon hydrate. This has led to the conclusion that these substances have acted as inhibitors of xenon hydrate. In addition, it was noticed that the inhibitory influence, based on mass fraction, was in the order of methanol > ethanol > ethylene glycol > diethylene glycol ≈ glycerol > triethylene glycol. Ferrari et al. explored the equilibrium circumstances of CO_2 hydrate, in the existence of 5 and 10 wt % of ethanol, in the temperature scope of 275.65−281.65 K and pressured up to 3.5 MPa, utilizing the isothermal method.[100] Their research demonstrated that the introduction of ethanol caused a displacement in the equilibria figure of hydrate toward regions considered by lower temperature and higher pressure. This outcome serves as an indicator of the thermodynamic hindrance exerted by ethanol on CO_2 hydrate. Akhfash et al. examined the effect of injection of monoethylene glycol and methyl diethanolamine inhibitors in preventing the creation of CH_4 hydrate and a methane, ethane, propane, and carbon dioxide gases mixture hydrate.[101] The findings indicate that, when comparing equal injection rates, monoethylene glycol exhibited nearly twice the efficiency of methyl diethanolamine in reducing the temperatures at which hydrate phase boundaries occur. Additionally, methyl diethanolamine was observed to produce a shift in hydrate phase boundaries ranging from 0.3 to 0.8 K. Furthermore, a decrease in the efficacy of both monoethylene glycol and methyl diethanolamine as thermodynamic inhibitors of hydrate has been noted. For instance, in a gas mixture system containing 21.719 wt % of monoethylene glycol, the addition of 7.231 wt % of methyl diethanolamine resulted in the prevention of hydrate formation at a level equivalent to 22.41 wt % of monoethylene glycol. Liu et al. conducted an examination of the phase equilibria circumstances of quaternary sour gases consisting of CH_4/CO_2/H_2S/N_2 in both methanol−water solutions and pure water.[102] The three samples of gas used in their research with different percentages of gases are given in Table 4.

Table 4. Composition of the Three Samples of Gas Utilized in the Research Conducted by Liu et al.[102]

component	M_1	M_2	M_3
CH_4	82.51	73.54	85.02
CO_2	11	17.5	9.47
H_2S	3.49	6.96	9.47
N_2	3	2	0.5

The outcomes of their investigations have demonstrated that the creation of hydrates for sour gas assortments in the existence of H_2S and CO_2 gases takes place at significantly higher temperatures under given pressures or lower pressures at given temperatures than methane hydrate. However, compared to pure H_2S hydrate, it occurs at much higher pressures. In addition, the formation pressures of such sour gases have been observed to decrease with an increase in the total amount of CO_2 and H_2S in the feed gas, according to the hydrate formation data of M_1 and M_2 samples in distilled water. For the M_3 sample, the total amount of CO_2 and H_2S was approximately the same as for the M_1 sample and much lower than that of the M_2 sample. Nevertheless, the M_3 sample has shown the lowest hydrate formation pressure at all temperatures, mainly due to the gradual increase of the mole fraction of H_2S from M_1, M_2 to M_3. Furthermore, the concentration value of N_2 has decreased from M_1, M_2 to M_3, which could reduce the hydrate formation pressures of gases. However, the changes in N_2 concentration are much less than those in H_2S. Therefore, it can be inferred that the formation conditions of hydrates for sour gases depend on the concentration of gas components, with hydrogen sulfide playing the most crucial role. On the other hand, for sample M_1 in the existence of methanol (15 wt %)−water solution, sample M_2 in the existence of methanol (20 wt %)−water, and sample M_3 in the existence of methanol (30 wt %)−water was found that, unlike distilled water, injection of methanol into water substantially augmented the hydrate creation pressure of the tested sour gases at all temperatures. For example, for the M_1 sample at a temperature of 277.65 K, the pressure obtained was 5.33 MPa, which is twice as much as distilled water (∼2.25 MPa). In addition, for the formation of hydrates of samples M_1 and M_2 in the prepared methanol−water solution, although for the second sample 5 wt % more than methanol was used, however, when the experiment temperature was less than the approximate temperature of 279.4 K, the creation pressure of M_2 sample hydrate is still lesser than the M_1 sample, which is the same as the experimental data obtained in distilled water. Nevertheless, after a temperature of 279.4 K, the M_2 sample showed a much higher hydrate formation pressure than the M_1 sample. These results indicated that the suppressive influence of methanol on the creation of CH_4/CO_2/H_2S/N_2 quaternary sour gases had a nonlinear relationship with the augmentation of methanol concentration in a solution comprising water.

Xu et al. measured synthetic gas hydrate equilibrium conditions, including CH_4 (91.12 mol %), C_2H_6 (5.03 mol %), C_3H_8 (1.49 mol %), n-C_4H_{10} (0.37 mol %), i-C_4H_{10} (0.32 mol %), n-C_5H_{12} (0.12 mol %), i-C_5H_{12} (0.16 mol %), n-C_6H_{14} (0.41 mol %), n-C_7H_{16} (0.033 mol %), CO_2 (0.48 mol %), and N_2 (0.46 mol %) in the presence of methanol (5, 10, 15, and 35 wt %) and ethylene glycol (5, 10, 15, 35, 40, and 55 wt %) inhibitors, in the temperature range of 267.74−298.53 K and the pressure of 4.22−34.72 MPa, utilizing isochoric pressure examination procedure on high pressure apparatus.[103] Their study has indicated that the movement of the hydrate equilibrium diagram toward the suppression zone can be achieved through an increase in the concentration of inhibitors. Furthermore, it was observed that the thermodynamic restraining impact of methanol proved to be more potent in comparison to that of ethylene glycol, when the same mass fraction was taken into account. For instance, once the amount of methanol and ethylene glycol was 5 wt %, a temperature depression of 2.5 and 1.25 K was observed, respectively. This particular observation brings to the fore the more pronounced inhibitory impact of methanol relative to ethylene glycol.

Saberi et al. explored the stimulus of the existence of ethylene glycol inhibitor on the creation condition of synthetic natural gas hydrates, including CH_4 (0.8040 mole fraction), C_2H_6 (0.1030 mole fraction), C_3H_8 (0.055 mole fraction), n-C_4H_{10} (0.0072 mole fraction), i-C_4H_{10} (0.0165 mole fraction), N_2 (0.0011 mole fraction), and CO_2 (0.0182 mole fraction), in the temperature scope of 289.9−294.1 K and pressure scope of 3.90−8.20 MPa, using step-heating method.[104] The outcomes demonstrate that the balance temperature of synthetic gas hydrate, while utilizing ethylene glycol inhibitor with a weight concentration of 10 and 20%, encountered a decrease of approximately 2.5 and 5 K, respectively. This serves as

https://doi.org/10.1021/acs.jced.5c00025
J. Chem. Eng. Data XXXX, XXX, XXX−XXX

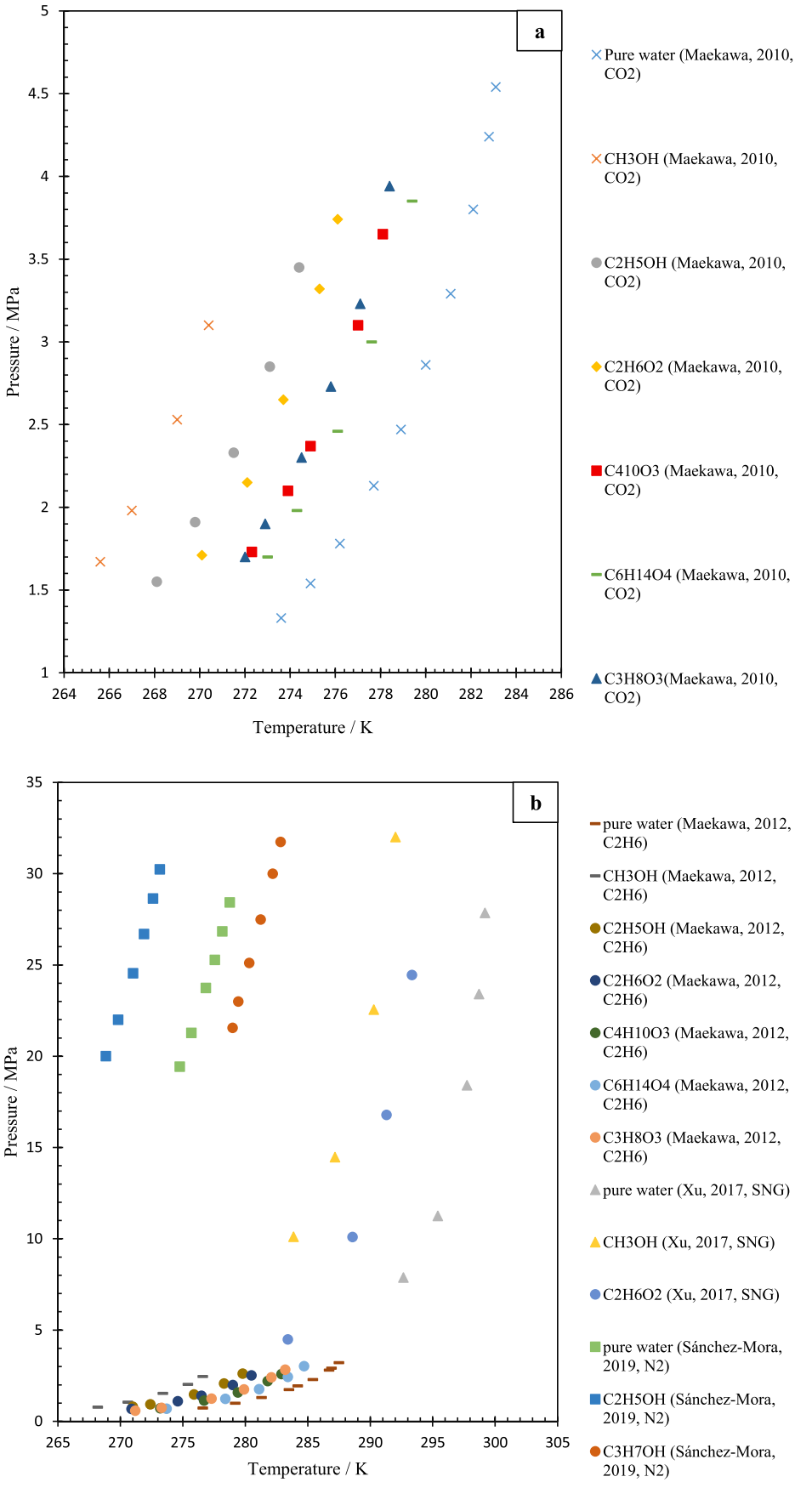

Figure 6. Comparison between the equilibria diagram of various gas hydrates in the existence of various commercial additives. (a) CO_2 gas with CH_3OH, C_2H_5OH, $C_2H_6O_2$, $C_4H_{10}O_3$, $C_6H_{14}O_4$, and $C_3H_8O_3$;[74] (b) C_2H_6 gas with CH_3OH, C_2H_5OH, $C_2H_6O_2$, $C_4H_{10}O_3$, $C_6H_{14}O_4$, and $C_3H_8O_3$,[96] synthetic gas hydrate with CH_3OH and $C_2H_6O_2$,[103] and N_2 gas with C_2H_5OH and C_3H_7OH.[106]

https://doi.org/10.1021/acs.jced.5c00025
J. Chem. Eng. Data XXXX, XXX, XXX−XXX

evidence for the inhibitory impact of ethylene glycol on hydrate.

Adisasmito and Parubak studied the influence of monoethylene glycol injection in gas transmission pipelines located in deep water on the creation circumstances of synthetic gas hydrates, the chief part of which includes CH_4 (87.24% mol), C_2H_6 (3.973 mol %), C_3H_8 (2.758 mol %), and CO_2 (1.254 mol %).[105] Based on the findings of their research, it can be inferred that, in the absence of ethylene glycol, alterations in production flow rate under comparable operational parameters, such as fluid composition, temperature, pressure, and pipeline dimensions, result in similar behavior of hydrate diagrams. Consequently, it can be deduced that changes in flow rate will not have a considerable influence on the conditions of hydrate creation. Nonetheless, a slight reduction in the production flow rate facilitates the hydrate creation conditions with a rise in temperature. Furthermore, the introduction of monoethylene glycol with a concentration of 0.6 wt % causes a decrease in hydrate creation temperature from 293.039 to 257.15 K, and for a greater dosage, the injection of monoethylene glycol in each of the production flow rates brings about a more substantial lessening of hydrate formation temperature. This indicates that the hydrate equilibrium diagram has transferred to the left of the area where there is a risk of hydrate formation. Sánchez-Mora et al.[106] have conducted an exploration into the experimental measurement of gas hydrate decomposition circumstances in systems that include CO_2/N_2 + ethanol/1-propanol/tetrabutylammonium fluoride/tetrabutylammonium bromide + H_2O. The alcohols were injected in mass fractions of 0.05, 0.10, 0.20, and 0.30, tetrabutylammonium fluoride in mass fractions of 0.05 and 0.10, and tetrabutylammonium bromide in mass fractions of 0.05 and 0.30.[106] The results of their study indicate that ethanol exhibited an inverse relationship with the dissociation temperature in the CO_2 hydrate system. The aforementioned observation suggests that the elevation in the quantity of ethanol triggers a decrement in the decomposition temperature of CO_2 hydrate, thereby signifying the thermodynamic hindrance of ethanol in the given system. Furthermore, increasing the concentration of tetrabutylammonium fluoride/tetrabutylammonium bromide in the CO_2 hydrate system and 75 mol % CO_2 + 25 mol % N_2 hydrates system, respectively, increased the hydrate dissociation temperature, which indicates the promotion effect of these substances. On the other hand, in the N_2 + ethanol + H_2O system at four different ethanol concentrations, it was found that the thermodynamic hindrance influence occurred with the addition of ethanol and augmented with growing ethanol concentration. This occurrence can be associated with the disruption caused by the thermodynamic inhibition in the hydrogen bonding arrangement among water particles. This disturbance makes the conversion of all water to hydrate arduous, thereby altering the hydrate equilibria figure to the prevention zone. Moreover, the results of the data obtained from the hydrate phase equilibria of the nitrogen + 1-propanol + water system with four different concentrations of 1-propanol showed that, unlike ethanol, injecting 1-propanol into the system resulted in the thermodynamic promotion effect, which was observed by increasing equilibrium temperature or decreasing equilibrium pressure that was due to the inclusion of 1-propanol molecules in hydrate cages. The promotion influences are also amplified by increasing the mass fraction of 1-propanol by only 20 wt %. However, in the mass fraction of 0.30 of this substance, a slight decrease has been observed because of the excessive existence of 1-propanol particles that are not surrounded by the hydrate enclosures, so in this case, it might act as a thermodynamic inhibitor.

Deka et al. evaluated the inhibitory efficacy of CH_4 hydrate by propylene glycol at the pressure scope of 70−190 bar by visual method and sapphire cell under isothermal conditions (constant pressure).[107] revealed that the equilibrium diagram of CH_4 hydrate, when coupled with propylene glycol inhibitor, experienced a shift toward regions with lower temperatures. Furthermore, the suppression equilibrium temperature of methane hydrate formation, when subjected to 20 wt % of propylene glycol, was recorded as 10.42 °C. Additionally, their report comparing the inhibitory potential of propylene glycol and monoethylene glycol demonstrated that the propylene glycol inhibitor exhibited a superior inhibition effect on CH_4 hydrate.

Aminolroayaei et al. scrutinized the experimental gas hydrate equilibria data of 99 mol % CH_4 + 1 mol % H_2S in the existence of 10, 15, and 20 wt % of monoethylene glycol within the temperature and pressure scope of 276.65−288.95 and 6.16−12.30 MPa, respectively, utilizing the stepwise heating isochoric pressure examination method.[108] The outcomes have demonstrated that the incorporation of a concentration ranging from 10 to 20 wt % of monoethylene glycol can effectively relocate the hydrate phase to the inhibition region. This shift occurs as the suppression temperature escalates from 2.47 to 6.17, which is directly proportional to the corresponding concentration of monoethylene glycol that is raised from 10 to 20 wt %.

Figure 6a,b portrays a graphical representation of the state of equilibrium between CO_2 and C_2H_6 gases in the company of methanol, ethanol, ethylene glycol, diethylene glycol, triethylene glycol, and glycerol, with a weight percentage of 20%, as observed in the research conducted by Maekawa.[94,96] Moreover, the equilibria diagram of synthetic gas hydrate is delineated under the influence of methanol and ethylene glycol, with a weight percentage of 15%, as observed in the research carried out by Xu et al.[103] Lastly, based on the survey of Sánchez-Mora et al., the equilibria circumstances of N_2 gas are depicted in the concentration of 20 wt % of ethanol and 1-propanol.[106] The graphical representation (Figure 5) demonstrates that methanol exhibits a remarkably superior inhibition effect in comparison to other chemical compounds. Additionally, when examining various glycols, it can be postulated that monoethylene glycol possesses the capability to act as an inhibitor that effectively impedes the formation of hydrates to a greater extent than other glycols.

Expounding on the outcomes of extensive research on commercial inhibitors, it can be stated that the inhibitory mechanism of this specific cohort of chemicals is predominantly linked to the existence of the hydroxyl group. These inhibitors act as a deterrent to the formation of hydrate masses by engaging in the formation of hydrogen ties with water particles via their hydroxyl cluster. However, among the gamut of commercial inhibitors, methanol has been identified as the unparalleled inhibitor, possessing the most substantial influence on the thermodynamic circumstances of different gas hydrates. Furthermore, the inhibitory prowess of glycolic inhibitors was observed to follow the order of monoethylene glycol > diethylene glycol > triethylene glycol > poly(ethylene glycol), respectively. Moreover, the quantum of commercial inhibitors requisite for different processes is subject to the

https://doi.org/10.1021/acs.jced.5c00025
J. Chem. Eng. Data XXXX, XXX, XXX−XXX

operational conditions. Nevertheless, their consumption is relatively exorbitant, necessitating the need for a recovery unit. Methanol recycling is a convoluted and expensive process; hence, these materials are typically utilized without recycling. As such, if the objective is to inhibit at high flow rates, the thermodynamic inhibitor of monoethylene glycol is often the preferred option. Table 5 summarizes the studies performed on the phase equilibria of gas hydrates while utilizing commercial inhibitors derived from the alcohol and glycol family. To summarize, the key findings in the field of commercial inhibitors are as follows:

- Alcohols and glycols function as thermodynamic inhibitors by forming hydrogen bonds with water molecules through their hydroxyl group, thereby impeding hydrate formation.
- Methanol and monoethylene glycol are commonly used in concentrations up to 60% to prevent hydrate formation, especially in pipelines. Methanol is more volatile and has a lower viscosity than monoethylene glycol, which makes it prone to evaporation in upstream points.
- Methanol, due to its high vapor pressure, tends to evaporate rapidly, leading to its loss in the gas phase. This makes it less efficient at high flow rates. In contrast, monoethylene glycol is often preferred at higher flow rates, though methanol regeneration is more common in specific regions (e.g., Russia).
- Although triethylene glycol is used in industry, it is less effective as a hydrate inhibitor compared to methanol and monoethylene glycol. Its low inhibitory efficacy restricts its use primarily to gas dehydration processes.
- Increasing the concentration of inhibitors (e.g., methanol, monoethylene glycol, triethylene glycol) shifts the hydrate equilibrium to lower temperatures and higher pressures, indicating enhanced inhibitory effects.
- Among glycols, the inhibitory effectiveness decreases in the order: monoethylene glycol > diethylene glycol > triethylene glycol > poly(ethylene glycol).
- The use of glycolic inhibitors, such as monoethylene glycol, requires a recovery unit due to the high consumption rate. Recycling methanol is complex and costly, leading to its usage without recycling in most scenarios.
- Methanol was consistently found to have the most significant impact on hydrate formation, with its inhibitory effectiveness surpassing that of other glycols and alcohols.
- PEG-400 showed the least effect as a hydrate inhibitor, especially in comparison with other glycols like ethylene glycol and diethylene glycol.
- Monoethylene glycol is particularly effective in gas transmission pipelines, especially in deep-water applications, where its introduction leads to a significant reduction in hydrate formation temperature.
- Ethylene glycol and ethanol also exhibited substantial inhibitory effects, with ethanol showing superior performance over other glycols in some systems.

4.5. Simultaneous Effect of Commercial Inhibitors, Including Alcohols or Glycols with Salts. In certain circumstances, the utilization of an inhibitor alone may not be feasible due to various concerns, including the absence of high subcooling temperature, financial constraints, and limited funds allocated to the establishment of chemical recovery units. Hence, the concept of synergy has garnered more attention. The principal purpose of the synergy is to augment the effectiveness of hydrate inhibition by selecting inhibitors that possess distinct functional groups and diverse mechanisms. The impediment of gas hydrate creation may be accomplished with greater efficacy through the application of substances that feature a hydroxyl group, as it is capable of establishing hydrogen bonds. Conversely, commercial inhibitors, namely, alcohols, glycols, and salts, have exhibited widespread efficacy in impeding the creation of gas hydrates in the realm of petroleum. Therefore, it is imperative to undertake a comparative study of the inhibitory power and synergistic effect of these two categories of chemicals.

Majumdar et al. steered a survey to evaluate the state of equilibria of H_2S, CO_2, and C_2H_6 hydrates in the existence of ethylene glycol aqueous solutions (at 15 and 30 wt %) and sodium chloride aqueous solutions (at 10 and 15 wt %) separately and simultaneously, within the temperature scope of 264−290 K and pressure scope of 0.23−3.18 MPa.[109] The study conducted by the aforementioned individuals has demonstrated that sodium chloride exhibits a more pronounced inhibitory effect when compared to ethylene glycol. Sun et al.'s[110] inquiry explored the requisite circumstances for hydrate decomposition in a gas amalgam comprising CH_4, C_2H_6, and C_3H_8. The examination was undertaken in the existence of an aqueous solution of ethylene glycol at 0.10, 0.20, and 0.30 mass fraction, as well as electrolytes such as sodium chloride and calcium chloride at 0.05 and 0.10 mass fraction. The pressure examination method was utilized in the study while implementing temperature and pressure ranges of 0.78−8.1 MPa and 263.52−288.96 K, respectively.[110] Upon analysis of the equilibria data derived from the conducted research, it has been deduced that the mixture of 0.10 mass fraction ethylene glycol and 0.10 mass fraction sodium chloride solutions displays a more pronounced inhibition impact, compared to its counterpart comprising 0.10 mass fraction ethylene glycol and 0.10 mass fraction calcium chloride solutions. Therefore, it can be inferred that sodium chloride is a more effective inhibitor as compared to calcium chloride. Additionally, as per the experimental data, it has been established that for the 0.10 mass fraction ethylene glycol and 0.10 mass fraction calcium chloride solution compared with the 0.20 mass fraction ethylene glycol solution, calcium chloride displays a lower inhibition effect than ethylene glycol, based on mass fraction. Hence, the inhibitory efficacy of different inhibitors follows the order of ethylene glycol < calcium chloride < sodium chloride, respectively.

Eichholz et al. conducted an inquiry into the potential impact of utilizing a blend of inhibitors comprising ethylene glycol and sodium chloride on the formation of CH_4 hydrate.[111] The findings of this research endeavor were disseminated in varying concentrations within the temperature span of 262−282 K and pressures ranging between 2.1 and 9.5 MPa. In accordance with their empirical evidence, the concomitant action of sodium chloride and ethylene glycol at 3.77 and 23.88 wt %, respectively, vis-a-vis the scenario in which the concentration of ethylene glycol was 3.77 wt %, was observed to elicit a shift in equilibrium toward lesser temperatures and greater pressures. As a result, the temperature at which hydrate creation occurs was detected to decline with the augmentation of ethylene glycol quantity, while the pressure exhibited an upward trend. Masoudi et al. investigated

https://doi.org/10.1021/acs.jced.5c00025
J. Chem. Eng. Data XXXX, XXX, XXX−XXX

Table 5. Research Studies on the Subject of Gas Hydrate Creation in the Existence of Commercial Inhibitors from the Family of Alcohols and Glycols

author (publication date)	gas	type of thermodynamic inhibitor	concentration of inhibitor (wt %)	T/K	P/MPa	result	ref
Wu et al. (2007)	NG mix. including CH_4, C_2H_6, C_3H_8, CO_2	CH_3OH, $C_2H_6O_2$	10, 20	259−312	1−9	by adding 10 wt % of methanol and glycol, the creation of hydrates inside the reactor can be effectively prevented	88
Afzal et al. (2007)	CO_2	$C_6H_{14}O_4$	5, 10, 15, 20	264.7−282.6	0.61−4.23	the presence of triethylene glycol inhibited the creation of CH_4 and CO_2 hydrates	89
	CH_4		24.5, 40, 50	264.8−275.8	3.07−5.12		
Afzal et al. (2008)	CH_4	$C_4H_{10}O_3$	6.6, 16.8	274.3−282.5	3.91−8.02	the presence of diethylene glycol inhibited the hydrate creation circumstances of the gases used in the experiments	90
	C_2H_6		7.1, 16.3	275.7−285.7	0.84−2.80		
	C_3H_8		7.3, 16.4	272.2−277	0.23−0.50		
	CO_2		16.3	272.1−281.4	1.43−3.83		
Mohammadi et al. (2008)	C_2H_6	CH_3OH, $C_2H_6O_2$, $C_6H_{14}O_4$	5, 15	268.2- 281.5	0.49−2.60	$CH_3OH > C_2H_6O_2 > C_6H_{14}O_4$	91
	C_3H_8			266.3−276.8	0.20−0.47		
Mohammadi et al. (2009)	CH_4	PEG-400	10	276.8−287.3	3.58−11.90	the low concentration of inhibitor PEG-400 (10 wt %) in an aqueous solution had almost no hindrance impact on the decomposition circumstances of CH_4 hydrate, while this efficacy was non-negligible at high concentrations	92
			40	276.1−285.6	5.15−17.37		
Mohammadi and Richon (2010)	CH_4	CH_3OH, $C_2H_6O_2$	10, 20, 35, 50 MEG, 55, 65 methanol	234.5−248.4	3.16−10.76	the methanol inhibitor performed better than ethylene glycol	93
	C_2H_6			251.6−278.5	0.39−1.29		
	CO_2			249.9−277.8	1.18−2.86		
	H_2S			262.7−287.8	0.13−1.02		
Maekawa (2010)	CO_2	CH_3OH, C_2H_5OH, $C_2H_6O_2$, $C_4H_{10}O_3$, $C_6H_{14}O_4$, $C_3H_8O_3$	10, 20 CH_3OH, C_2H_5OH, 10, 20, 30 $C_2H_6O_2$, $C_4H_{10}O_3$, 10, 20, 30, 40 $C_6H_{14}O_4$, 20, 30 $C_3H_8O_3$	264.1−283.1	1.33−4.54	$CH_3OH > C_2H_5OH > C_2H_6O_2 > C_3H_8O_3 > C_4H_{10}O_3 > C_6H_{14}O_4$	94
Mohammadi and Richon (2011)	CH_4	$C_2H_6O_2$	65	247.4−250.7	10.38−18.32	$C_2H_6O_2 > C_4H_{10}O_3 > C_6H_{14}O_4$	95
		$C_4H_{10}O_3$	20, 35, 50	265.0−283.2	4.94−14.50		
		$C_6H_{14}O_4$	20, 35, 50	266.3−284.6	4.64−12.52		
Maekawa (2012)	C_2H_6	CH_3OH, C_2H_5OH, $C_2H_6O_2$, $C_4H_{10}O_3$, $C_6H_{14}O_4$, $C_3H_8O_3$	10, 20, 30, 40, $C_3H_8O_3$, $C_4H_{10}O_3$, $C_6H_{14}O_4$, 10, 20, 30, 40 $C_2H_6O_2$, 10, 20, 30 CH_3OH, C_2H_5OH	261.6−285.9	0.59−3.12	$CH_3OH > C_2H_5OH > C_2H_6O_2 > C_3H_8O_3 \approx C_4H_{10}O_3 > C_6H_{14}O_4$	96
Cha et al. (2013)	synthetic NG contains a mix. of CH_4, C_2H_6, C_3H_8, n-C_4H_{10}	$C_2H_6O_2$	10, 30, 50	269.7−294.7	4.8−11.4	increasing the concentration of monoethylene glycol leads to an increase in its inhibition power	97
Mech et al. (2015)	CH_4	PEG-200, PEG-400, PEG-600	7.7, 20, 40, 44, 46	270.75−281.45	4.60−7.05	the suppressive efficacy of methane hydrate creation is more pronounced in low molecular weight PEG-200 as compared to PEG-400 and PEG-600 in equal mass fractions	98
Maekawa (2016)	xenon	CH_3OH, C_2H_5OH, $C_2H_6O_2$, $C_4H_{10}O_3$, $C_6H_{14}O_4$, $C_3H_8O_3$	10, 20, 30 CH_3OH, C_2H_5OH, $C_2H_6O_2$, 20, 40 $C_3H_8O_3$, $C_4H_{10}O_3$, $C_6H_{14}O_4$	263.6−289.6	0.145−0.981	$CH_3OH > C_2H_5OH > C_2H_6O_2 > C_3H_8O_3 \approx C_4H_{10}O_3 > C_6H_{14}O_4$	99
Ferrari et al. (2016)	CO_2	C_2H_5OH	5, 10	275.65−281.65	1.65−3.59	the addition of ethanol led to an alteration in the equilibria diagram of CO_2 hydrate toward areas with lower temperatures and higher pressures	100
Akhfash et al. (2017)	Pure CH_4 and a mix of CH_4, C_2H_6, C_3H_8, CO_2	$C_2H_6O_2$, $C_5H_{13}NO_2$	3.099, 7.231 $C_5H_{13}NO_2$, 7.231 $C_5H_{13}NO_2$ + 21.719 $C_2H_6O_2$	280.09−290.42	5.70−8.87	at equal injection rates, monoethylene glycol was almost twice as efficient as methyl diethanolamine in shifting the hydrate stage boundaries to lower temperatures	101

https://doi.org/10.1021/acs.jced.5c00025
J. Chem. Eng. Data XXXX, XXX, XXX−XXX

Table 5. continued

author (publication date)	gas	type of thermodynamic inhibitor	concentration of inhibitor (wt %)	T/K	P/MPa	result	ref
Liu et al. (2017)	$CH_4/CO_2/H_2S/N_2$ quaternary sour gases	CH_3OH	15, 20, 30	270.15−292.15	1.27−8.41	methanol injection into water considerably augmented the hydrate creation pressure of the tested sour gases at all temperatures	102
Xu et al. (2017)	synthetic gas hydrates include mixtures of CH_4, C_2H_6, C_3H_8, n-C_4H_{10}, i-C_4H_{10}, n-C_5H_{12}, i-C_5H_{12}, n-C_6H_{14}, n-C_7H_{16}, N_2, CO_2	CH_3OH, $C_2H_6O_2$	5, 10, 15, 35 CH_3OH, 5, 10, 15, 35, 40, 55 $C_2H_6O_2$	267.74−298−53	4.22−34.72	the thermodynamic hindrance impact of methanol was more substantial than that of ethylene glycol	103
Saberi et al. (2018)	synthetic NG including mixtures of CH_4, C_2H_6, C_3H_8, n-C_4H_{10}, i-C_4H_{10}, N_2, CO_2	$C_2H_6O_2$	10, 20	289.9−294.1	3.90−8.20	ethylene glycol inhibited synthetic natural gas hydrates by reducing the hydrate equilibria temperature by about 2.5 and 5 K in 10 and 20 wt %, respectively	104
Adisasmito and Parubak (2019)	synthetic NG	$C_2H_6O_2$	0.6, 0.668, 0.737	239.26−293.78	0.34−16.54	changing the flow rate will not affect the hydrate formation condition much; the addition of monoethylene glycol led to a decrease in hydrate formation temperature	105
Sánchez-Mora et al. (2019)	CO_2, N_2, CO_2 + N_2	C_2H_5OH, C_3H_8O, $C_{16}H_{36}FN$, $C_{16}H_{36}BrN$	5, 10, 20, 30 C_2H_5OH, C_3H_8O, 5, 10 $C_{16}H_{36}FN$, 5, 30 $C_{16}H_{36}BrN$	262.87−294.52	0.79−33.06	tetrabutylammonium fluoride/tetrabutylammonium bromide and 1-propanol had promotion effects; ethanol showed the thermodynamic inhibition effect	106
Deka et al. (2021)	CH_4	$C_3H_8O_2$, $C_2H_6O_2$	20	271.65−289.65	7−12	the propylene glycol inhibitor had a better inhibition effect than monoethylene glycol	107
Aminolroayaei et al. (2022)	CH_4 + H_2S	$C_2H_6O_2$	10, 15, 20	276.65−288.95	6.16−12.3	adding the concentration of 10−20 wt % of monoethylene glycol could substantially alter the hydrate stage to the inhibition zone	108

equilibria circumstances of CH_4 hydrate in the existence of concentrations of 21.3, 23, 30.8, and 35 wt % ethylene glycol along with sodium chloride (12 and 15 wt %) or potassium chloride (8 and 10 wt %) salts at pressures up to 50 MPa, using step-heating method.[112] Their research has demonstrated that the synergistic effect of salt and ethylene glycol has triggered a significant rise in the inhibition of CH_4 hydrates. Moreover, it has been observed that the concentration of inhibitors directly impacts the inhibition conditions. Additionally, the findings have indicated that the inhibitory influence of ethylene glycol is less than sodium chloride salt.

Masoudi et al. evaluated the equilibria circumstances of CH_4 hydrate in the existence of amounts of 14, 15, 15.3, and 18 wt % of calcium chloride along with the commercial inhibitor of ethylene glycol (13.4, 14, 21.3, and 26 wt %), at pressures up to 50 MPa using step-heating method.[113] It has been determined that the addition of salt and ethylene glycol has a positive stimulus on the inhibition potency of hydrate. Moreover, the inhibitory effect of calcium chloride on the CH_4 hydrate has been observed to exceed that of ethylene glycol.

Najibi et al. examined the impact of salts and their thermodynamic inhibition on the hydrate equilibrium condition along with commercial inhibitors on an aqueous solution, including CH_4/water/thermodynamic inhibitor/salt quaternary system, in the pressure scope of 4.27−28.90 MPa, utilizing isochoric step-heating method.[114] The system under investigation in their research included alcohols like methanol (9, 9.2, 14, and 30 wt %) and ethylene glycol (12 and 30 wt %), and prevalent salts like sodium chloride (3 and 8.3 wt %), potassium chloride (7 wt %) and calcium chloride (8 and 10 wt %). Their experiments demonstrated that the synergism of alcohols and salts had a favorable impact on the inhibitory potential of CH_4 hydrate. Additionally, it was observed that the inhibitory strength of methanol surpassed that of ethylene glycol. Mohammadi and Richon considered the decomposition circumstances of CH_4 hydrate in the existence of sodium chloride, potassium chloride, and calcium chloride salts and commercial inhibitors of ethylene glycol and methanol.[70] The isochoric pressure examination technique was employed in their survey, and the concentrations of salts were 5, 10, and 15 wt %, methanol concentrations were 10, 15, and 20 wt %, and the quantity of ethylene glycol used in the experiments was 20 wt %. Also, the temperature range of the experiment for methanol and the salt solution were 253.9−277.5 K, and for ethylene glycol and the salt solution, it was 260.6−278 K. Their research reveals that the interaction between alcohols and salts results in a modification of the hydrate equilibrium diagram, which tends to shift toward regions characterized by a lesser temperature or a greater pressure. Additionally, it has been observed that the concentration of inhibitors positively influences hydrate inhibition. Conversely, experimental data demonstrates that the inhibitory functionality of methanol with salts surpasses that of ethylene glycol and salts solution.

Lee and Kang investigated the inhibition efficacy of ethylene glycol (10−50 wt %) and methanol (10−30 wt %) with a constant concentration of 3.5 wt % of sodium chloride salt on a synthetic gas containing CH_4 (89.86 mol %), C_2H_6 (6.40 mol %), C_3H_8 (2.71 mol %), i-C_4H_{10} (0.48 mol %), n-C_4H_{10} (0.49 mol %), n-C_5H_{12} (0.02 mol %), and N_2 (0.04 mol %), in the temperature scope of 266.2−290.2 K and pressure of 0.99−8.86 MPa.[115] The findings indicate that the introduction of 10 wt % methanol into the system resulted in a temperature reduction of approximately 5 K. Conversely, when a

https://doi.org/10.1021/acs.jced.5c00025
J. Chem. Eng. Data XXXX, XXX, XXX−XXX

comparable concentration of ethylene glycol was added, a temperature decline of approximately 4 K was noted. Alternatively, the inclusion of 3.5 wt % of sodium chloride into a solution containing either ethylene glycol or methanol resulted in a decrease of equilibrium temperature between 2.8 and 3.2 K. Based on empirical evidence, the inhibitory capacity of methanol, either solely or in conjunction with sodium chloride, is greater compared to ethylene glycol as a result of its lower molecular weight.

Mohammadi and Richon[116] undertook an examination of the equilibria circumstances of hydrates containing H_2S and CO_2 in the existence of aqueous solutions. These solutions consisted of varying mass fractions of methanol (0.1, 0.2, 0.3, 0.4, and 0.5), methanol combined with sodium chloride (0.05 mass fraction), and ethylene glycol (0.15 mass fraction) combined with sodium chloride.[116] Their research showed that the augmentation of the methanol inhibitor concentration has the effect of shifting the equilibrium diagram of CO_2 and H_2S hydrates to regions characterized by lesser temperatures and greater pressures. Furthermore, it has been noted that under stable levels of ethylene glycol and sodium chloride inhibitors, CO_2 hydrate is subjected to a more pronounced decrease in temperature in comparison to H_2S. Lafond et al. ascertained the parameters surrounding the CH_4 hydrate phase boundary in the existence of thermodynamic inhibitors of sodium chloride in a concentration of 0.035 mass fraction and methanol in concentrations of 0.05, 0.10, and 0.20 mass fraction, within the pressure span of 7−20 MPa, employing the high-pressure differential scanning calorimeter (DSC) technique.[117] Their study divulged that rising the quantity of methanol improved the inhibition conditions of CH_4 hydrate, which infers that the hydrate equilibria diagram moves to zones with lower temperatures or higher pressures. Chapoy et al. investigated the equilibria circumstances of CH_4 and natural gas hydrates (containing 0.8879 of CH_4, 0.0530 of C_2H_6, 0.1550 of C_3H_8, 0.0017 of i-C_4H_{10}, 0.0030 of n-C_4H_{10}, 0.0100 of n-C_5H_{12}, 0.0168 of CO_2, and 0.0204 of N_2 mole fraction) in the existence of a combination of ethylene glycol (23, 30, and 40 wt %) and sodium chloride (5 and 10 wt %), utilizing the isochoric step-by-step heating method.[118] The outcomes of their experimentation have demonstrated that augmenting the quantity of monoethylene glycol in a steady proportion of sodium chloride has caused a shift of the equilibrium diagram for natural gas hydrate toward a region with a lower temperature. Furthermore, the increase in the concentration of both inhibitors concurrently has resulted in a notable reduction in the equilibria temperature of CH_4 hydrate. To illustrate, when CH_4 gas is at a 5 wt % concentration of sodium chloride and 30 wt % quantity of monoethylene glycol, the equilibrium temperature for hydrate formation was 269.55 K at a pressure of 5.96 MPa. However, upon elevating the amounts of monoethylene glycol and sodium chloride to 40 and 10 wt %, respectively, the equilibrium temperature for CH_4 hydrate formation was reduced to 248.25 K at a pressure of 1.75 MPa.

Nasir et al.[119] evaluated the hydrate equilibrium circumstances of two types of synthetic gas rich in CO_2, including CO_2 (70.353 mol %), C_2H_6 (26.551 mol %), and N_2 (3.096 mol %) (synthetic gas mixture type I) and CO_2 (69.103 mol %), C_2H_6 (26.197 mol %), N_2 (3.1 mol %), CH_4 (0.9 mol %), C_3H_8 (0.3 mol %), i-C_4H_{10} (0.2 mol %), and n-C_4H_{10} (0.2 mol %) (synthetic gas mixture type II), respectively, in the existence of commercial inhibitors of methanol and ethylene glycol along with sodium chloride and calcium chloride salts. The temperature and pressure scope of the experiments were 263.85−284.75 K and 2.76−12.08 MPa, respectively, and the experimental procedure was the isochoric pressure-search technique.[119] Their investigation has revealed that the existence of 10 and 20 wt % of solutions containing ethylene glycol or methanol yields a superior inhibition effect on the second gas mixture in comparison to the first. Conversely, the empirical data suggests that when alcohols are paired with salts, both at a constant concentration of 20 and 10 wt % respectively, the inhibitory potency of sodium chloride in combination with ethylene glycol or methanol surpasses that of the second type of synthetic gas mixture, whereas the first type is concerned. Moreover, the inhibition effect of the mixture of ethylene glycol or methanol with calcium chloride on type II gas mixture was higher than type I. Additionally, in accordance with the findings, it can be posited that the inhibitory influence of methanol supersedes that of ethylene glycol on both types of synthetic gas mixtures. Alqahtani investigated the effect of the existence of 5 wt % of methanol and 10 wt % of sodium chloride, 10 wt % of methanol and 10 wt % sodium chloride, and 10 wt % of methanol and 5 wt % of sodium chloride mixtures on the equilibria circumstances of CO_2 and C_2H_6 hydrate in the temperature ranges of 269.54−272.48 and 269.75−273.01 K and pressure of 1.993−3.092 and 0.674−1.090 MPa, respectively, utilizing isochoric pressure examination method.[5] The findings have indicated that the pressure necessary to generate hydrates in the company of a blend of inhibitors exceeded the pressure essential for the development of hydrates in unpolluted water. Furthermore, the restraining impact on CO_2 and C_2H_6 hydrates experienced a growth in tandem with the escalation in inhibitor mixture concentration. Conversely, the inhibitors solution had a superior restraining impact on CO_2 hydrate creation relative to C_2H_6 hydrate.

Mech and Sangwai's study focused on investigating the equilibria circumstances of CH_4 hydrate in the existence of diverse inhibitors, namely, ethylene glycol, methanol, and sodium chloride.[120] The study delved into two different mass fractions, 0.03 and 0.1, and explored the pressure scope of 2.25−6.43 MPa and temperature scope of 282.28−289.65 K. The isochoric pressure examination approach was employed in the experimentation process. The findings of their study demonstrate that the methanol inhibitor exhibited the utmost efficacy compared with sodium chloride and ethylene glycol in the methane hydrate system, in the existence of tetrabutylammonium bromide and tetrahydrofuran promoters. Additionally, an escalation in the amount of methanol resulted in an increased inhibitory effect on the formation of methane hydrate in the mixed promoter system. At a reduced concentration of sodium chloride, there was an observed increase in the creation of the mixed hydrate, whereas elevated concentrations of sodium chloride exhibited an inhibitory impact. Seo et al. directed an investigation into the equilibrium circumstances of artificial gas hydrates.[121] The composition of these hydrates consisted of CH_4 (0.90 mole fraction), C_2H_6 (0.06 mole fraction), C_3H_8 (0.03 mole fraction), and n-C_4H_{10} (0.01 mole fraction). The study was carried out in the existence of 20 wt % of ethylene glycol solution, with mixtures of either 3.5 or 20 wt % of sodium chloride, as well as an amount of 20 wt % ethylene glycol, utilizing the step-by-step heating method. The inquiry carried out by them has proven that a rise in the quantity of sodium chloride salt triggers a displacement in the equilibria of hydrate toward greater pressures and lesser temperatures. In addition, the combined

https://doi.org/10.1021/acs.jced.5c00025
J. Chem. Eng. Data XXXX, XXX, XXX−XXX

effect of salt and ethylene glycol resulted in a positive efficacy of the inhibitory capabilities of hydrate.

Dastanian et al. scrutinized the decomposition circumstances of CO_2 in the existence of 5 and 10 wt % aqueous solutions of potassium chloride with weight percentages of 10 and 20 methanol or ethylene glycol, using the isochoric pressure-search method.[122] Their research has revealed that the incorporation of inhibitors within the system has resulted in a displacement of the CO_2 hydrate equilibria diagram to lower temperatures and higher pressures. Furthermore, it has been observed that the augmentation of inhibitor concentration has led to a notable enhancement of inhibition conditions. Conversely, upon analysis of experimental data, it has been determined that methanol has exhibited a superior inhibition effect in comparison to ethylene glycol based on mass fractions. Kim et al. measured the decomposition circumstances of synthetic natural gas hydrates, counting CH_4 (0.90 mole fraction), C_2H_6 (0.06 mole fraction), C_3H_8 (0.03 mole fraction), and n-C_4H_{10} (0.01 mole fraction) in the existence of the commercial inhibitor of ethylene glycol (20 wt %) along with sodium chloride salt (3.5, 7, 10, and 20 wt %), utilizing the isochoric step-by-step heating method.[123] The existence of sodium chloride and monoethylene glycol within the aqueous phase appears to reduce the interaction between the hydrated particles through enveloping them with the aforementioned substances. Furthermore, the inhibition effect of hydrate was detected by moving the equilibrium diagram toward areas that possess lower temperature and greater pressure. The data also indicated that rising the salt concentration in an aqueous solution improved hydrate inhibitory circumstances. Accordingly, the hydrate formation temperature depression for a 0.20 mass fraction ethylene glycol, a mixture of 0.07 mass fraction sodium chloride and 0.20 mass fraction ethylene glycol, a mixture of 0.10 mass fraction sodium chloride and 0.20 mass fraction ethylene glycol, and a mixture of 0.20 mass fraction sodium chloride and 0.20 mass fraction ethylene glycol were 5.7, 9.1, 10.2, and 15.6 K, respectively.

Dastanian et al. executed measurements of the CO_2 hydrate's equilibrium circumstances in the presence of aqueous solutions of ethylene glycol or methanol with 10 and 20 wt % concentrations and a calcium chloride concentration of 5 and 10 wt % in the temperature range of 262.2−276.8 K and pressure of 1.49−3.36 MPa by applying the pressure examination approach.[124] According to the findings derived from this particular investigation, it was determined that the concomitant existence of methanol or ethylene glycol synergistically combined with calcium chloride salt demonstrated a beneficial impact on the inhibitory potential of CO_2. Furthermore, it was observed that, in terms of the same mass fraction, methanol exhibited a more pronounced inhibitory effect compared to ethylene glycol. Burgass et al. assessed the hydrate decomposition temperature for a multicomponent synthetic gas mixture (including 0.0219 of N_2, 0.0228 of CO_2, 0.8598 of CH_4, 0.0509 of C_2H_6, 0.0396 of C_3H_8, 0.0016 of i-C_4H_{10}, 0.0026 of n-C_4H_{10}, 0.0004 of i-C_5H_{12}, and 0.0004 of the n-C_5H_{12} mole fraction) in equilibria with deionized water, an aqueous sodium chloride solution, mixed aqueous ethylene glycol/sodium chloride, and ethylene glycol/sodium bromide solutions, applying the isochoric step-by-step heating procedure at pressures up to 150 MPa.[125] The results of their experiments have demonstrated that the equilibria temperature of synthetic gas hydrate is elevated in the existence of a 25 wt % sodium chloride solution, in comparison to the temperature achieved when utilizing the sodium chloride inhibitor (20 wt %) in conjunction with monoethylene glycol. Additionally, an escalation in the concentration of monoethylene glycol inhibitor (30, 40, and 50 wt %) has resulted in the transfer of the hydrate decomposition diagram toward the left of the temperature−pressure diagram, that is, toward regions with lower temperatures. Consequently, the creation of multicomponent gas mixture hydrates is impeded by the existence of monoethylene glycol inhibitor. Conversely, the hydrate equilibrium diagram's geometric location, in the existence of 40 wt % of sodium bromide solution and 40 wt % of ethylene glycol solution, in contrast to the case where solely 40 wt % of sodium bromide was employed, is positioned on the left-hand side of the temperature−pressure curve, that is, at points with lower temperatures and higher pressures. In the study conducted by Kwak and colleagues in 2018, an assessment was made of the phase equilibria states of both unadulterated CH_4 hydrate and a combination of CH_4 and C_3H_8 in the existence of mixtures containing 10 wt % of sodium chloride and 10 or 30 wt % of monoethylene glycol, utilizing the isochoric method.[126] The outcomes of the conducted experiment have signified that the incorporation of inhibitors has resulted in the repositioning of hydrate phase equilibrium boundaries, which have been shifted toward lesser temperatures and greater pressures. Furthermore, an augmentation in the level of the monoethylene glycol inhibitor within a consistent quantity of sodium chloride brought about an additional relocation of the area of stability for the hydrate toward the left of the temperature−pressure diagram. To illustrate, consider the equilibria temperature of CH_4 hydrate in the existence of a combination of 10 wt % monoethylene glycol and 10 wt % sodium chloride, which was observed to be 271.1 K at a pressure of 4.33 MPa. However, when the quantity of monoethylene glycol inhibitor was increased to 30 wt %, the equilibria temperature of hydrate creation reduced to 261.6 K.

Semenov et al. evaluated the hydrate decomposition circumstances of N_2, CO_2, CH_4, C_2H_6, and C_3H_8 gas combinations at concentrations of 3.16, 1.89, 79.55, 3.38, and 12.02 mol %, respectively, in the pressure scope of 0.87−4.70 MPa, and in systems containing a mixture of salts (sodium chloride, potassium chloride, calcium chloride, and magnesium chloride) with a steady amount of 18 wt % in all experiments, and also methanol inhibitor with a concentration of 10, 20, 30, 40, and 50 wt %, utilizing the isochoric approach in high-pressure cell.[127] Their study showed the existence of synergism, which is evident in the significant displacement of equilibrium diagrams toward lower temperatures and higher pressures as compared with systems that only contain a single thermodynamic hydrate inhibitor. The findings designate that the thermodynamic shift of the hydrate detachment temperature, near the brine one, can be achieved by introducing 20 wt % methanol in purified water. Furthermore, it has been observed that when the pressure exceeds 4 MPa, the thermodynamic inhibition can be achieved by combining 20 wt % methanol with brine, which is equivalent to the inhibitory effect of 50 wt % methanol in water. For instance, the equilibria temperature of hydrate decomposition can be reduced to 27.5 K by the blend of 20 wt % of methanol and brine at a pressure of 4 MPa, whereas the injection of 50 wt % methanol at the same pressure can reduce the equilibria temperature of hydrate detachment to 27.6 K. Park et al. explored the state of equilibrium for CH_4 hydrates while taking into account the

https://doi.org/10.1021/acs.jced.5c00025
J. Chem. Eng. Data XXXX, XXX, XXX−XXX

existence of ammonium chloride (5 and 10 wt %) and methanol/ethylene glycol (10 and 20 wt %), in the temperature and pressure ranges of 264−281 K and 4−12 MPa, respectively, using isochoric method.[128] Their research showed that the augmentation of inhibitor concentration has resulted in a notable increase in the inhibitory impact of the assortment of inhibitors. Also, methanol has the best inhibition effect among inhibitors on equilibrium conditions of CH_4 hydrates, and the inhibitory power of mixtures of inhibitors was in the form of 20 wt % methanol/ethylene glycol + 10 wt % ammonium chloride > 20 wt % methanol/ethylene glycol + 5 wt % ammonium chloride > 10 wt % methanol/ethylene glycol + 10 wt % ammonium chloride > 10 wt % methanol/ethylene glycol + 5 wt % ammonium chloride. Mu and Cui investigated the circumstances of hydrate stage equilibria for two artificial gas samples, one with a high amount of carbon dioxide and the other with a low amount (Table 6), in the existence of aqueous solutions containing 5 and 10 wt % of methanol and sodium chloride salt at concentrations of 3.5, 5, and 7.5 wt %, in the temperature scope of 267.71−287.64 K and pressure of 2.118−11.512 MPa, utilizing isochoric pressure examination method.[129] The outcomes of their experimentation have exhibited that a rise in the concentration of inhibitors triggers a reduction in the equilibrium temperature of the hydrate. Consequently, the hydrate inhibition effect of both synthetic gas samples has been enhanced. To illustrate, the addition of 10 wt % methanol and 7.5 wt % sodium chloride to pure water has resulted in the lowering of the equilibrium temperature of type I synthetic gas hydrate by approximately 7.61 K at experimental pressures.

Table 6. Composition of Artificial Natural Gas Samples Applied in the Research Conducted by Mu and Cui (mol %)[129]

component	SNG1	SNG2
CH_4	87.21	72.13
C_2H_6	1.26	1
C_3H_8	0.1	0.07
CO_2	5.08	21.86
N_2	6.35	4.94

Cordeiro et al. conducted an isobaric study to determine the equilibria figures of CO_2 hydrate in the existence of various amounts of ethylene glycol and sodium chloride salts in the pressure range of 8.5−25 MPa.[130] The concentrations studied included 0.10, 0.20, and 0.30 mass fractions of ethylene glycol, 0.05 and 0.10 mass fraction of sodium chloride salts, and a mixture of 0.05 mass fraction sodium chloride with 0.10, 0.20, and 0.30 mass fraction of ethylene glycol. The findings have revealed that the combined effect of sodium chloride and ethylene glycol has exhibited a positive influence on the inhibition potential of CO_2. Additionally, as per the experimental observations, sodium chloride has been found to have a stronger inhibition impact than ethylene glycol when compared at an equivalent mass fraction.

Kim et al. carried out an investigation to evaluate the phase equilibria circumstances of CH_4 hydrate in the existence of sodium chloride, sodium bromide, and sodium iodide salts (5 wt %) and a commercial inhibitor of ethylene glycol (10 wt %), within the temperature scope of 272−283 K and at a pressure of 5.3−11 MPa.[131] The outcomes of their evaluation exposed that the synergy of salts and ethylene glycol had a positive influence on improving the hydrates inhibition efficiency. The inhibitory power of the mixture of inhibitors was reduced in the form of 10 wt % of ethylene glycol + 5 wt % of sodium chloride > 10 wt % of ethylene glycol + 5 wt % of sodium bromide > 10 wt % of ethylene glycol + 5 wt % of sodium iodide.

Behnammotlagh et al. steered an inquiry into mixed ternary gas systems consisting of 0.9416 mol fraction CH_4, 0.0488 mol fraction C_3H_8, and 0.0096 mol fraction H_2S in the existence of 20 wt % monoethylene glycol, as well as in the concurrent existence of 20 wt % monoethylene glycol with salts encompassing 10 wt % calcium chloride, 10 wt % sodium chloride, and 6 wt % calcium chloride + 4 wt % sodium chloride, respectively.[132] The study involved measuring the equilibrium data in the temperature and pressure scope of 276.75−296.05 K and 2.29−12.08 MPa, respectively, utilizing the step-by-step heating isochoric technique. The outcomes of their research experiment have demonstrated that diverse substances have resulted in an alteration in the equilibrium chart of the ternary acidic hydrate comprising CH_4 + C_3H_8 + H_2S toward the left segment of the balance figure for the purified water setup, thereby signifying the efficiency of thermodynamic additives. Moreover, the consequences revealed that the inhibition strength of hydrates decreased as 20 wt % ethylene glycol + 10 wt % sodium chloride > 20 wt % ethylene glycol + 6 wt % calcium chloride + 4 wt % sodium chloride > 20 wt % ethylene glycol + 10 wt % calcium chloride > 20 wt % ethylene glycol.

The equilibria circumstances of different mixture gases in the existence of diverse commercial chemical materials and salts are depicted in Figure 7. The equilibrium diagram of hydrate conditions formation of 91.96 mol % CH_4 + 5.13 mol % C_2H_6 + 2.91 mol % C_3H_8 gas mixture in the existence of 10 wt % $C_2H_6O_2$, 10 wt % $C_2H_6O_2$ + 10 wt % NaCl, and 10 $C_2H_6O_2$ + 10 wt % $CaCl_2$ is drawn by using the research of Sun et al.[110] In addition, from the research done by Lee and Kang, the phase diagram of a gas mixture including 89.86 mol % CH_4 + 6.40 mol % C_2H_6 + 2.71 mol % C_3H_8 + 0.48 *i*-C_4H_{10} + 0.49 *n*-C_4H_{10} + 0.02 *n*-C_5H_{12} + 0.04 N_2 is presented in the presence of 20 wt % CH_3OH, 20 wt % $C_2H_6O_2$, 3.5 wt % NaCl, 20 wt % CH_3OH + 3.5 wt % NaCl, and 20 wt % $C_2H_6O_2$ + 3.5 wt % NaCl.[115] Furthermore, the creation circumstances of a gas assortment of 79.69 mol % CH_4 + 3.25 mol % C_2H_6 + 12.00 mol % C_3H_8 + 3.08 mol % N_2 + 1.98 mol % CO_2 is shown in the existence of 20 wt % CH_3OH, 13.15 wt % NaCl + 2.46 wt % KCl + 1.28 wt % $CaCl_2$ + 1.10 wt % $MgCl_2$, and 20 wt % CH_3OH + 13.15 wt % NaCl + 2.46 wt % KCl + 1.28 wt % $CaCl_2$ + 1.10 wt % $MgCl_2$, by considering Semenov et al.[127] Finally, by investigating the study done by Behnammotlagh et al., the equilibrium drawing of a synthesized gas mixture of 94.16 mol % CH_4, 4.88 mol % C_3H_8, and 0.96 mol % H_2S is plotted in the presence of 20 wt % $C_2H_6O_2$, 20 wt % $C_2H_6O_2$ + 10 wt % $CaCl_2$, 20 wt % $C_2H_6O_2$ + 10 wt % NaCl, and 20 wt % $C_2H_6O_2$ + 4 wt % NaCl + 6 wt % $CaCl_2$.[132] By undertaking a comprehensive comparison of a range of systems, as represented in Figure 6, it can be posited that those systems comprising a blend of inhibitors exhibit a substantially enhanced inhibition effect when juxtaposed against systems that solely incorporate commercial inhibitors or salts. Furthermore, it appears that methanol functions in a more efficacious capacity as an inhibitor. This suggests that methanol exhibits a higher capacity in preventing the development of diverse gas hydrates, both individually or in conjunction with

https://doi.org/10.1021/acs.jced.5c00025
J. Chem. Eng. Data XXXX, XXX, XXX−XXX

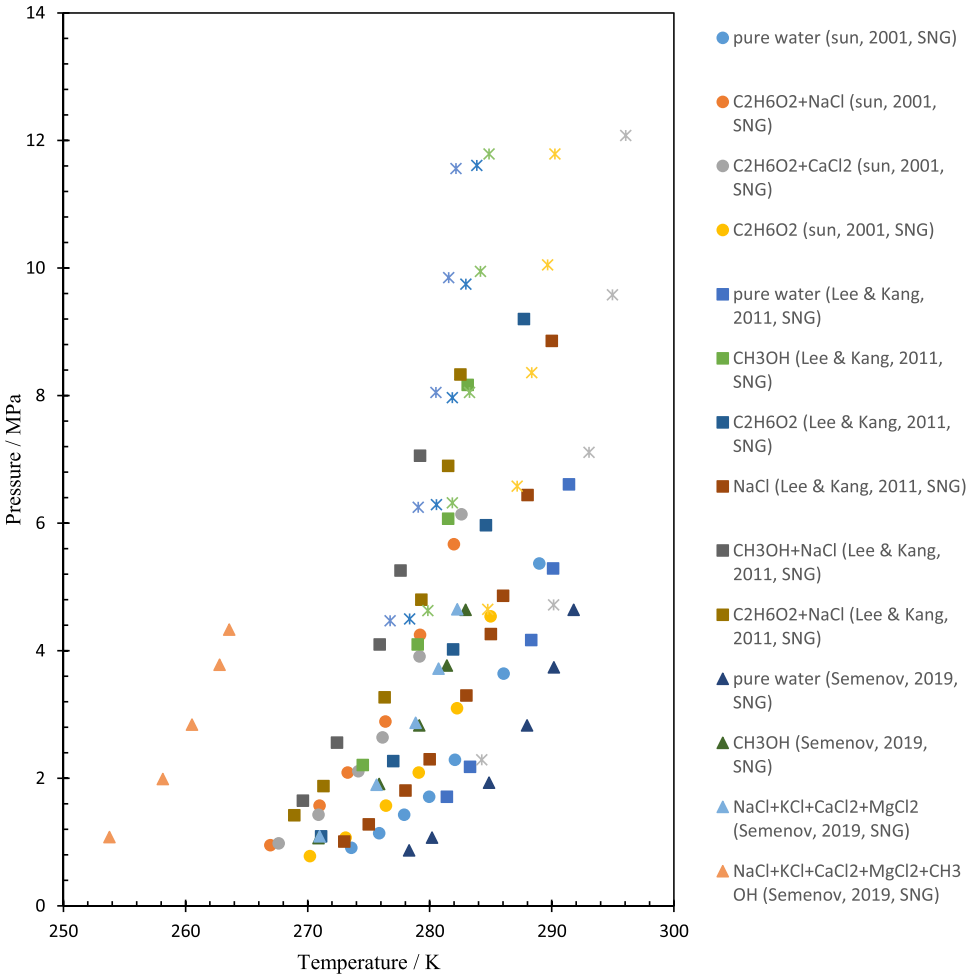

Figure 7. Comparison between the equilibrium diagram of different gas hydrates in the presence of mixtures of commercial additives and different salts, including synthetic gas hydrate and $C_2H_6O_2$, $C_2H_6O_2$ + NaCl, and $C_2H_6O_2$ + $CaCl_2$,[110] synthetic gas hydrate and CH_3OH, $C_2H_6O_2$, NaCl, CH_3OH + NaCl, and $C_2H_6O_2$ + NaCl,[115] synthetic gas hydrate and CH_3OH, NaCl + KCl + $CaCl_2$ + $MgCl_2$, and NaCl + KCl + $CaCl_2$ + $MgCl_2$ + CH_3OH,[127] and synthetic gas hydrate and $C_2H_6O_2$, $C_2H_6O_2$ + NaCl, $C_2H_6O_2$ + $CaCl_2$, and $C_2H_6O_2$ + NaCl + $CaCl_2$.[132132]

salts, to a greater extent than other commercial inhibitors such as monoethylene glycol.

The research findings of a comprehensive and collaborative study on commercial inhibitors in combination with various electrolytes have demonstrated that the concerted action of these two distinct groups of compounds, when synergistically employed, triggers a marked and substantial enhancement in the inhibition of hydrate creation by relocating the hydrate equilibrium figure toward regions characterized by lower temperatures and higher pressures. Furthermore, when compared with the inhibitory efficacy of different salts and commercial inhibitors, methanol has been found to be an exceedingly superior inhibitor with superior performance in the inhibition of hydrate formation. Table 7 summarizes the studies performed due to the simultaneous presence of commercial inhibitors of the family of alcohols and glycols and ionic salts on the gas hydrate phase equilibria. To summarize, the key findings in the field of commercial inhibitors from the family of alcohols and glycols with salts are as follows:

- The combination of commercial inhibitors (alcohols, glycols) and salts has proven to be more effective in preventing gas hydrate formation compared to using a single type of inhibitor. This synergy helps to shift the hydrate equilibrium to conditions of lower temperatures and higher pressures.
- Inhibitors containing a hydroxyl group, such as alcohols and glycols, can form hydrogen bonds with water molecules, which enhances their effectiveness in hydrate inhibition.
- The combination of sodium chloride and ethylene glycol significantly improved the inhibition of CH_4 hydrate formation, with more pronounced effects as the concentration of both inhibitors increased.
- In some studies, the inhibitory effect of calcium chloride was found to exceed that of ethylene glycol when used in combination with other salts, highlighting the importance of salt type in the overall effectiveness.
- Methanol, when combined with salts, was consistently found to have a stronger inhibitory effect on gas hydrate formation compared to other alcohols and glycols. Methanol's lower molecular weight and higher efficiency made it the most potent inhibitor in various systems.
- Studies on synthetic gas mixtures (e.g., CH_4, C_2H_6, CO_2) showed that the combination of inhibitors like methanol with salts provided superior inhibition effects compared to systems containing only alcohols, glycols, or salts alone.

https://doi.org/10.1021/acs.jced.5c00025
J. Chem. Eng. Data XXXX, XXX, XXX−XXX

Table 7. Research Studies on the Subject of Gas Hydrate Development in the Occurrence of Commercial Inhibitors from the Family of Alcohols and Glycols with Salts

author (publication date)	gas	type of thermodynamic inhibitor	concentration of inhibitor (wt %)	T/K	P/MPa	result	ref
Majumdar et al. (2000)	H_2S, CO_2, CH_4	$C_2H_6O_2$, NaCl	15, 30 $C_2H_6O_2$, 10, 15 $C_2H_6O_2$ + 10 NaCl, 10 $C_2H_6O_2$ + 15 NaCl	264−290	0.23−3.18	the inhibitory influence of sodium chloride surpasses that of ethylene glycol	109
Sun et al. (2001)	a ternary mixture of CH_4, C_2H_6, C_3H_8	$C_2H_6O_2$, NaCl, $CaCl_2$	10, 20, 30 $C_2H_6O_2$, 10, 20 $C_2H_6O_2$ + 10 NaCl, 10 $C_2H_6O_2$ + 10 $CaCl_2$, 15, 20 $C_2H_6O_2$ + 5 NaCl + 5 $CaCl_2$	263.52−288.96	0.78−8.1	the inhibitory power of different inhibitors is in the form of $C_2H_6O_2$ < $CaCl_2$ < NaCl	110
Eichholz et al. (2004)	CH_4	$C_2H_6O_2$, NaCl	19.16 $C_2H_6O_2$, 5.77, 15.36, 23.88 $C_2H_6O_2$ + 3.77 NaCl, 3.77 $C_2H_6O_2$ + 15.67 NaCl, 12.07 $C_2H_6O_2$ + 15.01 NaCl	262−282	2.1−9.5	with growing the amount of ethylene glycol, the temperature of hydrate creation decreased, and the pressure increased	111
Masoudi et al. (2004)	CH_4	$C_2H_6O_2$, NaCl, KCl	21.3, 30.8 $C_2H_6O_2$ + 15, 12 NaCl, 8, 10 KCl + 35, 23 $C_2H_6O_2$	259.30−283.90	3.93−46.69	the synergism of salt and ethylene glycol increased the inhibition effect of CH_4 hydrate	112
Masoudi et al. (2005)	CH_4	$C_2H_6O_2$, $CaCl_2$	21.3, 13.4, 14, 26 $C_2H_6O_2$ + 15, 15.3, 18, 14 $CaCl_2$	261.5−287.8	3.91−45.44	the incorporation of salt and ethylene glycol yielded a favorable outcome with regard to the obstructive capabilities of hydrate	113
Najibi et al. (2009)	CH_4	CH_3OH, $C_2H_6O_2$, NaCl, KCl, $CaCl_2$	8.3, 3 NaCl + 9.2, 30 CH_3OH, 3 NaCl + 30 $C_2H_6O_2$, 7 KCl + 9 CH_3OH, 8 $CaCl_2$ + 12 $C_2H_6O_2$, 10 $CaCl_2$ + 14 CH_3OH	269.30−286.35	4.27−28.90	the synergism of alcohols and salts positively affected the inhibition efficacy of CH_4 hydrate	114
Mohammadi and Richon (2009)	CH_4	CH_3OH, $C_2H_6O_2$, NaCl, KCl, $CaCl_2$	10 NaCl + 20 CH_3OH, 10 KCl + 15 CH_3OH, 5 $CaCl_2$ + 10 CH_3OH, 15 NaCl + 20 $C_2H_6O_2$, 10 KCl + 20 $C_2H_6O_2$, 15 $CaCl_2$ + 20 $C_2H_6O_2$	253.90−278.00	2.85−11.41	the combined effect of alcohols and salts resulted in the alteration of the hydrate equilibrium diagram, causing it to shift toward regions characterized by lesser temperatures or greater pressures	70
Lee and Kang (2011)	NG mixtures including CH_4, C_2H_6, C_3H_8, i-C_4H_{10}, n-C_4H_{10}, n-C_5H_{12}, N_2	$C_2H_6O_2$, CH_3OH, NaCl	10, 20, 30 CH_3OH, 10, 20, 30, 40, 50 $C_2H_6O_2$, 3.5 NaCl, 10,20, 30 $CH_3OH/C_2H_6O_2$ + 3.5 NaCl	266.20−290.20	0.99−8.86	the inhibitory power of methanol, whether alone or in combination with sodium chloride, is higher than that of ethylene glycol due to its lower molecular mass	115
Mohammadi and Richon (2012)	H_2S	$C_2H_6O_2$, CH_3OH, NaCl	15 $C_2H_6O_2$ + 5 NaCl, 10 CH_3OH + 5 NaCl, 30, 50 CH_3OH	254.10−290.10	0.18−1.10	elevating the methanol inhibitor amount resulted in a displacement of the equilibria figure for the hydrates of CO_2 and H_2S toward regions characterized by augmented pressures and decreased temperatures	116
	CO_2		15 $C_2H_6O_2$ + 5 NaCl, 10 CH_3OH + 5 NaCl, 10, 20, 30, 40, 50 CH_3OH	241.1−274.7	0.89−3.82		
Lafond et al. (2012)	CH_4	CH_3OH, NaCl	3.5 NaCl, 3.5 NaCl + 5, 10, 20 CH_3OH	272.00−290.10	7.00−20.00	increasing the concentration of methanol improved the inhibition conditions of CH_4 hydrate	117
Chapoy et al. (2012)	CH_4	$C_2H_6O_2$, NaCl	5 NaCl + 30 $C_2H_6O_2$, 10 NaCl + 40 $C_2H_6O_2$	248.25−279.85	1.75−22.73	elevating the concentration of monoethylene glycol in an unvarying proportion of sodium chloride resulted in a displacement of the equilibrium chart pertaining to natural gas hydrate toward a territory characterized by a reduced temperature	118
	NG mixtures including CH_4, C_2H_6, C_3H_8, i-C_4H_{10}, n-C_4H_{10}, n-C_5H_{12}, CO_2, N_2		5 NaCl + 30 $C_2H_6O_2$, 5 NaCl + 23 $C_2H_6O_2$	272.65−286.65	3.42−24.74		
Nasir et al. (2014)	two types of synthetic gas mixtures rich in CO_2	CH_3OH, $C_2H_6O_2$, NaCl, $CaCl_2$	10, 20 $CH_3OH/C_2H_6O_2$, 20 $CH_3OH/C_2H_6O_2$ + 10 $CaCl_2$/NaCl	263.85−284.75	2.76−12.08	the inhibition efficacy of methanol is greater than that of ethylene glycol on both types of synthetic gas mixtures	119
Alqahtani (2014)	CO_2	CH_3OH, NaCl	4.05, 10 NaCl + 10 CH_3OH, 10 NaCl + 5 CH_3OH	269.54−272.48	1.99−3.09	the inhibition effect on the CO_2 and C_2H_6 hydrates has increased with increasing the concentration of the mixture of inhibitors	5
	C_2H_6		5, 10 NaCl + 10 CH_3OH, 10 NaCl + 5 CH_3OH	269.75−273.01	0.67−1.09		
Mech and Sangwai (2016)	CH_4	$C_2H_6O_2$, CH_3OH, NaCl	3, 10, 3, 10 NaCl/$CH_3OH/C_2H_6O_2$ + 0.5, 0.5, 1, 1 C_4H_8O + 10 $C_{16}H_{36}BrN$	282.28−289.65	2.25−6.43	methanol exhibited the highest level of effectiveness when compared with the inhibitors named sodium chloride and ethylene glycol	120
Seo et al. (2016)	SG mixtures including CH_4, C_2H_6, C_3H_8, n-C_4H_{10}	$C_2H_6O_2$, NaCl	10, 20 $C_2H_6O_2$, 3.5, 20 NaCl + 20 $C_2H_6O_2$, 20 NaCl + 20 $C_2H_6O_2$	274.00−293.00	0.50−11.00	the combined influence of salt and ethylene glycol resulted in a beneficial impact on the ability to hinder the creation of hydrate.	121
Dastanian et al. (2017)	CO_2	CH_3OH, $C_2H_6O_2$, KCl	5 KCl + 10, 20 CH_3OH, 5 KCl + 10, 20 $C_2H_6O_2$, 10 KCl + 10 $C_2H_6O_2$	263.30−277.40	1.77−3.65	increasing the concentration of inhibitors led to the improvement of inhibition conditions	122

https://doi.org/10.1021/acs.jced.5c00025
J. Chem. Eng. Data XXXX, XXX, XXX−XXX

Table 7. continued

author (publication date)	gas	type of thermodynamic inhibitor	concentration of inhibitor (wt %)	T/K	P/MPa	result	ref
Kim et al. (2017)	SNG including CH_4, C_2H_6, C_3H_8, n-C_4H_{10}	$C_2H_6O_2$, NaCl	3.5 NaCl, 20 $C_2H_6O_2$, 3.5, 7, 10, 20 NaCl + 20 $C_2H_6O_2$	277.75−294.75	5.24−11.49	increasing salt concentration in an aqueous solution has improved hydrate inhibition conditions	123
Dastanian et al. (2018)	CO_2	CH_3OH, $C_2H_6O_2$, $CaCl_2$	5 $CaCl_2$ + 10, 20 $CH_3OH/C_2H_6O_2$, 10 $CaCl_2$ + 10 $CH_3OH/C_2H_6O_2$	262.20−276.80	1.49−3.36	the collaborative impact of calcium chloride salt with either methanol or ethylene glycol was observed to exert a favorable influence on the suppressive potential of CO_2	124
Burgass et al. (2018)	SG mixture including CH_4, C_2H_6, C_3H_8, i-C_4H_{10}, n-C_4H_{10}, i-C_5H_{12}, n-C_5H_{12}, CO_2, N_2	$C_2H_6O_2$, NaCl, NaBr	25 NaCl, 40 NaBr, 20 NaCl + 30, 40 $C_2H_6O_2$, 40 NaBr + 40 $C_2H_6O_2$	259.40−313.40	4.94−146.38	increasing the concentration of monoethylene glycol inhibitor has led to the transfer of the hydrate decomposition diagram to the left of the temperature−pressure chart, i.e., toward areas with lower temperatures	125
Kwak et al. (2018)	CH_4	$C_2H_6O_2$, NaCl	10 NaCl + 10, 30 $C_2H_6O_2$	261.6−279.4	3.64−12.35	by augmenting the degree of monoethylene glycol inhibitor within a consistent quantity of sodium chloride, the range in which hydrate stability is maintained has been detected to alter toward the left of the temperature−pressure diagram	126
	CH_4 + C_3H_8			275.8−289.8	3.92−14.31		
Semenov et al. (2019)	CH_4 + C_2H_6 + C_3H_8 + CO_2 + N_2	NaCl, KCl, $CaCl_2$, $MgCl_2$, CH_3OH	10, 20, 30, 40, 50 CH_3OH, 13.15 NaCl + 2.46 KCl + 1.28 $CaCl_2$ + 1.11 $MgCl_2$, 10, 20 CH_3OH + 13.15 NaCl + 2.46 KCl + 1.28 $CaCl_2$ + 1.11 $MgCl_2$	249.7−291.8	0.87−4.70	the phenomenon of synergism has been observed to result in a notable alteration of the equilibrium figures toward lower temperatures and higher pressures, when compared with systems that exclusively comprise a single thermodynamic hydrate inhibitor.	127
Park et al. (2019)	CH_4	CH_3OH, $C_2H_6O_2$, NH_4Cl	20 $CH_3OH/C_2H_6O_2$ + 10 NH_4Cl, 20 $CH_3OH/C_2H_6O_2$ + 5 NH_4Cl, 10 $CH_3OH/C_2H_6O_2$ + 10 NH_4Cl, 10 $CH_3OH/C_2H_6O_2$ + 5 NH_4Cl	264.00−281.00	4.00−12.00	20 wt % $CH_3OH/C_2H_6O_2$ + 10 wt % NH_4Cl > 20 wt % $CH_3OH/C_2H_6O_2$ + 5 wt % NH_4Cl > 10 wt % $CH_3OH/C_2H_6O_2$ + 10 wt % NH_4Cl > 10 wt % $CH_3OH/C_2H_6O_2$ + 5 wt % NH_4Cl	128
Mu and Cui (2019)	Two types of SNG, including CH_4, C_2H_6, C_3H_8, CO_2, N_2	CH_3OH, NaCl	3.5, 5, 7.5 NaCl, 3.5 NaCl + 5 CH_3OH, 5, 7.5 NaCl + 10 CH_3OH	267.71−287.64	2.12−11.51	augmenting the quantity of inhibitors triggered a decrease in the equilibria temperature of the hydrate	129
Cordeiro et al. (2019)	CO_2	CH_3OH, NaCl	10, 20, 30 CH_3OH, 5, 10 NaCl, 5 NaCl + 10, 20, 30 CH_3OH	267.02−285.21	8.50−25.00	the synergistic of sodium chloride and ethylene glycol was observed to produce a beneficial outcome in the suppression of CO_2	130
Kim et al. (2020)	CH_4	$C_2H_6O_2$, NaCl NaBr, NaI	10 $C_2H_6O_2$ + 5 NaCl/NaBr/NaI	272.00−283.00	5.30−11.00	10 wt % of $C_2H_6O_2$ + 5 wt % of NaCl > 10 wt % of $C_2H_6O_2$ + 5 wt % of NaBr > 10 wt % of $C_2H_6O_2$ + 5 wt % of NaI	131
Behnammotlagh et al. (2022)	CH_4 + C_3H_8 + H_2S	$C_2H_6O_2$, NaCl, $CaCl_2$	20 $C_2H_6O_2$, 20 $C_2H_6O_2$ + 10 NaCl, 20 $C_2H_6O_2$ + 6 $CaCl_2$ + 4 NaCl, 20 $C_2H_6O_2$ + 10 $CaCl_2$	276.75−296.05	2.29−12.08	20 wt % MEG + 10 wt % NaCl > 20 wt % MEG + 6 wt % $CaCl_2$ + 4 wt % NaCl > 20 wt % MEG + 10 wt % $CaCl_2$ > 20 wt % MEG	132

https://doi.org/10.1021/acs.jced.5c00025
J. Chem. Eng. Data XXXX, XXX, XXX−XXX

- The combination of ethylene glycol with calcium chloride led to a more significant reduction in hydrate formation temperature compared to ethylene glycol alone, further emphasizing the value of salt in combination with glycolic inhibitors.
- Combining alcohols (methanol) and glycols (ethylene glycol) with salts (sodium chloride, calcium chloride) resulted in a significant improvement in the inhibition of gas hydrate formation, with methanol being the most effective inhibitor.

5. MODELING SECTION

5.1. Data Sets. The experimental hydrate phase equilibrium data utilized for building the machine learning model (MLM) were sourced from previously published articles. Overall, 213 data sets were collected for various gases, including CO_2, CH_4, C_2H_6, C_3H_8, *iso*-C_4H_{10}, *n*-C_4H_{10}, *n*-C_5H_{12}, *iso*-C_5H_{12}, N_2, H_2S, *n*-C_6H_{14}, and *n*-C_7H_{16}, examined in the presence of six amino acids: glycine, alanine, valine, proline, serine, and arginine. In addition, nine different salts were included in the study: LiBr, LiCl, NaCl, $CaCl_2$, KCl, $MgCl_2$, $MgBr_2$, $CaBr_2$, and $ZnBr_2$. The research also incorporated seven types of commercial inhibitors, namely, CH_3OH, C_2H_5OH, $C_2H_6O_2$, $C_4H_{10}O_3$, $C_6H_{14}O_4$, $C_3H_8O_3$, and C_3H_7OH. Furthermore, 18 different ionic liquids were evaluated, such as [OH-EMIM][Cl], [OH-EMIM][Br], [BMIM][HSO_4], [BMIM][Cl], [BMIM][$N(CN)_2$], [BMIM]-[Br], [BMIM][CF3SO3], [BMIM][$MeSO_4$], [BMIM][ClO_4], TMACl, TEAOH, TPrAOH, TMAOH, TEA-I, HMIM-I, MOIM-Cl, H-MIM-HSO_4, and TBAOH. To accurately predict hydrate formation temperature (HFT) and pressure in the presence of distilled water and various inhibitors, two different independent variables were utilized: the concentration of the inhibitors and the molar composition of the gases. Prior to model development, the data set underwent normalization (or scaling) to a uniform range of 0−1 to prevent larger numerical values from dominating smaller ones, which was crucial for ensuring balanced input data, particularly when there were significant value disparities. This normalization was achieved by calculating the minimum and maximum values of each variable (x_i) in the data set, and then applying eq 1 to compute the scaled value (x_i^*). This preprocessing ensured that each recorded value was normalized to the closed interval [0, 1], facilitating consistent input data for the model.[133]

$$X_i^* = \frac{x_i - \min(x_i)}{\max(x_i) - \min(x_i)} \tag{1}$$

5.2. Machine Learning Models. Four machine learning models (random forest (RF), convolutional neural networks (CNN), deep neural networks (DNN), and support vector machine (SVM)) were evaluated to predict hydrate formation temperature and pressure with various inhibitors using a collected data set. Python was used for model development, and model details are briefly outlined, as they are extensively covered in previous studies.[134−137] These models were chosen for their ability to handle complex, nonlinear relationships and high-dimensional data, providing robust predictions under varying conditions. The selection of these models is based on their proven effectiveness in addressing the challenges of predicting hydrate formation in the presence of multiple inhibitors, ensuring accurate and reliable results. The diversity of the models allows for a comprehensive comparison, leveraging each model's unique strengths: random forest for handling high-dimensional data and identifying influential factors, support vector machine for classification and regression in nonlinear spaces, convolutional neural networks for pattern recognition and feature extraction in complex data sets, and deep neural networks for capturing hierarchical relationships and intricate patterns. This approach helps in determining the most effective method for hydrate prediction, improving prediction accuracy, and optimizing inhibitor selection.

5.2.1. Random Forest (RF). Random forest (RF) is an ensemble learning method introduced by Breiman that builds multiple decision trees by randomly splitting the training data and training the trees simultaneously. A decision tree represents a decision-making pathway with three main components: the root node (initial decision point), branches (options), and leaf nodes (outcomes). In RF, each tree is independently constructed using a random subset of data and features. The algorithm uses bootstrap aggregation (bagging) and random feature selection to improve predictive accuracy by averaging the outputs of all trees. Splits are determined using the decrease of Gini impurity (DGI) criterion.[133,134] In this study, the RF model was developed by constructing 100 decision trees using bootstrap samples. The out-of-bag (OOB) error rate was calculated with data not included in the bootstrap samples to evaluate performance.

5.2.2. Support Vector Machine (SVM). SVM is a machine learning technique applicable to both classification and regression tasks, rooted in the Vapnik−Chervonenkis theory, which is part of computational learning theory connected to statistical learning theory.[138] The core concept of support vector regression (SVR) involves mapping input data into a high-dimensional space and then performing linear regression within this space. This approach allows disorganized or nonlinearly separable data to become linearly separable, facilitating the minimization of training error during the optimization process. The full set of SVR equations has been thoroughly discussed in the existing literature,[139,140] so the derivation process will not be repeated here; instead, the final equation is presented directly as follows:

$$f(x) = \sum_{i,j=1}^{n} (\alpha_i - \alpha_i^*)\langle \phi(x_i)\cdot\phi(x_j)\rangle + b \tag{2}$$

where b represents the offset of the regression function, while α_i and α_i^* are the Lagrange multipliers that must meet the condition $0 \le \alpha_i, \alpha_i^* \le C$. Only the nonzero α_i and α_i^* contribute to the final regression model and are referred to as support vectors. The parameter C is the complexity constant that balances the complexity of the SVR model with the allowed margin of error. The function $\phi(x)$ is a mapping function that is typically unknown and challenging to identify. As a result, the inner product $\langle \phi(x_i)\cdot\phi(x_j)\rangle$ is often replaced with a kernel function for computational simplicity.

$$K(x_i, x_j) = \langle \phi(x_i)\cdot\phi(x_j)\rangle \tag{3}$$

The kernel function calculates the dot product and is represented as a symmetric square matrix known as the kernel matrix. This function restructures the original nonlinear input space into a higher-dimensional feature space, which then serves as the new input for the model. This transformation effectively converts a nonlinear problem into a linear one. Various kernel functions, such as linear, polynomial, radial basis function (RBF), and sigmoid, can be applied to introduce

https://doi.org/10.1021/acs.jced.5c00025
J. Chem. Eng. Data XXXX, XXX, XXX−XXX

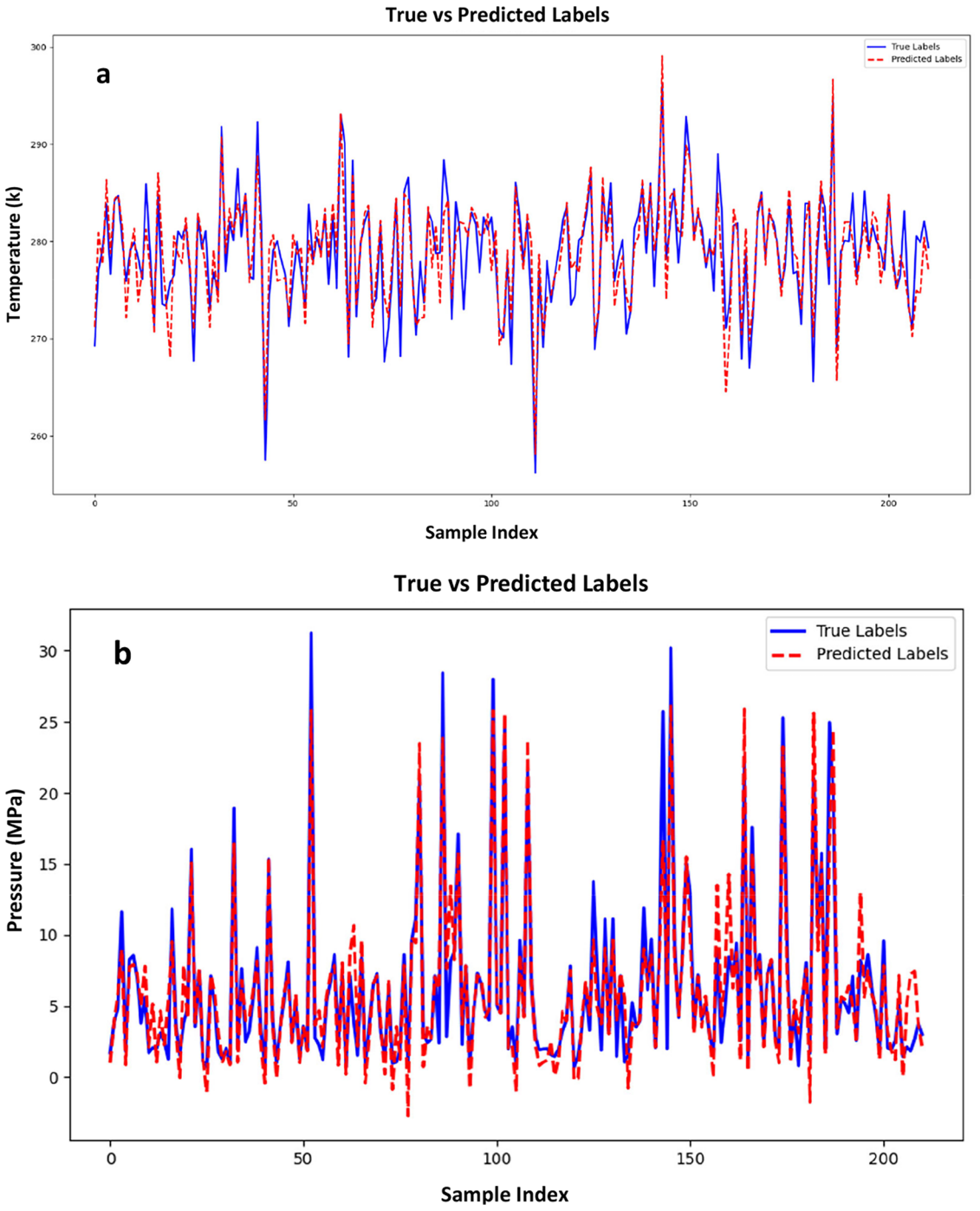

Figure 8. Comparison of actual and predicted data for hydrate formation using a DNN model: (a) temperature predictions and (b) pressure predictions.

different levels of nonlinearity and flexibility to the model. There is currently no universal standard for selecting the most accurate kernel for SVR; the choice depends on the specific characteristics of the data being analyzed. In this study, polynomial kernels, commonly used due to their effectiveness, were applied with adjustments to their parameters. The sequential minimal optimization (SMO) algorithm was employed during the iterative training process to minimize the error function.[141]

5.2.3. Convolutional Neural Networks (CNNs). CNNs are deep learning models inspired by the human visual cortex, widely used for tasks like image processing, classification, and pattern recognition. They automatically detect features from input data using convolutional layers, which apply filters to generate feature maps, followed by pooling layers to reduce dimensions and maintain key information. Activation functions like ReLU add nonlinearity, and fully connected layers produce the final output. CNNs excel due to weight sharing, reduced parameters, and hierarchical feature extraction, making them highly efficient for applications like image classification, object detection, and facial recognition.[136]

5.2.4. Deep Neural Networks (DNNs). DNNs are artificial neural networks with multiple hidden layers, enabling them to model complex patterns in data for tasks like image

https://doi.org/10.1021/acs.jced.5c00025
J. Chem. Eng. Data XXXX, XXX, XXX−XXX

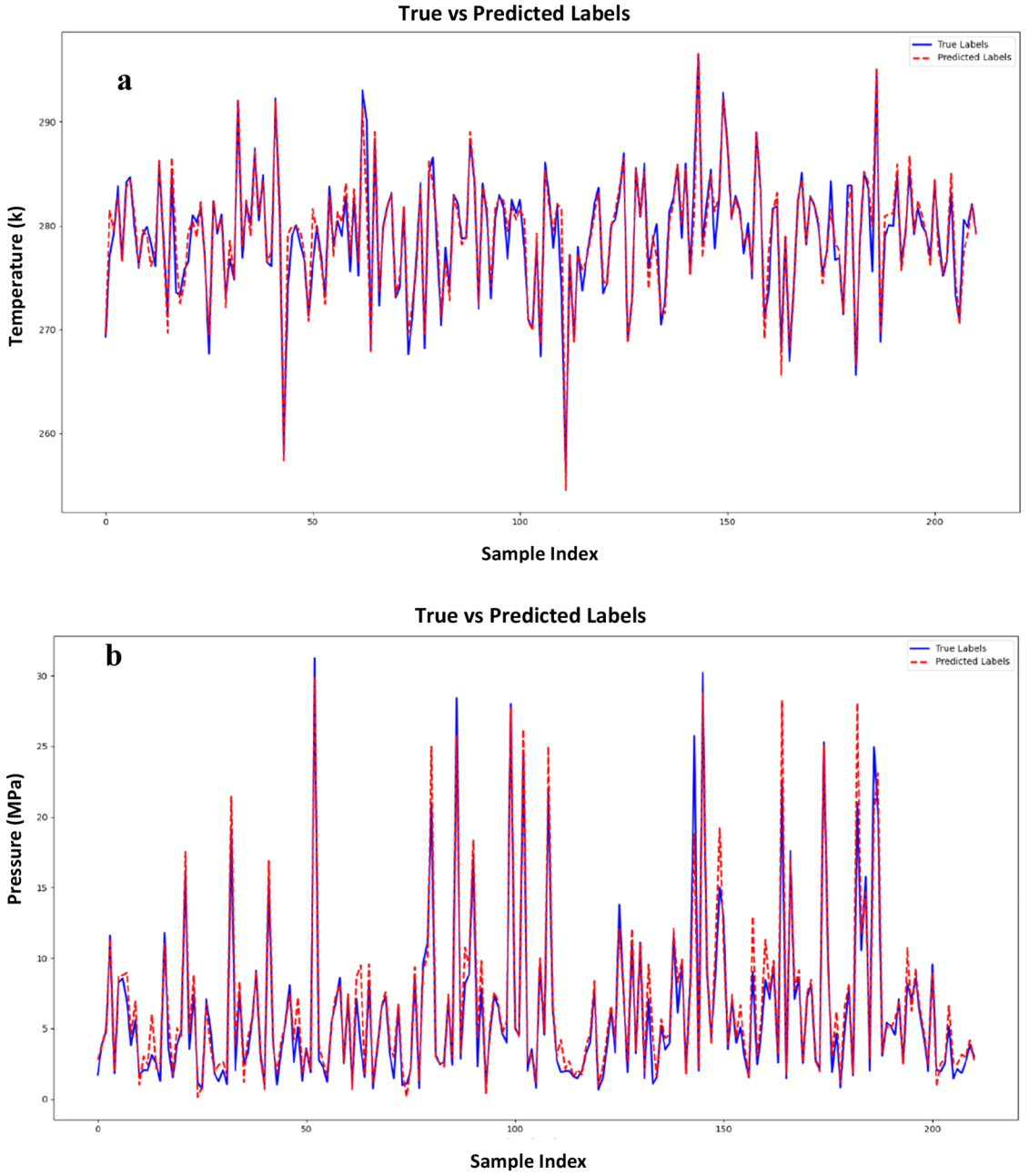

Figure 9. Comparison of actual and predicted data for hydrate formation using a CNN model: (a) temperature predictions and (b) pressure predictions.

recognition, speech processing, and natural language understanding. They process inputs layer by layer, using activation functions like ReLU and sigmoid to capture nonlinear relationships. Training involves forward propagation to produce outputs, backward propagation to calculate errors, and optimization methods like SGD or Adam to adjust weights. DNNs excel at learning hierarchical representations, capturing basic features in initial layers and complex patterns in deeper ones. Despite challenges like computational demands and overfitting, mitigated by techniques like dropout and data augmentation, DNNs have revolutionized AI, achieving breakthroughs in fields such as computer vision and natural language processing.

5.3. Model Validation. The entire data set was randomly split into two groups: a training data set (80%) and a testing data set (20%). The training data set was utilized for developing the predictive model, which was fine-tuned using a 5-fold cross-validation method. The essence of cross-validation involves dividing the training data set into 5 equal parts (folds), where 4 folds are used for training and the remaining 1-fold serves as the validation set. This process is repeated 5 times, with a different fold being used for validation in each iteration.[142] The performance of the trained model was then evaluated with the testing data set, which was not involved in the model's development. The model's accuracy and predictive power were measured using the coefficient of determination (R^2) and the mean squared error (MSE).

$$R^2 = 1 - \frac{\sum_{i=1}^{n} (Y_i^{\exp} - Y_i^{\text{pred}})^2}{\sum_{i=1}^{n} (Y_i^{\exp} - \overline{Y}^{\exp})^2} \quad (4)$$

https://doi.org/10.1021/acs.jced.5c00025
J. Chem. Eng. Data XXXX, XXX, XXX−XXX

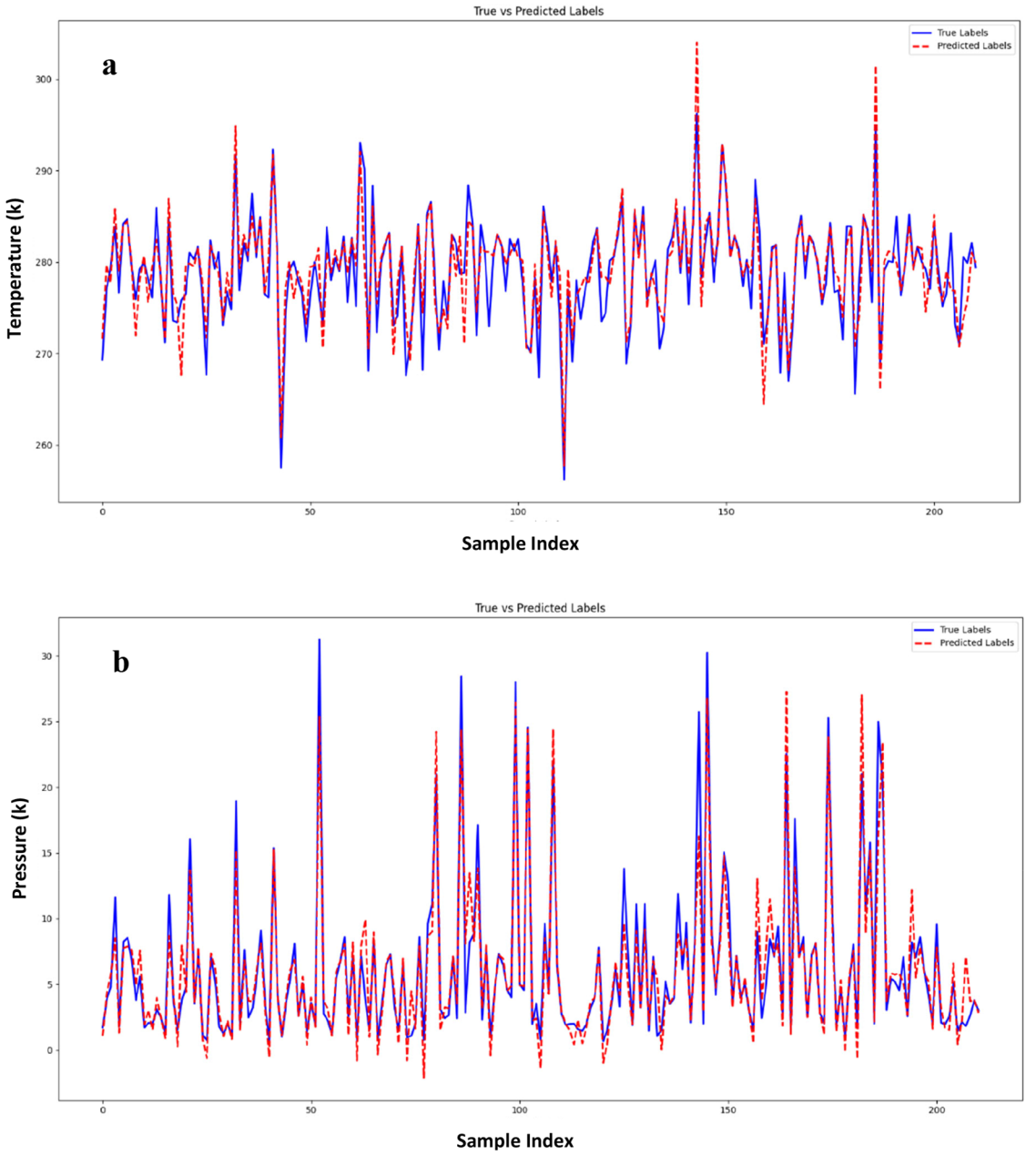

Figure 10. Comparison of actual and predicted data for hydrate formation using an SVM model: (a) temperature predictions and (b) pressure predictions.

$$\mathrm{MSE} = \frac{1}{n}\sum_{i=1}^{n}(Y_i^{\mathrm{exp}} - Y_i^{\mathrm{pred}})^2 \tag{5}$$

where Y_i^{exp} and Y_i^{pred} denote the hydrate formation temperature and pressure obtained from the experiments and predicted by the model, respectively, and $\overline{Y}^{\mathrm{exp}}$ represents the average hydrate formation temperature and pressure measured during the experiments.

6. RESULTS AND DISCUSSION

6.1. Comparative Analysis of Different Models for Temperature and Pressure of Hydrate Formation. This study compared DNN, CNN, SVM, and RF models to predict hydrate formation temperature and pressure, aiming to identify the most accurate model for industrial applications. Figure 8 illustrates the performance of a DNN model in predicting hydrate formation conditions. Figure 8a shows the comparison of actual (blue line) and predicted (red dashed line) temperature values. The DNN model effectively captured the general temperature trends, with close alignment in most cases. However, discrepancies were observed around sample indices 50 and 150, likely due to sudden fluctuations, indicating potential areas for improvement through architecture refinement and enhanced training data. Figure 8b displays the comparison of actual (blue line) and predicted (red dashed line) pressure values. The model successfully captured the overall pressure trends and variability, with close alignment in most sections. Nonetheless, deviations at certain peaks highlight challenges in predicting extreme values, suggesting the need for further refinement to enhance accuracy and consistency.

https://doi.org/10.1021/acs.jced.5c00025
J. Chem. Eng. Data XXXX, XXX, XXX−XXX

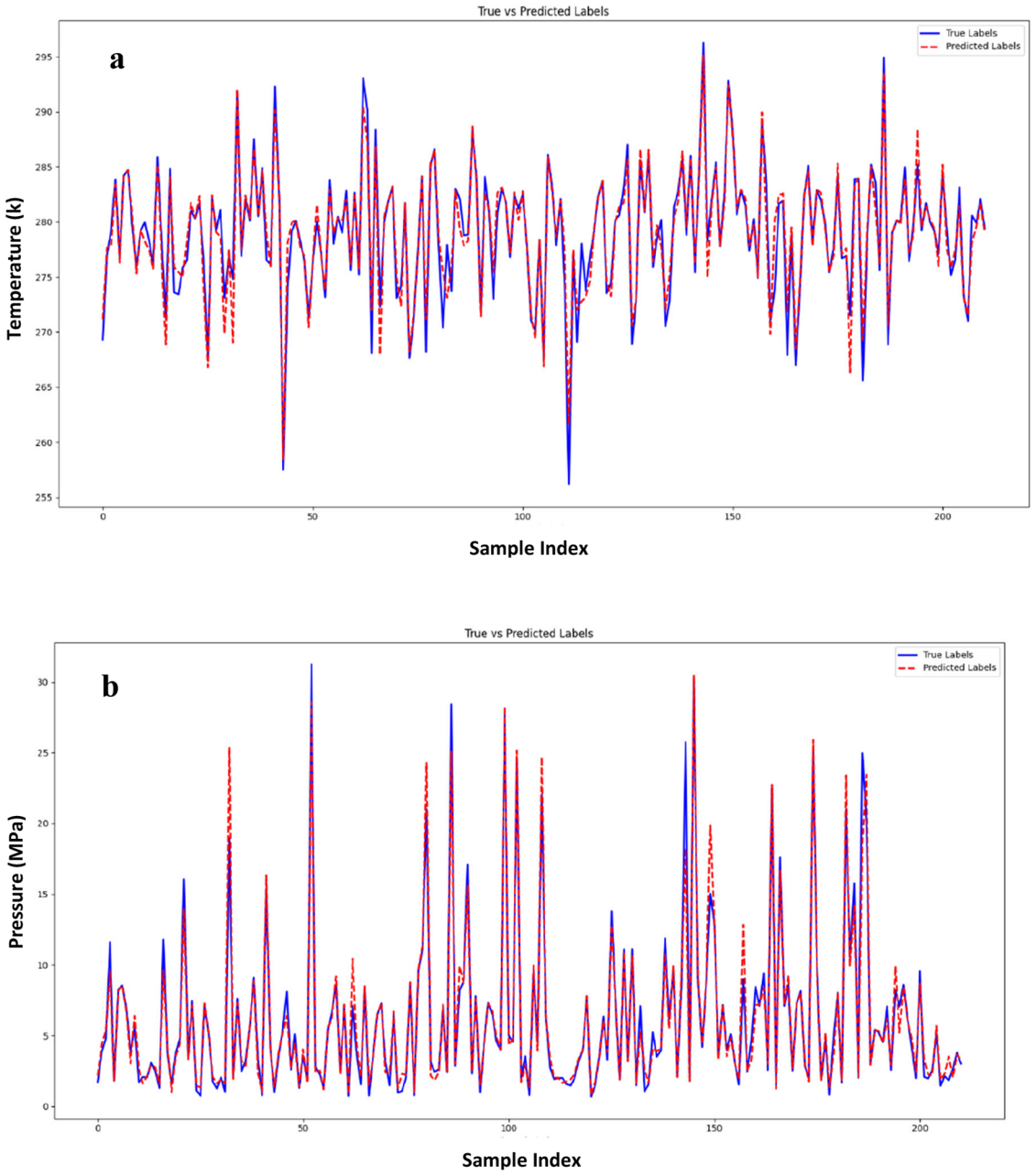

Figure 11. Comparison of actual and predicted data for hydrate formation using a RF model: (a) temperature predictions and (b) pressure predictions.

Figure 9a illustrates temperature predictions, showing the CNN model's reliability in capturing general trends and variability in hydrate formation temperatures. Minor deviations at peaks and dips indicate challenges in predicting rapid or extreme fluctuations, suggesting the need for further refinement or feature enhancement. Figure 9b depicts pressure predictions, highlighting the model's effectiveness in capturing overall trends and dynamic behavior. However, deviations at certain peaks reveal limitations in handling extreme pressure changes, likely due to nonlinear interactions or data set outliers.

Figure 10a illustrates temperature predictions, where the close alignment between actual and predicted values demonstrates the SVM model's good accuracy in capturing general temperature patterns. However, minor deviations at peaks and troughs indicate challenges in handling rapid or extreme fluctuations, suggesting that further tuning or alternative kernel functions may improve performance. Figure 10b shows pressure predictions, highlighting the SVM model's effectiveness in capturing general trends and variations. Nonetheless, discrepancies at peaks reveal limitations in handling extreme, nonlinear changes in pressure, possibly due to sensitivity to outliers or inappropriate kernel selection. Using a radial basis function kernel could enhance the model's ability to manage complex variations effectively.

Figure 11a illustrates temperature predictions, where the RF model shows strong performance in capturing general trends, with close alignment between actual and predicted values. Minor deviations at peaks and troughs suggest areas for refinement, such as adjusting tree depth or incorporating additional features, to improve accuracy for extreme temperature fluctuations. Figure 11b presents pressure predictions,

https://doi.org/10.1021/acs.jced.5c00025
J. Chem. Eng. Data XXXX, XXX, XXX−XXX

demonstrating reliable trend-capture by the RF model. The strong alignment highlights its robustness, but slight deviations at extreme values point to potential limitations due to averaging in the ensemble approach or insufficient representation of complex interactions in the feature set. Refining model parameters or expanding features could enhance the model's ability to predict extreme pressure variations more accurately.

6.2. Comparison among Different Models. In this study, we evaluated the performance of four different machine learning models—CNN, DNN, SVM, and RF—in predicting pressure and temperature during hydrate formation. The models were assessed based on MSE and R^2 values to determine their accuracy and reliability in capturing the complex patterns of hydrate formation data. Table 8 shows the performance of various MLMs for pressure and temperature prediction in hydrate formation.

Table 8. Performance Comparison of Different Machine Learning Models for Pressure and Temperature Prediction in Hydrate Formation

		pressure (MPa)		temperature (K)	
statistical metrics		MSE	R^2 (%)	MSE	R^2 (%)
model	CNN	2.15	94	7.39	79
	DNN	3.94	89	2.38	72
	SVM	3.68	90	7.12	80
	RF	1.51	96	2.66	92

Based on Table 8, the RF model demonstrated the highest accuracy for both pressure and temperature predictions, with an MSE of 1.51 and an R^2 of 96% for pressure, and an MSE of 2.66 and an R^2 of 92% for temperature. Its strong performance is attributed to the ensemble approach, which reduces overfitting and handles complex data effectively. The CNN model followed, showing strong results for pressure (MSE 2.15, R^2 94%) and temperature (MSE 7.39, R^2 79%), thanks to its ability to capture spatial patterns. SVM achieved moderate performance, with an MSE of 3.68 and an R^2 of 90% for pressure, and an MSE of 7.12 and an R^2 of 80% for temperature, reflecting its limitations in handling nonlinear dynamics. The DNN model showed the lowest accuracy, with an MSE of 3.94 and an R^2 of 89% for pressure, and an MSE of 2.38 and an R^2 of 72% for temperature, suggesting a need for further tuning or more advanced architectures. Overall, the RF model emerged as the most reliable, followed by CNN, highlighting the suitability of ensemble and spatial pattern-capturing models for complex data sets in hydrate formation studies.

Figure 12 presents a comparative analysis of the predictive performance of four machine learning models—DNN, CNN, SVM, and RF—in forecasting the temperature of hydrate formation. Each graph compares the predicted values (y-axis) with the actual values (x-axis), using both training and testing data sets, represented by solid and hollow markers, respectively. The diagonal dashed line signifies the ideal case where predicted values perfectly match the actual values. The DNN model shows moderate accuracy, with an R^2 of 0.6924 and a root-mean-square error (RMSE) of 3.2784. While it captures general temperature trends, deviations at extremes suggest limitations in generalization, requiring architectural optimization and more diverse training data. The CNN model performs better, achieving an R^2 of 0.7878 and an RMSE of 2.7232. It effectively captures spatial patterns, showing improved alignment with actual values, though minor deviations at temperature extremes indicate room for further refinement. The SVM model achieves competitive results, with an R^2 of 0.7964 and an RMSE of 2.6676. Its predictions align well for midrange temperatures but show challenges at extremes, suggesting that kernel optimization could enhance its ability to model nonlinear complexities. The RF model outperforms all others, with an R^2 of 0.9240 and an RMSE of 1.6297. Its ensemble learning approach ensures robust generalization, accurately predicting temperature trends across all ranges, including extremes, with minimal error or outliers. Overall, the RF model demonstrates superior reliability and accuracy, making it the most suitable for predicting hydrate formation temperatures. CNN and SVM perform moderately well, excelling in midrange predictions, while DNN requires significant improvements to handle extreme values effectively. These findings underscore the importance of model selection based on data set complexity and desired accuracy, particularly for industrial applications in hydrate formation management.

Figure 13 illustrates the predictive performance of four machine learning models—CNN, DNN, SVM, and RF—in estimating the pressure of hydrate formation using R^2 and RMSE metrics. The x-axis represents the actual pressure values, while the y-axis indicates the predicted values. Both training and testing data sets are included, with solid markers representing training data and hollow markers representing testing data. The diagonal dashed line represents the ideal fit ($y = x$), where the predicted values perfectly align with the actual values. The RF model outperforms all, with an R^2 of 0.9588 and RMSE of 1.2305, demonstrating superior accuracy and consistency across all pressure ranges due to its ensemble learning approach. The CNN model follows closely, achieving an R^2 of 0.9274 and an RMSE of 1.6341, with accurate predictions but slight deviations at higher pressures. The SVM and DNN models perform moderately well, with R^2 values of 0.9000 and 0.8945, respectively, but show higher errors and struggle with extreme pressures. These findings confirm the RF model as the most reliable choice for accurate and robust pressure predictions in industrial applications.

6.3. Parameter Optimization for Each Model. We evaluate the hyperparameter optimization process for various machine learning models, with a specific focus on their application to predict hydrate formation temperature and pressure. Through a systematic analysis of performance metrics, such as R^2 and RMSE, this section aims to identify the optimal configurations that enhance predictive accuracy while maintaining robust generalization.

Figure 14 illustrates the performance evaluation of an SVM regression model for predicting temperature data, assessed using two critical metrics, R^2 and RMSE, as functions of the polynomial order and complexity parameter (C). These metrics are visualized in three-dimensional bar plots, providing insights into how hyperparameter choices influence model performance. Higher polynomial orders improve R^2 and reduce RMSE, reflecting better modeling of nonlinear temperature patterns. Midrange C values strike a balance between fitting the data and avoiding overfitting, achieving peak R^2 (~0.8) and minimal RMSE (~1.5). Low C values lead to underfitting with poor performance, while excessive C may risk overfitting. The results highlight the importance of tuning these hyperparameters for robust and accurate temperature predictions, with applications in fields like climate studies and energy systems.

https://doi.org/10.1021/acs.jced.5c00025
J. Chem. Eng. Data XXXX, XXX, XXX−XXX

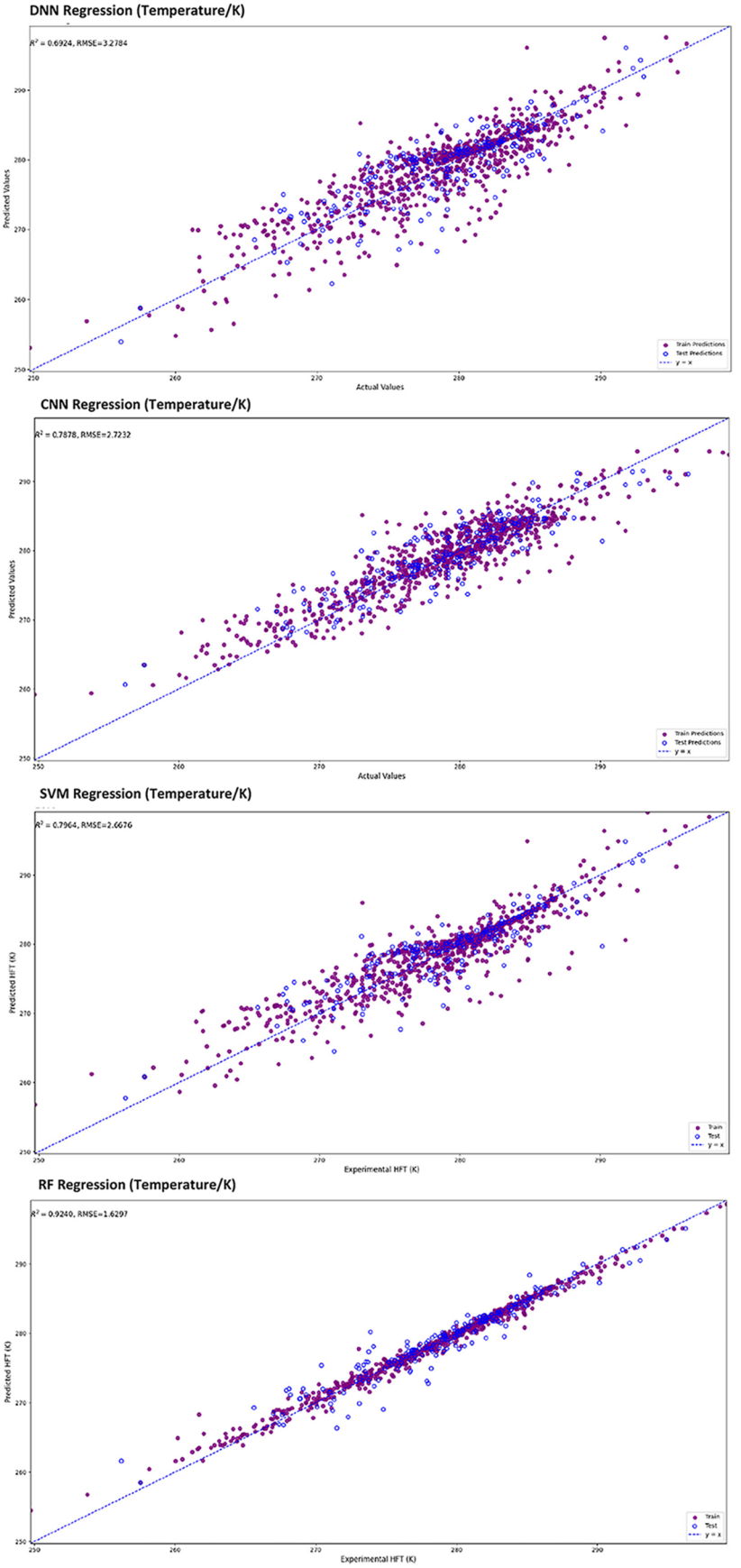

Figure 12. Comparative scatter plots of predicted vs actual hydrate formation temperatures using DNN, CNN, SVM, and RF models.

https://doi.org/10.1021/acs.jced.5c00025
J. Chem. Eng. Data XXXX, XXX, XXX−XXX

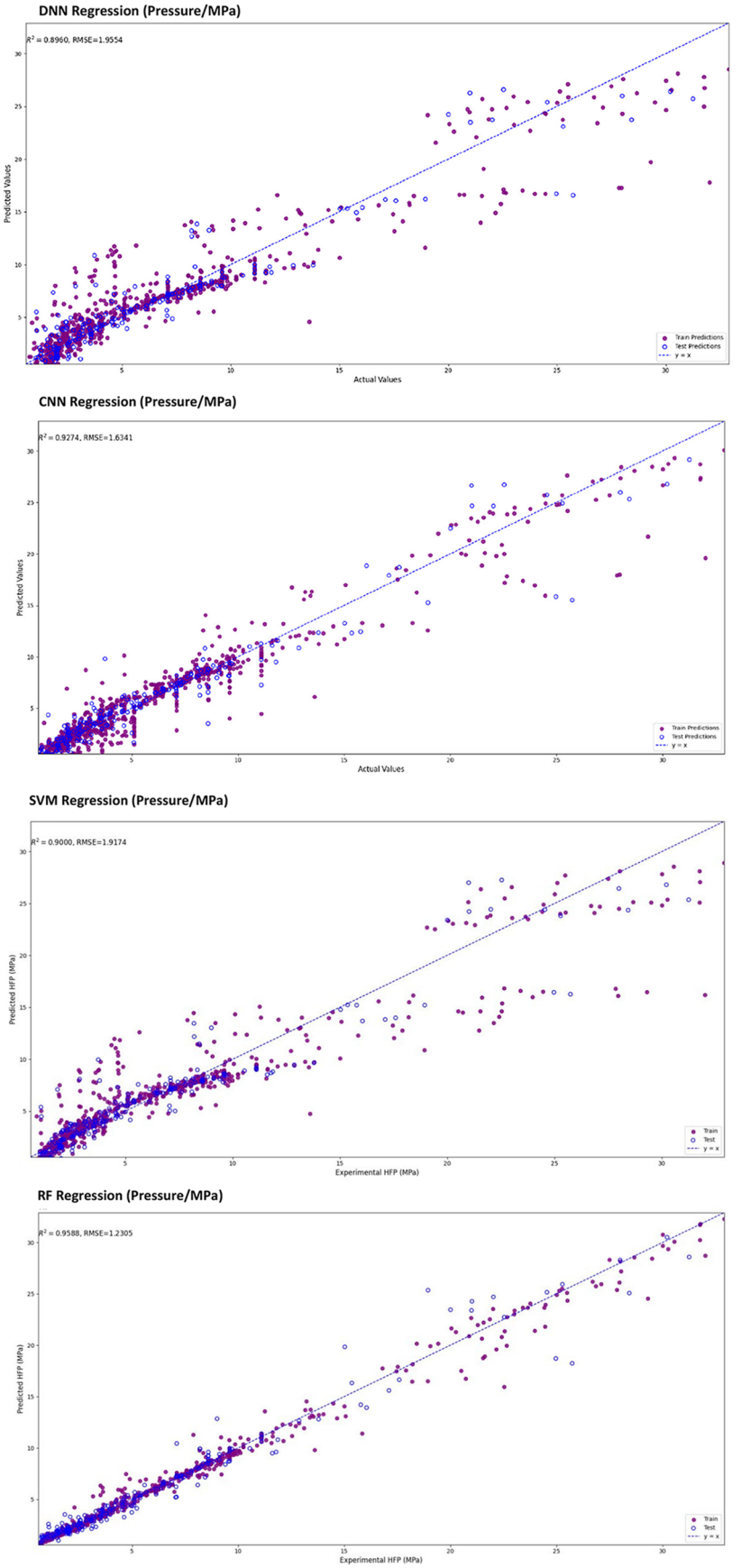

Figure 13. Comparative scatter plots of predicted vs actual hydrate formation pressures using DNN, CNN, SVM, and RF models.

https://doi.org/10.1021/acs.jced.5c00025
J. Chem. Eng. Data XXXX, XXX, XXX−XXX

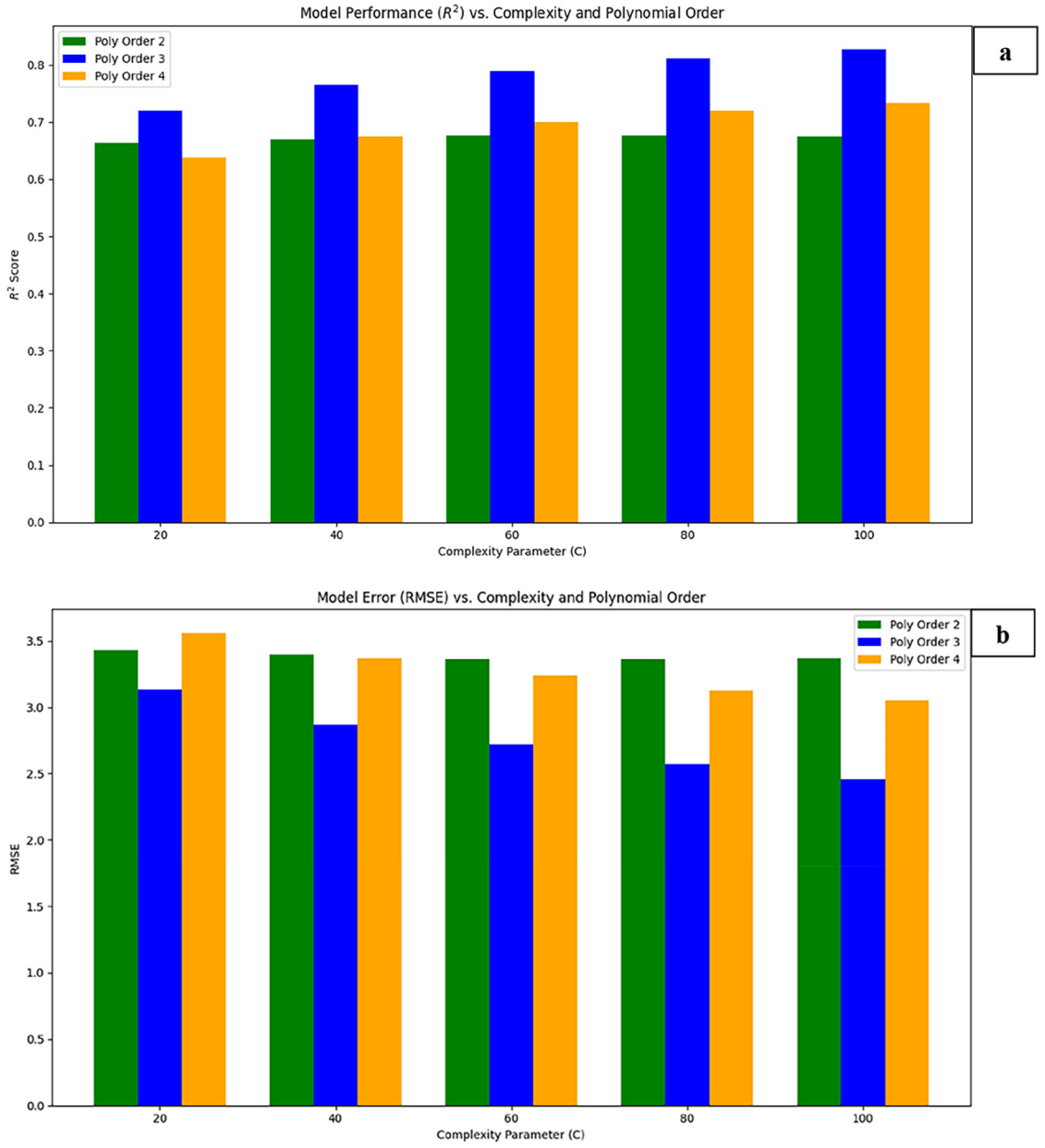

Figure 14. Performance evaluation of the SVM model for hydrate formation temperature prediction: (a) R^2 score vs complexity parameter and polynomial order and (b) RMSE vs complexity parameter and polynomial order.

Figure 15 presents the performance evaluation of the SVM regression model in predicting hydrate formation pressure (HFP). Two evaluation metrics, R^2 and RMSE, are plotted across different combinations of the polynomial order and the complexity parameter to determine how these hyperparameters influence the model's predictive accuracy. High polynomial orders (3.5−4.0) and moderate to high C values (40−100) yield the best results, with maximum R^2 and minimal RMSE, capturing nonlinear data patterns effectively. Low polynomial orders or low C values lead to underfitting, while excessively high C values risk overfitting, reducing generalizability. The analysis underscores the importance of optimizing hyperparameters for robust and accurate HFP predictions.

In this context, RF regression models are evaluated for their capability to predict hydrate formation temperature and pressure, with a focus on the number of trees (n_{trees}), a key hyperparameter. The performance metrics used for this analysis include the R^2 and RMSE, which together reflect the model's accuracy and error levels. The analysis explores how varying n_{trees} impacts the ability of the RF model to capture variance in the data and reduce prediction errors.

Figure 16 illustrates the performance evaluation of the RF regression model for predicting hydrate formation temperature, as influenced by n_{trees} used in the ensemble. The evaluation is presented through two critical metrics: R^2 in Figure 16A and RMSE in Figure 16B, offering insights into how the number of trees affects the model's accuracy and error. The R^2 metric measures the proportion of variance in the temperature data that is explained by the model. The x-axis represents the number of trees used in the RF model, ranging from a few trees to 2000. The y-axis indicates the R^2 values. At very low numbers of trees (<50), the R^2 value fluctuates, reflecting model instability due to the insufficient number of trees to form a reliable ensemble. In this range, the model

AQ

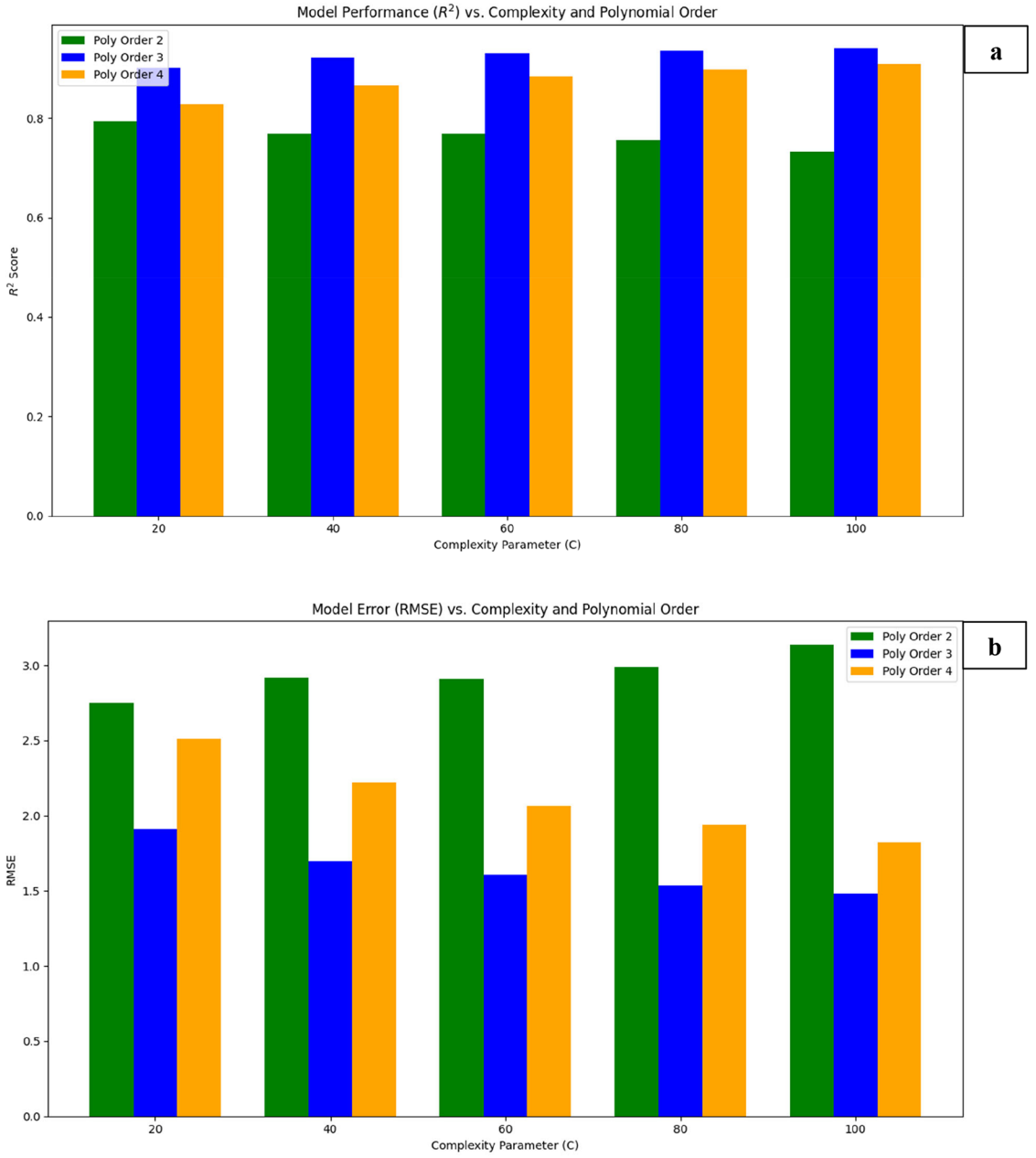

Figure 15. Performance evaluation of the SVM model for hydrate formation pressure prediction: (a) R^2 score vs complexity parameter and polynomial order and (b) RMSE vs complexity parameter and polynomial order.

struggles to generalize well, resulting in lower performance. As the number of trees increases, R^2 stabilizes, reaching a plateau between n_{trees} = 500 and 2000. In this range, the R^2 value consistently remains above 0.912, indicating that the model is capturing a significant portion of the variance in the temperature data. The highest R^2 is observed at n_{trees} = 2000, with a value of approximately 0.914. This suggests that adding more trees marginally improves performance, but the improvement diminishes as the model approaches its optimal configuration. The stability observed at higher tree counts highlights the robustness of the random forest model. However, beyond a certain point (n_{trees} > 1000), the computational cost of adding more trees outweighs the marginal gains in R^2. Based on Figure 16B, it can be stated that at very low tree counts, RMSE values exhibit instability and relatively higher error rates, reflecting the inability of the model to generalize effectively due to underfitting. From n_{trees} = 500 onward, RMSE values stabilize and maintain low error levels. The lowest RMSE observed is approximately 1.75, corresponding to the same range where R^2 achieves its optimal values (n_{trees} = 1000−2000). The consistent RMSE trend at higher tree counts indicates that increasing the number of trees reduces prediction variance. However, the negligible improvement in RMSE beyond n_{trees} = 1000 underscores the diminishing returns of additional trees in terms of error reduction. The analysis shows that the Random Forest model achieves its best balance between accuracy (R^2) and error reduction (RMSE) when the number of trees is between 1000 and 2000. Beyond this range, additional trees do not significantly improve performance but increase computational complexity. Both metrics indicate that the RF model is robust at higher tree counts, capturing the complexity of the

https://doi.org/10.1021/acs.jced.5c00025
J. Chem. Eng. Data XXXX, XXX, XXX−XXX

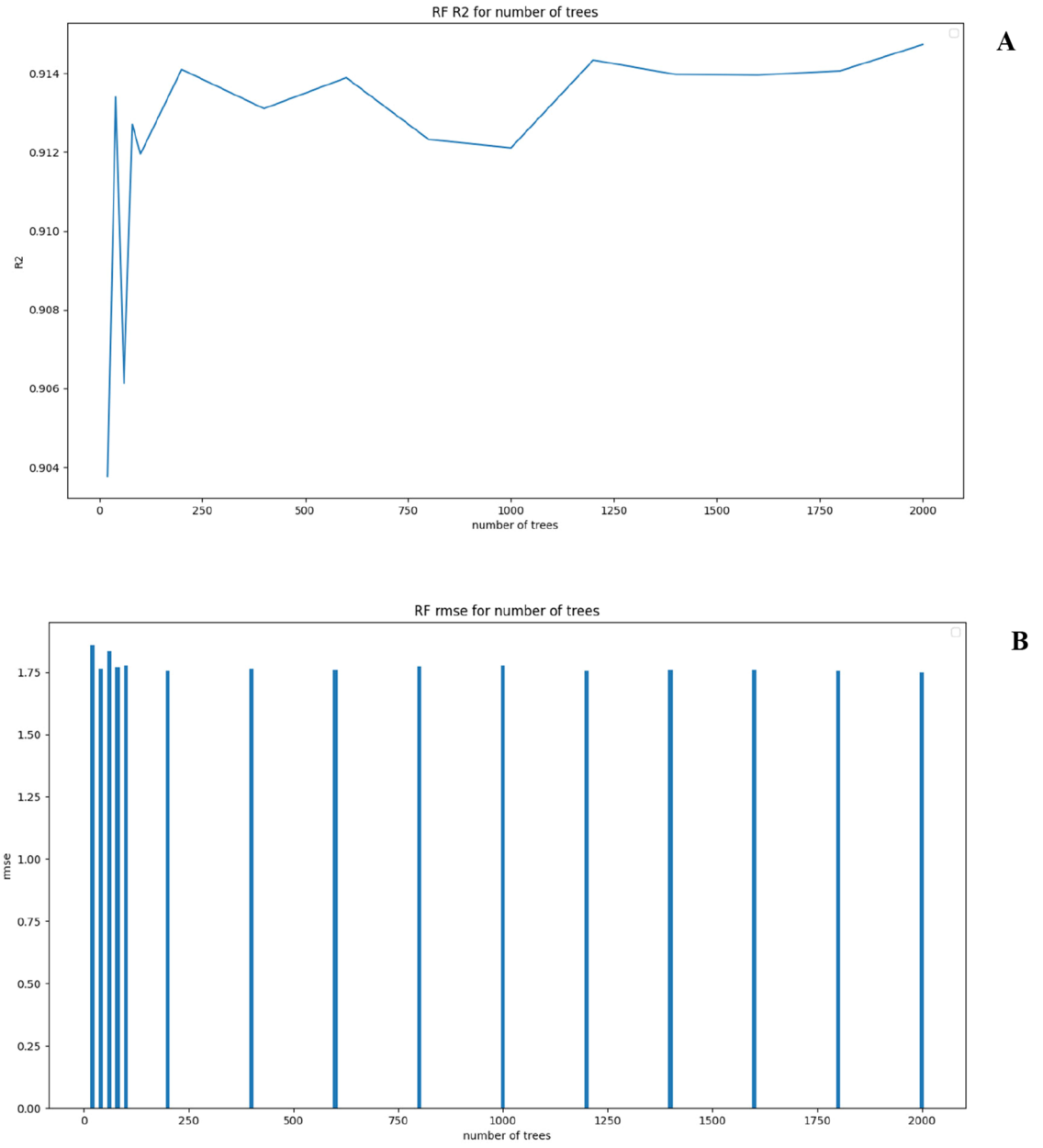

Figure 16. Performance analysis of random forest regression model: (A) impact of tree count on R^2 and (B) RMSE for hydrate formation temperature prediction.

temperature data effectively. However, care must be taken to avoid overfitting or excessive computational cost. For practical applications, selecting $n_{trees} \approx 1000$ is recommended, as it provides an optimal trade-off between performance and computational efficiency. This is particularly important for real-time predictions or scenarios with limited computational resources.

Figure 17 illustrates the performance evaluation of the RF regression model for predicting HFP, focusing on two key metrics: R^2 and RMSE. The analysis investigates the influence of the number of trees, a critical hyperparameter, on model performance. Both plots provide insights into the trade-offs between accuracy and error as the number of trees increases from 0 to 2000. At a very low number of trees (fewer than 100), R^2 shows significant variability and a rapid initial increase. This indicates that adding trees during the early stages substantially improves the model's predictive capacity by capturing additional variance in the data set. As the number of trees increases beyond approximately 500, the R^2 values stabilize around 0.928−0.930, indicating diminishing returns in predictive accuracy. This plateau suggests that the model has captured the majority of the information in the data set, and adding more trees does not significantly enhance performance. Small fluctuations in R^2 at higher tree counts may reflect inherent randomness in training subsets or variations in how features contribute to predictions. However, these fluctuations are minimal and do not compromise overall performance. At very low tree counts, RMSE is considerably higher (around 1.5), reflecting insufficient model complexity and a lack of ensemble diversity to generalize well on the HFP data. RMSE decreases sharply as the number of trees increases to approximately 100, highlighting the importance of ensemble size in reducing prediction error by aggregating outputs from multiple weak learners. Beyond 500 trees, RMSE stabilizes at

https://doi.org/10.1021/acs.jced.5c00025
J. Chem. Eng. Data XXXX, XXX, XXX−XXX

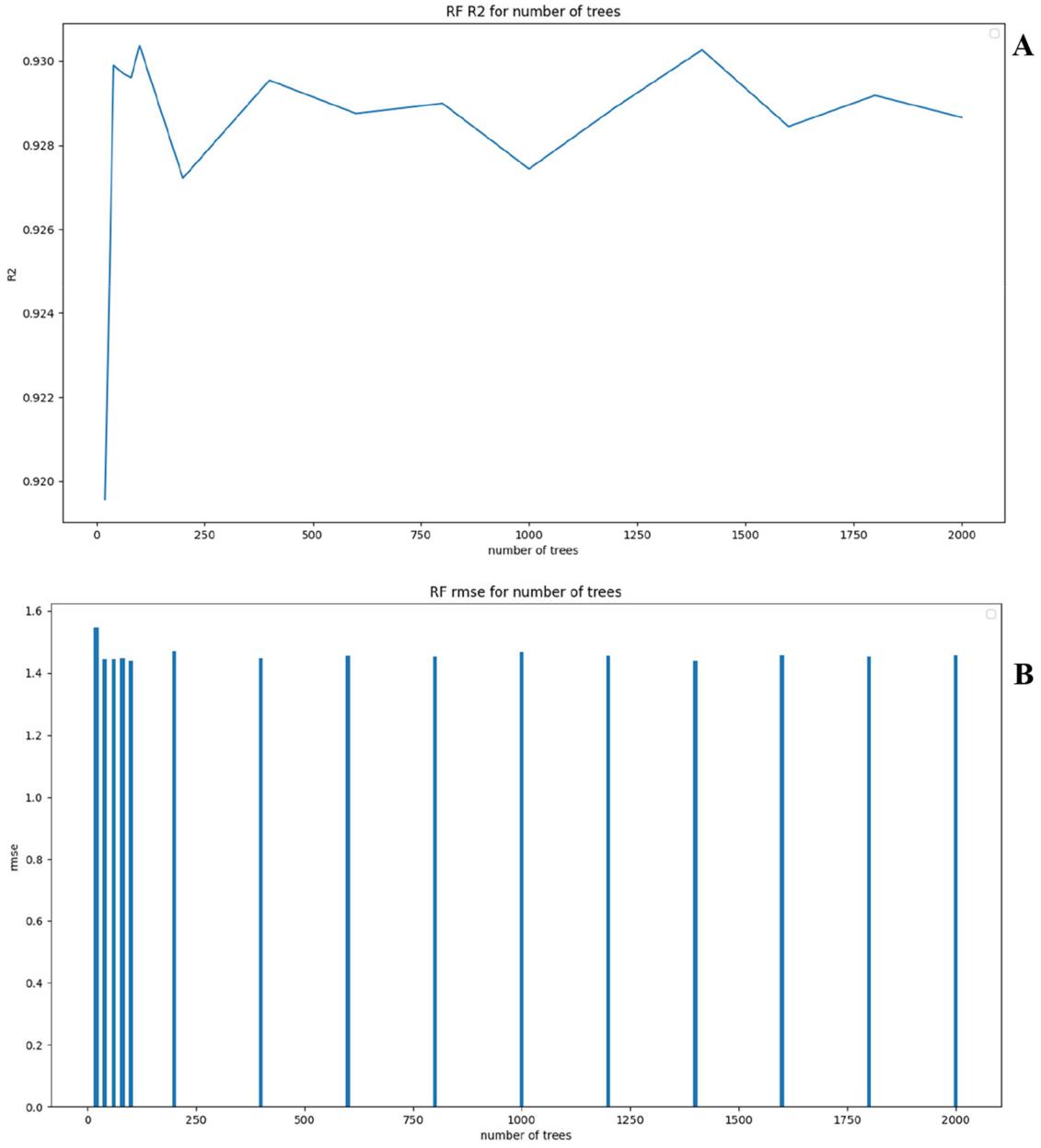

Figure 17. Performance analysis of random forest regression model: (A) impact of tree count on R^2 and (B) RMSE for hydrate formation pressure prediction.

around 0.8−0.9, consistent with the stabilization of R^2. This indicates that further increasing the number of trees does not reduce errors significantly, as the model has already achieved its optimal error reduction. These results underscore the random forest model's capability to predict hydrate formation pressure with high accuracy and low error when appropriately tuned. An ensemble size of approximately 500−1000 trees strike the best balance, achieving high R^2 (approximately 0.930) and low RMSE (approximately 0.8). The analysis highlights the robustness of RF models in handling nonlinear relationships in HFP data, making them a valuable tool for predictive tasks in industrial and scientific applications.

7. EVALUATION OF MACHINE LEARNING MODELS IN HYDRATE PREDICTION: A COMPARISON WITH THERMODYNAMIC MODELS

In this study, we applied machine learning models—including RF, SVM, DNN, and CNN—to predict hydrate formation conditions under diverse thermodynamic scenarios (pressure, temperature, inhibitor type and concentration). These models showed high predictive accuracy, particularly RF and CNN models, which achieved R^2 values of 96 and 94% for pressure prediction, respectively. To provide meaningful physical insight, a thorough comparison was performed between our ML models and classical thermodynamic models, notably the widely used CPAHYD-MF (from Multiflash 7.0), Ballard and Sloan model (B&S), and the recent CaSH-e model introduced by Zhu.[16,143] Thermodynamic models such as CPAHYD-MF and B&S rely on physical principles, including fugacity and

https://doi.org/10.1021/acs.jced.5c00025
J. Chem. Eng. Data XXXX, XXX, XXX−XXX

Table 9. Comparison of Model Strengths and Limitations in Predicting Gas Hydrate Formation

feature	ML models	classical thermodynamic models (e.g., CaSH-e, CPAHYD-MF)
physical basis	data-driven; do not require thermodynamic assumptions	based on equations of state and activity models
accuracy in complex systems	higher accuracy especially with multivariable, high-inhibitor data sets	good for ideal systems; struggles with high inhibitor complexity
data requirements	requires large, high-quality data sets for training	performs well with limited but well-characterized data
interpretability	often seen as black-box; low interpretability	high interpretability based on physical laws
generalization	high flexibility for unseen data	needs recalibration for new compositions or inhibitors
parameterization	no need for manual tuning or electrolyte-specific parameters	requires electrolyte-specific tuning (e.g., CaSH-e uses 3 parameters per salt)

water activity correlations. For example, in CH_4−NaCl systems, Zhu reports the following average absolute deviations from temperature (AADT): CaSH-e: 0.489 K, CPAHYD-MF: 1.21 K, and B&S: 1.071 K, indicating the superior performance of the CaSH-e model at high salt concentrations. Similarly, in CH_4−KCl systems with high wt %, the AADT values were as follows: CaSH-e: 0.194 K, CPAHYD-MF: 1.10 K, and B&S: 0.641 K, further highlighting the better performance of the CaSH-e model compared to other thermodynamic models.

Observations on deviations and outliers revealed some notable trends in the performance of the models. While ML models, particularly RF and CNN, generally exhibited low MSE and strong generalization across data sets, certain patterns emerged. ML models tended to show larger deviations at very high inhibitor concentrations, possibly due to underrepresentation of such conditions in the training data. The CaSH-e model demonstrated a consistent and tight deviation spread, even for high electrolyte systems (e.g., 15−20 wt %), and performed consistently better than CPAHYD-MF in systems with ≥20 wt % salt. In systems with synergistic inhibitors, such as MEG combined with salts, classical models like B&S significantly overestimated dissociation temperatures, with deviations reaching up to 8 K, while the CaSH-e and ML models maintained smaller errors. Table 9 provides a qualitative comparison of the strengths and limitations of various thermodynamic and machine learning models used for predicting gas hydrate formation. It highlights key aspects such as accuracy, generalization capability, performance under different conditions (e.g., high inhibitor concentrations or salt systems), and the handling of complex interactions between variables. This comparison serves to contextualize the performance of each model and guide their application in different scenarios, emphasizing the trade-offs between established thermodynamic approaches and advanced machine learning techniques.

To sum up, while traditional thermodynamic models like CPAHYD-MF and B&S have been foundational in hydrate modeling, they often exhibit limitations under complex, multicomponent systems, particularly those with high inhibitor concentrations. The CaSH-e model improves upon these through a more compact parametrization and predictive accuracy. However, machine learning models surpass even CaSH-e in many real-world scenarios by capturing nonlinear interactions and adapting to diverse data sets without the need for thermodynamic formulations. Despite their black-box nature, ML models offer a promising complementary approach to classical methods, especially for rapid screening, optimization of inhibitors, and operational risk management in hydrate control.

8. PRACTICAL AND ECONOMIC VIABILITY OF ML-BASED HYDRATE MONITORING SYSTEMS

The application of ML models in hydrate prediction has progressed beyond academic exploration and is increasingly being considered for practical deployment in industrial settings. In this study, the models developed—including random forest (RF), support vector machines (SVM), deep neural networks (DNNs), and convolutional neural networks (CNNs)—were evaluated not only for their predictive performance but also for their suitability for integration into real-time hydrate monitoring and flow assurance systems. One of the key advantages of ML models in operational environments is their low inference cost. Although training deep learning models can be computationally intensive, this step is performed offline. Once trained, the models generate predictions rapidly and with minimal computational overhead. This makes them well suited for deployment on edge devices or standard industrial control systems, eliminating the need for specialized high-performance computing infrastructure. Furthermore, the models rely solely on readily available operational parameters—including temperature, pressure, and inhibitor concentration—which are already monitored in most hydrate-prone pipelines and offshore production units. As a result, the integration of these models requires no additional instrumentation or costly sensor upgrades, significantly reducing implementation barriers. From an economic standpoint, the preventive capabilities of the models are particularly noteworthy. Accurate and timely prediction of hydrate formation conditions enables operators to optimize inhibitor injection, prevent flow blockages, and avoid unplanned shutdowns, all of which can result in substantial operational cost savings. This proactive approach not only improves system reliability but also enhances safety and environmental compliance. Moreover, the models are implemented using flexible and open-source tools such as python, tensorflow, and scikit-learn, which facilitates easy integration with existing digital infrastructure and SCADA systems. This technology compatibility reduces deployment cost and promotes scalability across multiple assets or fields. In summary, the ML models developed in this study demonstrate not only strong predictive accuracy but also high economic and operational viability. Their low computational demands, reliance on existing field data, and potential to reduce hydrate-related risks make them promising candidates for real-time field deployment in hydrate monitoring and management systems.

9. CONCLUSIONS

The conducted research on thermodynamic inhibitors for gas hydrates has provided comprehensive insights into their mechanisms and effectiveness. These findings, combined with

https://doi.org/10.1021/acs.jced.5c00025
J. Chem. Eng. Data XXXX, XXX, XXX−XXX

the application of machine learning models, allow for more robust conclusions. The results reveal that increasing the concentration of thermodynamic inhibitors shifts the equilibrium diagram of gas hydrates toward regions of lower temperatures or higher pressures, thereby enhancing their inhibitory effectiveness. Among amino acids, glycine has emerged as the most effective thermodynamic inhibitor when evaluated by weight percentage. Additionally, glycine functions as a suitable synergist, amplifying the inhibition efficiency of commercial inhibitors such as methanol. In the realm of ionic liquids, the inhibitory performance is heavily influenced by the structure of their functional groups and the length of their side chains. Shorter side chain lengths and the presence of hydrogen bonding functional groups, such as OH, NH_2, and NHCO, significantly improve their inhibition potency. Among these, the hydroxyl (OH−) group stands out as the most effective functional group for hydrogen bonding, contributing to the superior performance of ionic liquids in hydrate inhibition. For systems containing salts, the ionic charge distribution and size are critical factors influencing inhibitory potential. Salts with higher ionic charges or smaller ionic radii disrupt hydrogen bonds more effectively, impeding hydrate formation. Among all salts studied, magnesium chloride ($MgCl_2$) and magnesium ions (Mg^{2+}) exhibit superior inhibitory capabilities due to their highly distributed ionic charges. Furthermore, the anion's properties generally exert a greater influence on hydrate stability than the cation in electrolyte solutions. Commercial inhibitors, particularly methanol, have demonstrated strong efficacy in preventing hydrate formation across a range of gas systems. Glycolic inhibitors also follow a descending order of inhibition potency as monoethylene glycol > diethylene glycol > triethylene glycol > poly(ethylene glycol). Monoethylene glycol is preferred over methanol in high-flow-rate applications due to its higher efficiency and reduced operational complexity, eliminating the need for costly recovery units associated with methanol. Moreover, the synergistic use of commercial inhibitors with various salts shows promising results, with salts enhancing the inhibition efficiency by shifting hydrate equilibrium to zones of lower temperatures and higher pressures. Methanol, however, remains the most effective standalone inhibitor, outperforming other commercial inhibitors and salts in preventing hydrate formation. Integrating machine learning models into this research, particularly RF, CNN, SVM, and DNN, has significantly advanced the understanding and prediction of hydrate formation conditions. The RF model outperformed other approaches, achieving an R^2 value of 0.96 and an RMSE of 1.51 for pressure prediction, and an R^2 value of 0.92 and an RMSE of 2.66 for temperature prediction. These results highlight the RF model's superior accuracy and robustness in handling complex data sets. In comparison, CNN and SVM models also delivered strong performance, with CNN achieving an R^2 of 0.94 and RMSE of 2.15 for pressure, and SVM achieving an R^2 of 0.80 and RMSE of 7.12 for temperature prediction. However, the DNN model showed relatively lower accuracy, with an R^2 of 0.72 and RMSE of 2.38 for temperature prediction. The combination of experimental insights and machine learning predictions enables a precise and systematic selection of inhibitors, optimizing their use in industrial applications. By integrating predictive modeling with experimental data, the study ensures both efficacy and economic feasibility, offering a robust framework for hydrate formation management in oil and gas operations.

10. RECOMMENDATIONS

(1) Optimization of machine learning models

- Further refinement of machine learning models, such as RF, CNN, SVM, and DNN, is recommended to enhance predictive accuracy. This could include exploring advanced architectures, such as hybrid models or ensemble techniques, and optimizing hyperparameters for specific data sets.
- Expanding the training data set with additional experimental data, especially at extreme temperature and pressure conditions, can improve the models' ability to generalize and predict rare or complex scenarios.

(2) Targeted use of inhibitors

- Glycine and $MgCl_2$ should be prioritized as effective thermodynamic inhibitors due to their superior performance in shifting hydrate equilibrium conditions. Their combination with commercial inhibitors like methanol may provide enhanced results and should be further investigated.
- For high-flow-rate applications, monoethylene glycol is recommended over methanol due to its cost-effectiveness and ease of recovery.

(3) Development of synergistic formulations

- Research on the synergistic effects of ionic liquids, salts, and commercial inhibitors should continue to identify combinations that maximize inhibition efficacy while minimizing costs.
- Ionic liquids with hydrogen bonding functional groups, such as OH, NH_2, and NHCO, should be explored further, particularly for applications requiring environmentally friendly and highly efficient solutions.

(4) Industrial implementation

- Machine learning models like RF should be integrated into industrial workflows to provide real-time predictions of hydrate formation temperature and pressure. This can optimize inhibitor dosing and reduce operational risks.
- Pilot-scale studies are recommended to validate the practical applicability of machine learning-enhanced inhibitor strategies under real field conditions.

(5) Future research directions

- Investigate the impact of additional environmental and operational factors, such as salinity, gas composition, and flow dynamics, on the performance of thermodynamic inhibitors.
- Explore the use of emerging technologies, such as explainable AI, to better understand the interaction between inhibitors and hydrate formation processes, enhancing model interpretability and reliability.
- In this study, we focused on evaluating machine learning models (RF, SVM, DNN, CNN) for predicting hydrate formation conditions. While these models provide accurate predictions, we recommend future research on hybrid models that combine domain knowledge (thermodynamics and kinetics) with machine learning techniques. This approach could enhance prediction accuracy and robustness, especially under varying environmental conditions.

https://doi.org/10.1021/acs.jced.5c00025
J. Chem. Eng. Data XXXX, XXX, XXX−XXX

AUTHOR INFORMATION

Corresponding Author

Rohallah Hashemi − *Department of Chemical Engineering, Isfahan University of Technology, Isfahan 84156-83111, Iran;* orcid.org/0000-0001-7095-6014; Email: rhashemi@cc.iut.ac.ir

Authors

Mohammad Amin Behnam Motlagh − *Department of Chemical Engineering, Isfahan University of Technology, Isfahan 84156-83111, Iran;* orcid.org/0000-0003-0742-7720

Zahra Taheri Rizi − *Research Institute of Petroleum Industry, RIPI, Tehran 14857-33111, Iran*

Mohsen Mohammadi − *Department of Chemical Engineering, Isfahan University of Technology, Isfahan 84156-83111, Iran;* orcid.org/0000-0001-9035-9997

Mahbobeh Mohammadtaheri − *Research Institute of Petroleum Industry, RIPI, Tehran 14857-33111, Iran*

Behnam Zarei Eslam − *Department of Chemical Engineering, Isfahan University of Technology, Isfahan 84156-83111, Iran*

Complete contact information is available at: https://pubs.acs.org/10.1021/acs.jced.5c00025

Notes

The authors declare no competing financial interest.

ACKNOWLEDGMENTS

The authors would like to express their sincere gratitude to the Research Institute of Petroleum Industry and Isfahan University of Technology for their valuable support and collaboration throughout this research. Their contributions have significantly enhanced the quality of this work.

REFERENCES

(1) Sloan, E. D., Jr.; Koh, C. A. *Clathrate Hydrates of Natural Gases*; CRC Press, 2007.

(2) McMullan, R. K.; Jeffrey, G. A. Polyhedral Clathrate Hydrates. IX. Structure of Ethylene Oxide Hydrate. *J. Chem. Phys.* **1965**, *42* (8), 2725−2732.

(3) Sloan, E. D. Fundamental Principles and Applications of Natural Gas Hydrates. *Nature* **2003**, *426* (6964), 353−359.

(4) Mak, T. C. W.; McMullan, R. K. Polyhedral Clathrate Hydrates. X. Structure of the Double Hydrate of Tetrahydrofuran and Hydrogen Sulfide. *J. Chem. Phys.* **1965**, *42* (8), 2732−2737.

(5) Alqahtani, F. Equilibrium Conditions of Carbon Dioxide and Ethane Gas Hydrate in the Presence of Binary Mixtures of Methanol and Sodium Chloride. Master's Thesis, University of Calgary, 2014.

(6) Ripmeester, J. A.; Tse, J. S.; Ratcliffe, C. I.; Powell, B. M. A New Clathrate Hydrate Structure. *Nature* **1987**, *325* (6100), 135−136.

(7) Sloan, E. D. *Natural Gas Hydrates in Flow Assurance*; Gulf Professional Publishing, 2010.

(8) Jozian, S.; Vafajoo, L. Mathematical Modeling of the Gas Hydrate Formation in a 90° Elbow Utilizing CFD Technique. *Chem. Eng. Trans.* **2018**, *70*, 2167−2172.

(9) Lal, B.; Nashed, O. *Chemical Additives for Gas Hydrates*; Springer Nature, 2019.

(10) Max, M. D. *Natural Gas Hydrate in Oceanic and Permafrost Environments*; Springer Science & Business Media, 2003; Vol. *5*.

(11) Zhao, J.; Song, Y.; Lim, X.-L.; Lam, W.-H. Opportunities and Challenges of Gas Hydrate Policies with Consideration of Environmental Impacts. *Renewable Sustainable Energy Rev.* **2017**, *70*, 875−885.

(12) Han, S.; Shin, J.-Y.; Rhee, Y.-W.; Kang, S.-P. Enhanced Efficiency of Salt Removal from Brine for Cyclopentane Hydrates by Washing, Centrifuging, and Sweating. *Desalination* **2014**, *354*, 17−22.

(13) Nyayapathi, L. *Performance and Economics of Methane Hydrate Reservoirs*; West Virginia University, 2010.

(14) Tariq, M.; Rooney, D.; Othman, E.; Aparicio, S.; Atilhan, M.; Khraisheh, M. Gas Hydrate Inhibition: A Review of the Role of Ionic Liquids. *Ind. Eng. Chem. Res.* **2014**, *53* (46), 17855−17868.

(15) Mokwenye, P. O. Evaluation of Gas Hydrate in Gas Pipeline Transportation. Ph.D. Thesis, University of North Dakota, 2020.

(16) Zhu, D. A. Cage-Based Hydrate Model for Industrially Relevant Systems in Offshore Energy. Doctoral Thesis, University of Western Australia, 2025.

(17) Saleh, J. M. *Fluid Flow Handbook*; McGraw-Hill Education, 2002.

(18) Othman, E. A. Gas Hydrate Equilibrium Measurements for Multi-Component Gas Mixtures and Effect of Ionic Liquid Inhibitors., Texas A&M University, 2014.

(19) Mohanty, K.; Cook, B.; Hakimuddin, M.; Pitchumani, R.; Ogunlana, D.; Burger, J.; Shillinglaw, J. *Petrophysical Characterization and Reservoir Simulator for Methane Gas Production from Gulf of Mexico Hydrates*; Westport Technology Center, 2006.

(20) Iyowu, T. O. Prevention of Hydrates in Pipelines Using Hybrid Thermodynamic Inhibitors. Ph.D. Thesis, African University of Science and Technology, Abuja, Nigeria, 2010.

(21) Sami, N. A.; Sangwai, J.; Subramanian, B. Gas Hydrate Applications and Problems in Oil and Gas Industry. *Int. J. Sci. Eng. Res.* **2013**, *4* 81-5

(22) Igboanusi, U. P.; Opara, A. C. The Advancement from Thermodynamic Inhibitors to Kinetic Inhibitors and Anti-Agglomerants in Natural Gas Flow Assurance. *Int. J. Chem. Environ. Eng.* **2011**, 22131-134

(23) Hu, Y. Measurements and Modeling of Gas Hydrates Formation in Inhibited Systems: High Pressure, High Salinity, and Mixture of Inhibitors. Ph.D. Thesis, Colorado School of Mines, 2018.

(24) Kelland, M. A. Gas Hydrate Control. *Prod. Chem. Oil Gas Ind.* **2014**, *2*, 219−245.

(25) Igor, W.; Erdila, I. Comparison of Methanol and Ethylene Glycol Effectiveness as Chemical Inhibitors in the Prevention of Gas Hydrates in Well Testing Barge DT-05 Well Z Mahakam Field. *IOP Conf. Ser.: Earth Environ.* **2024**, *1339*, No. 012023, DOI: 10.1088/1755-1315/1339/1/012023.

(26) Bavoh, C. B.; Lal, B.; Osei, H.; Sabil, K. M.; Mukhtar, H. A Review on the Role of Amino Acids in Gas Hydrate Inhibition, CO2 Capture and Sequestration, and Natural Gas Storage. *J. Nat. Gas Sci. Eng.* **2019**, *64*, 52−71.

(27) Hecht, D.; Tadesse, L.; Walters, L. Correlating Hydration Shell Structure with Amino Acid Hydrophobicity. *J. Am. Chem. Soc.* **1993**, *115* (8), 3336−3337.

(28) Nigam, A.; Srihari, K. REPORT ON "Alanine Water Complex.", 2013.

(29) Pertsemlidis, A.; Saxena, A. M.; Soper, A. K.; Head-Gordon, T.; Glaeser, R. M. Direct Evidence for Modified Solvent Structure within the Hydration Shell of a Hydrophobic Amino Acid. *Proc. Natl. Acad. Sci. U.S.A.* **1996**, *93* (20), 10769−10774.

(30) Sa, J.-H.; Lee, B. R.; Park, D.-H.; Han, K.; Chun, H. D.; Lee, K.-H. Amino Acids as Natural Inhibitors for Hydrate Formation in CO2 Sequestration. *Environ. Sci. Technol.* **2011**, *45* (13), 5885−5891.

(31) Sa, J.-H.; Kwak, G.-H.; Han, K.; Ahn, D.; Cho, S. J.; Lee, J. D.; Lee, K.-H. Inhibition of Methane and Natural Gas Hydrate Formation by Altering the Structure of Water with Amino Acids. *Sci. Rep.* **2016**, *6* (1), No. 31582.

(32) Roosta, H.; Dashti, A.; Mazloumi, S. H.; Varaminian, F. Inhibition Properties of New Amino Acids for Prevention of Hydrate Formation in Carbon Dioxide−Water System: Experimental and Modeling Investigations. *J. Mol. Liq.* **2016**, *215*, 656−663.

(33) Bavoh, C. B.; Partoon, B.; Lal, B.; Gonfa, G.; Khor, S. F.; Sharif, A. M. Inhibition Effect of Amino Acids on Carbon Dioxide Hydrate. *Chem. Eng. Sci.* **2017**, *171*, 331−339.

(34) Bavoh, C. B.; Partoon, B.; Lal, B.; Kok Keong, L. Methane Hydrate-Liquid-Vapour-Equilibrium Phase Condition Measurements in the Presence of Natural Amino Acids. *J. Nat. Gas Sci. Eng.* **2017**, *37*, 425−434.
(35) Mannar, N.; Bavoh, C. B.; Baharudin, A. H.; Lal, B.; Mellon, N. B. Thermophysical Properties of Aqueous Lysine and Its Inhibition Influence on Methane and Carbon Dioxide Hydrate Phase Boundary Condition. *Fluid Phase Equilib.* **2017**, *454*, 57−63.
(36) Bavoh, C. B.; Khan, M. S.; Lal, B.; Bt Abdul Ghaniri, N. I.; Sabil, K. M. New Methane Hydrate Phase Boundary Data in the Presence of Aqueous Amino Acids. *Fluid Phase Equilib.* **2018**, *478*, 129−133.
(37) Long, Z.; Zhou, X.; He, Y.; Li, D.; Liang, D. Performance of Mixture of Ethylene Glycol and Glycine in Inhibiting Methane Hydrate Formation. *J. Nat. Gas Sci. Eng.* **2018**, *56*, 134−140.
(38) Lee, D.; Go, W.; Seo, Y. Experimental and Computational Investigation of Methane Hydrate Inhibition in the Presence of Amino Acids and Ionic Liquids. *Energy* **2019**, *182*, 632−640.
(39) Qureshi, M. F.; Khraisheh, M.; Almomani, F. Doping Amino Acids with Classical Gas Hydrate Inhibitors to Facilitate the Hydrate Inhibition Effect at Low Dosages. *Greenhouse Gases: Sci. Technol.* **2020**, *10* (4), 783−794.
(40) Qureshi, M. F.; Khraisheh, M.; AlMomani, F. Probing the Effect of Various Water Fractions on Methane (CH4) Hydrate Phase Equilibria and Hydrate Inhibition Performance of Amino Acid L-Proline. *J. Mol. Liq.* **2021**, *333*, No. 115888.
(41) Bharathi, A.; Nashed, O.; Lal, B.; Foo, K. S. Experimental and Modeling Studies on Enhancing the Thermodynamic Hydrate Inhibition Performance of Monoethylene Glycol via Synergistic Green Material. *Sci. Rep.* **2021**, *11* (1), No. 2396.
(42) Rehman, A. N.; Bavoh, C. B.; Khan, M. Y.; Lal, B. Amino Acid-Assisted Effect on Hydrate-Based CO 2 Storage in Porous Media with Brine. *RSC Adv.* **2024**, *14* (13), 9339−9350.
(43) Matuszek, K.; Piper, S. L.; Brzęczek-Szafran, A.; Roy, B.; Saher, S.; Pringle, J. M.; MacFarlane, D. R. Unexpected Energy Applications of Ionic Liquids. *Adv. Mater.* **2024**, *36* (23), No. 2313023.
(44) Yaqub, S.; Lal, B.; Partoon, B.; Mellon, N. B. Investigation of the Task Oriented Dual Function Inhibitors in Gas Hydrate Inhibition: A Review. *Fluid Phase Equilib.* **2018**, *477*, 40−57.
(45) Li, X.-S.; Liu, Y.-J.; Zeng, Z.-Y.; Chen, Z.-Y.; Li, G.; Wu, H.-J. Equilibrium Hydrate Formation Conditions for the Mixtures of Methane + Ionic Liquids + Water. *J. Chem. Eng. Data* **2011**, *56* (1), 119−123.
(46) Tumba, K.; Reddy, P.; Naidoo, P.; Ramjugernath, D.; Eslamimanesh, A.; Mohammadi, A. H.; Richon, D. Phase Equilibria of Methane and Carbon Dioxide Clathrate Hydrates in the Presence of Aqueous Solutions of Tributylmethylphosphonium Methylsulfate Ionic Liquid. *J. Chem. Eng. Data* **2011**, *56* (9), 3620−3629.
(47) Keshavarz, L.; Javanmardi, J.; Eslamimanesh, A.; Mohammadi, A. H. Experimental Measurement and Thermodynamic Modeling of Methane Hydrate Dissociation Conditions in the Presence of Aqueous Solution of Ionic Liquid. *Fluid Phase Equilib.* **2013**, *354*, 312−318.
(48) Zare, M.; Haghtalab, A.; Ahmadi, A. N.; Nazari, K. Experiment and Thermodynamic Modeling of Methane Hydrate Equilibria in the Presence of Aqueous Imidazolium-Based Ionic Liquid Solutions Using Electrolyte Cubic Square Well Equation of State. *Fluid Phase Equilib.* **2013**, *341*, 61−69.
(49) Richard, A. R.; Adidharma, H. The Performance of Ionic Liquids and Their Mixtures in Inhibiting Methane Hydrate Formation. *Chem. Eng. Sci.* **2013**, *87*, 270−276.
(50) Sabil, K. M.; Nashed, O.; Lal, B.; Ismail, L.; Japper-Jaafar, A. Experimental Investigation on the Dissociation Conditions of Methane Hydrate in the Presence of Imidazolium-Based Ionic Liquids. *J. Chem. Thermodyn.* **2015**, *84*, 7−13.
(51) Su, Y.; Bernardi, S.; Searles, D. J.; Wang, L. Effect of Carbon Chain Length of Organic Salts on the Thermodynamic Stability of Methane Hydrate. *J. Chem. Eng. Data* **2016**, *61* (5), 1952−1960.
(52) Khan, M. S.; Lal, B.; Partoon, B.; Keong, L. K.; Bustam, A. B.; Mellon, N. B. Experimental Evaluation of a Novel Thermodynamic Inhibitor for CH4 and CO2 Hydrates. *Procedia Eng.* **2016**, *148*, 932−940.
(53) Khan, M. S.; Bavoh, C. B.; Partoon, B.; Lal, B.; Bustam, M. A.; Shariff, A. M. Thermodynamic Effect of Ammonium Based Ionic Liquids on CO 2 Hydrates Phase Boundary. *J. Mol. Liq.* **2017**, *238*, 533−539.
(54) Long, Z.; He, Y.; Zhou, X.; Li, D.; Liang, D. Phase Behavior of Methane Hydrate in the Presence of Imidazolium Ionic Liquids and Their Mixtures. *Fluid Phase Equilib.* **2017**, *439*, 1−8.
(55) Khan, M. S.; Bavoh, C. B.; Partoon, B.; Nashed, O.; Lal, B.; Mellon, N. B. Impacts of Ammonium Based Ionic Liquids Alkyl Chain on Thermodynamic Hydrate Inhibition for Carbon Dioxide Rich Binary Gas. *J. Mol. Liq.* **2018**, *261*, 283−290.
(56) Nashed, O.; Dadebayev, D.; Khan, M. S.; Bavoh, C. B.; Lal, B.; Shariff, A. M. Experimental and Modelling Studies on Thermodynamic Methane Hydrate Inhibition in the Presence of Ionic Liquids. *J. Mol. Liq.* **2018**, *249*, 886−891.
(57) Gupta, P.; Sakthivel, S.; Sangwai, J. S. Effect of Aromatic/Aliphatic Based Ionic Liquids on the Phase Behavior of Methane Hydrates: Experiments and Modeling. *J. Chem. Thermodyn.* **2018**, *117*, 9−20.
(58) Gupta, P.; Chandrasekharan Nair, V.; Sangwai, J. S. Phase Equilibrium of Methane Hydrate in the Presence of Aqueous Solutions of Quaternary Ammonium Salts. *J. Chem. Eng. Data* **2018**, *63* (7), 2410−2419.
(59) Khan, M. S.; Lal, B.; Keong, L. K.; Sabil, K. M. Experimental Evaluation and Thermodynamic Modelling of AILs Alkyl Chain Elongation on Methane Riched Gas Hydrate System. *Fluid Phase Equilib.* **2018**, *473*, 300−309.
(60) Khan, M. S.; Lal, B.; Keong, L. K.; Ahmed, I. Tetramethyl Ammonium Chloride as Dual Functional Inhibitor for Methane and Carbon Dioxide Hydrates. *Fuel* **2019**, *236*, 251−263.
(61) Kazemi, F.; Javanmardi, J.; Aftab, S.; Mohammadi, A. H. Experimental Study and Thermodynamic Modeling of the Stability Conditions of Methane Clathrate Hydrate in the Presence of TEACl and/or BMIM-BF4 in Aqueous Solution. *J. Chem. Thermodyn.* **2019**, *130*, 95−103.
(62) de Menezes, D. É. S.; Pessôa Filho, P. d. A.; Robustillo Fuentes, M. D. Use of 1-Butyl-3-Methylimidazolium-Based Ionic Liquids as Methane Hydrate Inhibitors at High Pressure Conditions. *Chem. Eng. Sci.* **2020**, *212*, No. 115323.
(63) Qasim, A.; Khan, M. S.; Lal, B.; Ismail, M. C.; Rostani, K. Quaternary Ammonium Salts as Thermodynamic Hydrate Inhibitors in the Presence and Absence of Monoethylene Glycol for Methane Hydrates. *Fuel* **2020**, *259*, No. 116219.
(64) Soromenho, M. R. C.; Keba, A.; Esperança, J. M.; Tariq, M. Effect of Thiouronium-Based Ionic Liquids on the Formation and Growth of CO2 (sI) and THF (sII) Hydrates. *Int. J. Mol. Sci.* **2022**, *23* (6), No. 3292.
(65) Wang, L.; Chen, Y.; Xu, Y.; Zhang, Y.; Li, Y.; Wang, Y.; Wei, J.; Chu, T. Thermodynamic and Kinetic Effects of Quaternary Ammonium and Phosphonium Ionic Liquids on CO2 Hydrate Formation. *ACS Omega* **2023**, *8*, 1191−1205, DOI: 10.1021/acsomega.2c06621.
(66) Lu, H.; Matsumoto, R.; Tsuji, Y.; Oda, H. Anion Plays a More Important Role than Cation in Affecting Gas Hydrate Stability in Electrolyte Solution?—A Recognition from Experimental Results. *Fluid Phase Equilib.* **2001**, *178* (1−2), 225−232.
(67) Jager, M. D.; Sloan, E. D. The Effect of Pressure on Methane Hydration in Pure Water and Sodium Chloride Solutions. *Fluid Phase Equilib.* **2001**, *185* (1−2), 89−99.
(68) Atik, Z.; Windmeier, C.; Oellrich, L. R. Experimental Gas Hydrate Dissociation Pressures for Pure Methane in Aqueous Solutions of MgCl2 and CaCl2 and for a (Methane+ Ethane) Gas Mixture in an Aqueous Solution of (NaCl+ MgCl2). *J. Chem. Eng. Data* **2006**, *51* (5), 1862−1867.

https://doi.org/10.1021/acs.jced.5c00025
J. Chem. Eng. Data XXXX, XXX, XXX−XXX

(69) Mohammadi, A. H.; Afzal, W.; Richon, D. Gas Hydrates of Methane, Ethane, Propane, and Carbon Dioxide in the Presence of Single NaCl, KCl, and CaCl2 Aqueous Solutions: Experimental Measurements and Predictions of Dissociation Conditions. *J. Chem. Thermodyn.* **2008**, *40* (12), 1693−1697.
(70) Mohammadi, A. H.; Richon, D. Methane Hydrate Phase Equilibrium in the Presence of Salt (NaCl, KCl, or CaCl2)+ Ethylene Glycol or Salt (NaCl, KCl, or CaCl2)+ Methanol Aqueous Solution: Experimental Determination of Dissociation Condition. *J. Chem. Thermodyn.* **2009**, *41* (12), 1374−1377.
(71) Haghighi, H.; Chapoy, A.; Tohidi, B. Methane and Water Phase Equilibria in the Presence of Single and Mixed Electrolyte Solutions Using the Cubic-plus-Association Equation of State. *Oil Gas Sci. Technol.* **2009**, *64* (2), 141−154.
(72) Sabil, K. M.; Román, V. R.; Witkamp, G.-J.; Peters, C. J. Experimental Observations on the Competing Effect of Tetrahydrofuran and an Electrolyte and the Strength of Hydrate Inhibition among Metal Halides in Mixed CO2 Hydrate Equilibria. *J. Chem. Thermodyn.* **2010**, *42* (3), 400−408.
(73) Ngema, P. T.; Petticrew, C.; Naidoo, P.; Mohammadi, A. H.; Ramjugernath, D. Experimental Measurements and Thermodynamic Modeling of the Dissociation Conditions of Clathrate Hydrates for (Refrigerant+ NaCl+ Water) Systems. *J. Chem. Eng. Data* **2014**, *59* (2), 466−475.
(74) Windmeier, C.; Oellrich, L. R. Experimental Methane Hydrate Dissociation Conditions in Aqueous Solutions of Lithium Salts. *J. Chem. Eng. Data* **2014**, *59* (2), 516−518.
(75) Ngema, P. T.; Naidoo, P.; Mohammadi, A. H.; Richon, D.; Ramjugernath, D. Thermodynamic Stability Conditions of Clathrate Hydrates for Refrigerant (R134a or R410a or R507) with MgCl2 Aqueous Solution. *Fluid Phase Equilib.* **2016**, *413*, 92−98.
(76) Sylva, T. Y.; Kinoshita, C. K.; Masutani, S. M. Inhibiting Effects of Transition Metal Salts on Methane Hydrate Stability. *Chem. Eng. Sci.* **2016**, *155*, 10−15.
(77) Cai, L.; Pethica, B. A.; Debenedetti, P. G.; Sundaresan, S. Formation of Cyclopentane Methane Binary Clathrate Hydrate in Brine Solutions. *Chem. Eng. Sci.* **2016**, *141*, 125−132.
(78) Holzammer, C.; Finckenstein, A.; Will, S.; Braeuer, A. S. How Sodium Chloride Salt Inhibits the Formation of CO_2 Gas Hydrates. *J. Phys. Chem. B* **2016**, *120* (9), 2452−2459.
(79) Hu, Y.; Lee, B. R.; Sum, A. K. Phase Equilibrium Data of Methane Hydrates in Mixed Brine Solutions. *J. Nat. Gas Sci. Eng.* **2017**, *46*, 750−755.
(80) Ho-Van, S.; Bouillot, B.; Douzet, J.; Babakhani, S. M.; Herri, J. M. Experimental Measurement and Thermodynamic Modeling of Cyclopentane Hydrates with NaCl, KCl, CaCl2, or NaCl-KCl Present. *AIChE J.* **2018**, *64* (6), 2207−2218.
(81) Lv, Q.; Zang, X.; Li, X.; Li, G. Effect of Seawater Ions on Cyclopentane-Methane Hydrate Phase Equilibrium. *Fluid Phase Equilib.* **2018**, *458*, 272−277.
(82) Choi, W.; Lee, Y.; Mok, J.; Lee, S.; Lee, J. D.; Seo, Y. Thermodynamic and Kinetic Influences of NaCl on HFC-125a Hydrates and Their Significance in Gas Hydrate-Based Desalination. *Chem. Eng. J.* **2019**, *358*, 598−605.
(83) Li, S.; Wang, J.; Lv, X.; Ge, K.; Jiang, Z.; Li, Y. Experimental Measurement and Thermodynamic Modeling of Methane Hydrate Phase Equilibria in the Presence of Chloride Salts. *Chem. Eng. J.* **2020**, *395*, No. 125126.
(84) Pourranjbar, M.; Pahlavanzadeh, H.; Askari Zadeh Mahani, A.; Mohammadi, A. H. Hydrate Phase Equilibria of Methane+ TBAC+ Water System in the Presence and Absence of NaCl and/or MgCl2. *J. Chem. Eng. Data* **2020**, *65* (9), 4684−4691.
(85) Bhawangirkar, D. R.; Sangwai, J. S. Phase Equilibrium of Methane Hydrates in the Presence of MgBr2, CaBr2, and ZnBr2 Aqueous Solutions. *J. Chem. Eng. Data* **2021**, *66* (6), 2519−2530.
(86) Porgar, S.; Rahmanian, N. Phase Equilibrium for Hydrate Formation in the Methane and Ethane System and Effect of Inhibitors. *Chem. Rev. Lett.* **2022**, *5*, 2−11.
(87) Satenov, K. G.; Tkenbayev, S. M.; Tashenov, Z. A.; Akhmetov, Z. E.; Kadyrov, S. R. Processes of Methanol Regeneration from Water-Methanol Solutions in the Oil and Gas Industry. *Kaz. J. Oil Gas Ind.* **2024**, *6* (1), 99−109.
(88) Wu, M.; Wang, S.; Liu, H. A Study on Inhibitors for the Prevention of Hydrate Formation in Gas Transmission Pipeline. *J. Nat. Gas Chem.* **2007**, *16* (1), 81−85.
(89) Afzal, W.; Mohammadi, A. H.; Richon, D. Experimental Measurements and Predictions of Dissociation Conditions for Carbon Dioxide and Methane Hydrates in the Presence of Triethylene Glycol Aqueous Solutions. *J. Chem. Eng. Data* **2007**, *52* (5), 2053−2055.
(90) Afzal, W.; Mohammadi, A. H.; Richon, D. Experimental Measurements and Predictions of Dissociation Conditions for Methane, Ethane, Propane, and Carbon Dioxide Simple Hydrates in the Presence of Diethylene Glycol Aqueous Solutions. *J. Chem. Eng. Data* **2008**, *53* (3), 663−666.
(91) Mohammadi, A. H.; Afzal, W.; Richon, D. Experimental Data and Predictions of Dissociation Conditions for Ethane and Propane Simple Hydrates in the Presence of Methanol, Ethylene Glycol, and Triethylene Glycol Aqueous Solutions. *J. Chem. Eng. Data* **2008**, *53* (3), 683−686.
(92) Mohammadi, A. H.; Laurens, S.; Richon, D. Experimental Study of Methane Hydrate Phase Equilibrium in the Presence of Polyethylene Glycol-400 Aqueous Solution. *J. Chem. Eng. Data* **2009**, *54* (11), 3118−3120.
(93) Mohammadi, A. H.; Richon, D. Gas Hydrate Phase Equilibrium in the Presence of Ethylene Glycol or Methanol Aqueous Solution. *Ind. Eng. Chem. Res.* **2010**, *49* (18), 8865−8869.
(94) Maekawa, T. Equilibrium Conditions for Carbon Dioxide Hydrates in the Presence of Aqueous Solutions of Alcohols, Glycols, and Glycerol. *J. Chem. Eng. Data* **2010**, *55* (3), 1280−1284.
(95) Mohammadi, A. H.; Richon, D. Gas Hydrate Phase Equilibrium in Methane+ Ethylene Glycol, Diethylene Glycol, or Triethylene Glycol+ Water System. *J. Chem. Eng. Data* **2011**, *56* (12), 4544−4548.
(96) Maekawa, T. Equilibrium Conditions of Ethane Hydrates in the Presence of Aqueous Solutions of Alcohols, Glycols, and Glycerol. *J. Chem. Eng. Data* **2012**, *57* (2), 526−531.
(97) Cha, M.; Shin, K.; Kim, J.; Chang, D.; Seo, Y.; Lee, H.; Kang, S.-P. Thermodynamic and Kinetic Hydrate Inhibition Performance of Aqueous Ethylene Glycol Solutions for Natural Gas. *Chem. Eng. Sci.* **2013**, *99*, 184−190.
(98) Mech, D.; Pandey, G.; Sangwai, J. S. Effect of Molecular Weight of Polyethylene Glycol on the Equilibrium Dissociation Pressures of Methane Hydrate System. *J. Chem. Eng. Data* **2015**, *60* (6), 1878−1885.
(99) Maekawa, T. Equilibrium Conditions of Xenon Hydrates in the Presence of Aqueous Solutions of Alcohols, Glycols, and Glycerol. *J. Chem. Eng. Data* **2016**, *61* (1), 662−665.
(100) Ferrari, P. F.; Guembaroski, A. Z.; Neto, M. A. M.; Morales, R. E.; Sum, A. K. Experimental Measurements and Modelling of Carbon Dioxide Hydrate Phase Equilibrium with and without Ethanol. *Fluid Phase Equilib.* **2016**, *413*, 176−183.
(101) Akhfash, M.; Arjmandi, M.; Aman, Z. M.; Boxall, J. A.; May, E. F. Gas Hydrate Thermodynamic Inhibition with MDEA for Reduced MEG Circulation. *J. Chem. Eng. Data* **2017**, *62* (9), 2578−2583.
(102) Liu, H.; Guo, P.; Du, J.; Wang, Z.; Chen, G.; Li, Y. Experiments and Modeling of Hydrate Phase Equilibrium of CH4/CO2/H2S/N2 Quaternary Sour Gases in Distilled Water and Methanol-Water Solutions. *Fluid Phase Equilib.* **2017**, *432*, 10−17.
(103) Xu, S.; Fan, S.; Yao, H.; Wang, Y.; Lang, X.; Lv, P.; Fang, S. The Phase Equilibria of Multicomponent Gas Hydrate in Methanol/Ethylene Glycol Solution Based Formation Water. *J. Chem. Thermodyn.* **2017**, *104*, 212−217.
(104) Saberi, A.; Alamdari, A.; Shariati, A.; Mohammadi, A. H. Experimental Measurement and Thermodynamic Modeling of Equilibrium Condition for Natural Gas Hydrate in MEG Aqueous Solution. *Fluid Phase Equilib.* **2018**, *459*, 110−118.

https://doi.org/10.1021/acs.jced.5c00025
J. Chem. Eng. Data XXXX, XXX, XXX−XXX

(105) Adisasmito, S.; Parubak, E. Ethylene Glycol Injection for Hydrate Formation Prevention in Deepwater Gas Pipelines. *MATEC Web Conf.* **2019**, *268*, No. 02003, DOI: 10.1051/matecconf/201926802003.
(106) Sánchez-Mora, M. F.; Galicia-Luna, L. A.; Pimentel-Rodas, A.; Mohammadi, A. H. Experimental Determination of Gas Hydrates Dissociation Conditions in CO2/N2+ Ethanol/1-Propanol/TBAB/TBAF+ Water Systems. *J. Chem. Eng. Data* **2019**, *64* (2), 763−770.
(107) Deka, B.; Barifcani, A.; Al Helal, A.; Badi, D.; Mahto, V.; Vuthaluru, H. Generation of Methane Gas Hydrate Equilibrium Curve for the Thermodynamic Gas Hydrate Inhibitor Propylene Glycol. *J. Pet. Sci. Eng.* **2021**, *199*, No. 108312.
(108) Aminolroayaei, M. A.; Taheri Rizi, Z.; Mohammad-Taheri, M.; Kamran Pirzaman, A.; Dehbandi Baladehi, M.; Ehsani, M. R. Experimental Measurements and Thermodynamic Modeling of CH_4 + H_2 S + MEG Hydrate Phase-Equilibrium Conditions at 6.2−12.3 MPa. *J. Chem. Eng. Data* **2022**, *67*, 2384−2392, DOI: 10.1021/acs.jced.2c00111.
(109) Majumdar, A.; Mahmoodaghdam, E.; Bishnoi, P. R. Equilibrium Hydrate Formation Conditions for Hydrogen Sulfide, Carbon Dioxide, and Ethane in Aqueous Solutions of Ethylene Glycol and Sodium Chloride. *J. Chem. Eng. Data* **2000**, *45* (1), 20−22.
(110) Sun, Z.-G.; Fan, S.-S.; Shi, L.; Guo, Y.-K.; Guo, K.-H. Equilibrium Conditions Hydrate Dissociation for a Ternary Mixture of Methane, Ethane, and Propane in Aqueous Solutions of Ethylene Glycol and Electrolytes. *J. Chem. Eng. Data* **2001**, *46* (4), 927−929.
(111) Eichholz, C.; Majumdar, A.; Clarke, M. A.; Oellrich, L. R.; Bishnoi, P. R. Experimental Investigation and Calculation of Methane Hydrate Formation Conditions in the Presence of Ethylene Glycol and Sodium Chloride. *J. Chem. Eng. Data* **2004**, *49* (4), 847−851.
(112) Masoudi, R.; Tohidi, B.; Anderson, R.; Burgass, R. W.; Yang, J. Experimental Measurement and Thermodynamic Modelling of Clathrate Hydrate Equilibria and Salt Solubility in Aqueous Ethylene Glycol and Electrolyte Solutions. *Fluid Phase Equilib.* **2004**, *219* (2), 157−163.
(113) Masoudi, R.; Tohidi, B.; Danesh, A.; Todd, A. C.; Anderson, R.; Burgass, R. W.; Yang, J. Measurement and Prediction of Gas Hydrate and Hydrated Salt Equilibria in Aqueous Ethylene Glycol and Electrolyte Solutions. *Chem. Eng. Sci.* **2005**, *60* (15), 4213−4224.
(114) Najibi, H.; Chapoy, A.; Haghighi, H.; Tohidi, B. Experimental Determination and Prediction of Methane Hydrate Stability in Alcohols and Electrolyte Solutions. *Fluid Phase Equilib.* **2009**, *275* (2), 127−131.
(115) Lee, J.-W.; Kang, S.-P. Phase Equilibria of Natural Gas Hydrates in the Presence of Methanol, Ethylene Glycol, and NaCl Aqueous Solutions. *Ind. Eng. Chem. Res.* **2011**, *50* (14), 8750−8755.
(116) Mohammadi, A. H.; Richon, D. Phase Equilibria of Hydrogen Sulfide and Carbon Dioxide Simple Hydrates in the Presence of Methanol, (methanol+NaCl) and (Ethylene glycol+NaCl) Aqueous Solutions. *J. Chem. Thermodyn.* **2012**, *44* (1), 26−30.
(117) Lafond, P. G.; Olcott, K. A.; Dendy Sloan, E.; Koh, C. A.; Sum, A. K. Measurements of Methane Hydrate Equilibrium in Systems Inhibited with NaCl and Methanol. *J. Chem. Thermodyn.* **2012**, *48*, 1−6.
(118) Chapoy, A.; Mazloum, S.; Burgass, R.; Haghighi, H.; Tohidi, B. Clathrate Hydrate Equilibria in Mixed Monoethylene Glycol and Electrolyte Aqueous Solutions. *J. Chem. Thermodyn.* **2012**, *48*, 7−12.
(119) Nasir, Q.; Lau, K. K.; Lal, B.; Sabil, K. M. Hydrate Dissociation Condition Measurement of CO_2 -Rich Mixed Gas in the Presence of Methanol/Ethylene Glycol and Mixed Methanol/Ethylene Glycol + Electrolyte Aqueous Solution. *J. Chem. Eng. Data* **2014**, *59* (11), 3920−3926.
(120) Mech, D.; Sangwai, J. S. Phase Equilibrium of the Methane Hydrate System in the Presence of Mixed Promoters (THF + TBAB) and the Effect of Inhibitors (NaCl, Methanol, and Ethylene Glycol). *J. Chem. Eng. Data* **2016**, *61* (10), 3607−3617.
(121) Seo, Y.; Kim, H.; Park, J. In *Investigation of Synergistic Thermodynamic Inhibition Effect of MEG and Salt Solution on Gas Hydrate*, Volume 8: Polar and Arctic Sciences and Technology; Petroleum Technology; American Society of Mechanical Engineers: Busan, South Korea, 2016; V008T11A021.
(122) Dastanian, M.; Izadpanah, A. A.; Mofarahi, M. Phase Equilibria of Carbon Dioxide Hydrates in the Presence of Methanol/Ethylene Glycol and KCl Aqueous Solutions. *J. Chem. Eng. Data* **2017**, *62* (5), 1701−1707.
(123) Kim, H.; Park, J.; Seo, Y.; Ko, M. Hydrate Risk Management with Aqueous Ethylene Glycol and Electrolyte Solutions in Thermodynamically Under-Inhibition Condition. *Chem. Eng. Sci.* **2017**, *158*, 172−180.
(124) Dastanian, M.; Izadpanah, A. A.; Mofarahi, M. Experimental Measurement of Dissociation Condition for Carbon Dioxide Hydrates in the Presence of Methanol/Ethylene Glycol and $CaCl_2$ Aqueous Solutions. *J. Chem. Eng. Data* **2018**, *63* (5), 1675−1681.
(125) Burgass, R.; Chapoy, A.; Li, X. Gas Hydrate Equilibria in the Presence of Monoethylene Glycol, Sodium Chloride and Sodium Bromide at Pressures up to 150 MPa. *J. Chem. Thermodyn.* **2018**, *118*, 193−197.
(126) Kwak, G.-H.; Lee, K.-H.; Hong, S. Y.; Seo, S. D.; Lee, J. D.; Lee, B. R.; Sum, A. K. Phase Behavior and Raman Spectroscopic Analysis for CH_4 and CH_4/C_3H_8 Hydrates Formed from NaCl Brine and Monoethylene Glycol Mixtures. *J. Chem. Eng. Data* **2018**, *63* (6), 2179−2184.
(127) Semenov, A. P.; Stoporev, A. S.; Mendgaziev, R. I.; Gushchin, P. A.; Khlebnikov, V. N.; Yakushev, V. S.; Istomin, V. A.; Sergeeva, D. V.; Vinokurov, V. A. Synergistic Effect of Salts and Methanol in Thermodynamic Inhibition of sII Gas Hydrates. *J. Chem. Thermodyn.* **2019**, *137*, 119−130.
(128) Park, K. H.; Jeong, D.; Yoon, J.-H.; Cha, M. Experimental Measurements of Phase Equilibria Conditions for Methane Hydrates Containing Methanol/Ethylene Glycol and NH4Cl Solutions. *Fluid Phase Equilib.* **2019**, *493*, 43−49.
(129) Mu, L.; Cui, Q. Hydrate Phase Equilibrium Condition of the Synthetic Natural Gas with High Content of CO2 in the Electrolyte Solutions Containing Methanol. *J. Chem. Thermodyn.* **2019**, *132*, 383−389.
(130) Cordeiro, J. C.; Marcelino Neto, M. A.; Morales, R. E. M.; Sum, A. K. Phase Equilibrium of Carbon Dioxide Hydrates Inhibited with MEG and NaCl above the Upper Quadruple Point. *J. Chem. Eng. Data* **2020**, *65* (1), 280−286.
(131) Kim, D. H.; Park, K. H.; Cha, M. Phase Equilibria and Formation Behaviors of Methane Hydrate with Ethylene Glycol and Salts. *Korean Chem. Eng. Res.* **2020**, *58* (4), 635−641.
(132) Behnammotlagh, M. A.; Hashemi, R.; Taheri Rizi, Z.; Mohammadtaheri, M.; Mohammadi, M. Experimental Study of the Effect of the Combined Monoethylene Glycol with NaCl/$CaCl_2$ Salts on Sour Gas Hydrate Inhibition with Low-Concentration Hydrogen Sulfide. *J. Chem. Eng. Data* **2022**, *67* (5), 1250−1258.
(133) Wu, G.; Coulon, F.; Feng, J.-C.; Yang, Z.; Jiang, Y.; Zhang, R. Machine Learning Models for Fast Selection of Amino Acids as Green Thermodynamic Inhibitors for Natural Gas Hydrate. *J. Mol. Liq.* **2023**, *370*, No. 120952.
(134) Breiman, L. Random Forests. *Mach. Learn.* **2001**, *45* (1), 5−32.
(135) Gholami, R.; Fakhari, N. Support Vector Machine: Principles, Parameters, and Applications. *Handbook of neural computation*; Elsevier, 2017; pp 515−535.
(136) Alzubaidi, L.; Zhang, J.; Humaidi, A. J.; Al-Dujaili, A.; Duan, Y.; Al-Shamma, O.; Santamaría, J.; Fadhel, M. A.; Al-Amidie, M.; Farhan, L. Review of Deep Learning: Concepts, CNN Architectures, Challenges, Applications, Future Directions. *J. Big Data* **2021**, *8* (1), No. 53.
(137) Zhang, J.; Zheng, Y.; Qi, D.; Li, R.; Yi, X. In *DNN-Based Prediction Model for Spatio-Temporal Data*, Proceedings of the 24th ACM SIGSPATIAL International Conference on Advances in Geographic Information Systems; ACM: Burlingame, California, 2016; pp 1−4.
(138) Vapnik, V. *The Nature of Statistical Learning Theory*; Springer Science & Business Media, 2013.

(139) Cristianini, N.; Shawe-Taylor, J. *An Introduction to Support Vector Machines and Other Kernel-Based Learning Methods*; Cambridge University Press, 2000.
(140) Schölkopf, B. Learning with Kernels: Support Vector Machines, Regularization, Optimization, and Beyond, 2002. https://direct.mit.edu/books/monograph/1821/bookpreview-pdf/2411769 (accessed Nov 09, 2024).
(141) Flake, G. W.; Lawrence, S. Efficient SVM Regression Training with SMO. *Mach. Learn.* **2002**, *46* (1−3), 271−290.
(142) Wu, G.; Kechavarzi, C.; Li, X.; Wu, S.; Pollard, S. J.; Sui, H.; Coulon, F. Machine Learning Models for Predicting PAHs Bioavailability in Compost Amended Soils. *Chem. Eng. J.* **2013**, *223*, 747−754.
(143) Ballard, A. L.; Sloan, E. D., Jr. The next Generation of Hydrate Prediction: Part III. Gibbs Energy Minimization Formalism. *Fluid Phase Equilib.* **2004**, *218* (1), 15−31.

https://doi.org/10.1021/acs.jced.5c00025
J. Chem. Eng. Data XXXX, XXX, XXX−XXX